


12-2014

# MODELING SUSTAINABILITY IN RENEWABLE ENERGY SUPPLY CHAIN SYSTEMS

Fei Xie

Clemson University, feix@clemson.edu

Follow this and additional works at: [https://tigerprints.clemson.edu/all\\_dissertations](https://tigerprints.clemson.edu/all_dissertations)

 Part of the [Civil Engineering Commons](#), [Operations Research, Systems Engineering and Industrial Engineering Commons](#), and the [Power and Energy Commons](#)

---

## Recommended Citation

Xie, Fei, "MODELING SUSTAINABILITY IN RENEWABLE ENERGY SUPPLY CHAIN SYSTEMS" (2014). *All Dissertations*. 1504.

[https://tigerprints.clemson.edu/all\\_dissertations/1504](https://tigerprints.clemson.edu/all_dissertations/1504)

This Dissertation is brought to you for free and open access by the Dissertations at TigerPrints. It has been accepted for inclusion in All Dissertations by an authorized administrator of TigerPrints. For more information, please contact [kokeefe@clemson.edu](mailto:kokeefe@clemson.edu).

MODELING SUSTAINABILITY IN RENEWABLE ENERGY SUPPLY CHAIN  
SYSTEMS

---

A Dissertation  
Presented to  
the Graduate School of  
Clemson University

---

In Partial Fulfillment  
of the Requirements for the Degree of  
Doctor of Philosophy  
Transportation Engineering

---

by  
Fei Xie  
December 2014

---

Accepted by:  
Dr. Yongxi (Eric) Huang, Committee Chair  
Dr. Mashrur Chowdhury  
Dr. C. Hsein Juang  
Dr. Margaret Wiecek

## **ABSTRACT**

This dissertation aims at modeling sustainability of renewable fuel supply chain systems against emerging challenges. In particular, the dissertation focuses on the biofuel supply chain system design, and manages to develop advanced modeling framework and corresponding solution methods in tackling challenges in sustaining biofuel supply chain systems. These challenges include: (1) to integrate “environmental thinking” into the long-term biofuel supply chain planning; (2) to adopt multimodal transportation to mitigate seasonality in biofuel supply chain operations; (3) to provide strategies in hedging against uncertainty from conversion technology; and (4) to develop methodologies in long-term sequential planning of the biofuel supply chain under uncertainties. All models are mixed integer programs, which also involves multi-objective programming method and two-stage/multistage stochastic programming methods. In particular for the long-term sequential planning under uncertainties, to reduce the computational challenges due to the exponential expansion of the scenario tree, I also developed efficient ND-Max method which is more efficient than CPLEX and Nested Decomposition method. Through result analysis of four independent studies, it is found that the proposed modeling frameworks can effectively improve the economic performance, enhance environmental benefits and reduce risks due to systems uncertainties for the biofuel supply chain systems.

## **ACKNOWLEDGEMENT**

I would like to express my deepest gratitude to my academic advisor, Dr. Yongxi Huang, for his excellent tutoring, mentoring, caring, patience and providing me with the best support for doing my doctorate research. Also, I would like to show my great appreciation to other committee members, Dr. Mashrur Chowdhury, Dr. C. Hsein Juang, Dr. Margaret Wiecek for spending their valuable time and efforts in reviewing, correcting, and making suggestions to improve my PhD dissertation.

In addition to the Dissertation Committee, I would like to thank Shengyin Li, Jie Lu, Yiming He, Xi Zhao, Mizan Rahman, Kakan Dey, Parth Bhavsar, Kweku Brown and many of my friends for their insights and assistants with various collaborations over the last four years.

Also, I would like to thank my parents and parents in law for their emotional and financial support along my graduate studies.

Finally, and most importantly, I will show my deep and heartfelt thanks to my wife, Nawei Liu, for her patience and understanding over the long journey with me. She sacrificed a lot for my career development, and she was always there cheering me up and stood by me through the good times and bad. Without her, I would not come to today's achievements.

# CONTENTS

<b>TITLE PAGE .....</b>	<b>i</b>
<b>ABSTRACT .....</b>	<b>ii</b>
<b>ACKNOWLEDGEMENT .....</b>	<b>iii</b>
<b>LIST OF TABLES .....</b>	<b>vi</b>
<b>LIST OF FIGURES.....</b>	<b>vii</b>
<b>CHAPTER 1 INTRODUCTION.....</b>	<b>1</b>
1.1. BACKGROUND OF RENEWABLE FUELS.....	1
1.2 RESEARCH CONTRIBUTIONS .....	2
1.3 STRUCTURE OF THIS DISSERTATION .....	5
<b>CHAPTER 2 LITERATURE REVIEW.....</b>	<b>6</b>
2.1. DETERMINISTIC BIOFUEL SUPPLY CHAIN SYSTEMS DESIGN.....	6
2.2. STOCHASTIC BIOFUEL SUPPLY CHAIN DESIGN .....	9
<b>CHAPTER 3 MULTISTAGE OPTIMIZATION OF SUSTAINABLE SUPPLY CHAIN OF BIOFUELS.....</b>	<b>12</b>
3.1 PROBLEM STATEMENT.....	12
3.2. METHODS .....	14
3.3 CASE STUDY.....	23
3,4 RESULTS AND DISCUSSION .....	28
3.5 SUMMARY .....	39
<b>CHAPTER 4 INTEGRATING MULTIMODAL TRANSPORT INTO CELLULOSIC BIOFUEL SUPPLY CHAIN DESIGN UNDER FEEDSTOCK SEASONALITY .....</b>	<b>40</b>
4.1 PROBLEM STATEMENT.....	40
4.2 METHODS .....	42
4.3 CASE STUDY.....	53
4.4 RESULTS AND DISCUSSION .....	58
4.5 SUMMARY .....	65
<b>CHAPTER 5 SUSTAINABLE BIOFUEL SUPPLY CHAIN PLANNING AND MANAGEMENT UNDER UNCERTAINTY .....</b>	<b>67</b>
5.1 PROBLEM STATEMENT.....	67
5.2 METHODS .....	68
5.3 CASE STUDY.....	74
5.4 RESULTS AND DISCUSSION .....	80
5.5 SUMMARY .....	83
<b>CHAPTER 6 MULTISTAGE SEQUENTIAL PLANNING OF LONG-TERM BIOFUEL SUPPLY CHAIN PLANNING UNDER UNCERTAINTIES .....</b>	<b>85</b>
6.1 BACKGROUND .....	85
6.2 METHODS .....	88
6.3 CASE STUDY.....	105
6.4 RESULTS AND DISCUSSION .....	111
6.5 SUMMARY .....	120

<b>CHAPTER 7 CONCLUSIONS .....</b>	<b>121</b>
7.1 SUMMARY OF DISSERTATION .....	121
7.2 RESEARCH IMPACTS OF DISSERTATION .....	121
7.3 LIMITATIONS OF DISSERTATIONS.....	122
7.4 FUTURE WORKS .....	123
<b>BIBLIOGRAPHY .....</b>	<b>125</b>

## LIST OF TABLES

TABLE 3-1 NOTATION .....	16
TABLE 3-2 GHG EMISSION DATA .....	27
TABLE 3-3 REFINERY CAPACITY EXPANSION (MGY) BY LOCATIONS OVER YEARS (2015~2025).....	31
TABLE 4-1 FEEDSTOCK PARAMETERS <sup>A</sup> .....	55
TABLE 4-2 REFINERY PARAMETERS .....	55
TABLE 4-3 TRANSPORTATION PARAMETERS <sup>A</sup> .....	57
TABLE 4-4 MEASURES OF EFFICIENCY AND COST FOR SINGLE-MODE AND MULTIMODAL TRANSPORTS.....	63
TABLE 4-5 OUTCOMES OF INCLUDING TRUCKING DISTANCE LIMIT OF 50 MILES .....	64
TABLE 5-1 NOTATIONS .....	69
TABLE 5-2 TECHNICAL AND ECONOMIC INPUTS OF BIOFUEL SUPPLY CHAIN.....	75
TABLE 5-3 GHG EMISSION ESTIMATES.....	77
TABLE 5-4 SCENARIO-DEPENDENT CONVERSION RATES AND EMISSIONS .....	79
TABLE 5-5 SYSTEM PLANNING STRATEGIES AND OUTCOMES .....	80
TABLE 6-1 TRANSPORTATION INPUTS .....	111
TABLE 6-2 PERFORMANCES OF SOLUTION METHODS FOR DIFFERENT NETWORK SIZES .....	112
TABLE 6-3 PERFORMANCES OF SOLUTION METHODS FOR DIFFERENT PLANNING HORIZONS* .....	113
TABLE 6-4 PERFORMANCES OF SOLUTION METHODS FOR DIFFERENT NUMBER OF REALIZATIONS EACH YEAR* .....	113
TABLE 6-5 REFINERY CAPACITIES BY SCENARIOS .....	117
TABLE 6-6 THE VSSS BY STAGES .....	119

## LIST OF FIGURES

FIGURE 3-1 MAPS OF FEEDSTOCK SUPPLY AND ETHANOL DEMAND .....	26
FIGURE 3-2 EXAMPLE OF SYSTEM EXPANSION STRATEGIES (BEST-COMPROMISED DESIGN WITH $\lambda=1$ ) .....	32
FIGURE 3-3 ANNUAL DELIVERED AVERAGE COST AND TOTAL GHG EMISSION IN EACH GALLON OF ETHANOL.....	33
FIGURE 3-4 OPTIMAL FEEDSTOCK PROCUREMENT PORTFOLIO AND USE OF CORN ETHANOL .....	37
FIGURE 3-5 RELATIONSHIP BETWEEN COST AND GHG .....	38
FIGURE 3-6 IMPACT OF CORN ETHANOL COST ON CELLULOSIC ETHANOL PRODUCTION .....	39
FIGURE 4-1 MULTISTAGE MULTIMODAL CELLULOSIC BIOFUEL SUPPLY CHAIN NETWORK.....	43
FIGURE 4-2 GEOGRAPHIC DISTRIBUTIONS OF FEEDSTOCK FIELDS, CANDIDATE REFINERIES, HUBS, TERMINALS AND MAJOR MARKETS .....	54
FIGURE 4-3 ETHANOL INFRASTRUCTURE SYSTEMS .....	60
FIGURE 4-4 THE DIAGRAM OF FEEDSTOCK AND ETHANOL FLOWS OVER SEASONS IN THE SUPPLY CHAIN....	62
FIGURE 4-5 THE EFFECTS OF DISTANCE LIMITS ON THE DELIVERED FUEL COST .....	65
FIGURE 5-1 SCENARIO GENERATIONS FOR UNCERTAIN CONVERSION RATES OF CORN STOVER.....	79
FIGURE 5-2 BOX PLOTS OF RELATIVE COST SAVINGS BY THE SP SOLUTION .....	83
FIGURE 6-1 A SCENARIO TREE WITH THREE PERIODS AND TWO REALIZATIONS FOR EACH PERIOD.....	92
FIGURE 6-2 MAPS OF FEEDSTOCK FIELDS, REFINERIES AND DEMAND CENTERS.....	110
FIGURE 6-3 CUMULATIVE DISTRIBUTIONS OF THE RATIOS OF SOLVING TIMES OF ND AND ND-MAX TO THE SOLVING TIMES OF CPLEX .....	114
FIGURE 6-4 A DIAGRAM OF PLANNING DECISIONS OVER TIME .....	116
FIGURE 6-5 REFINERY LAYOUTS UNDER TWO DEMAND SCENARIOS .....	117
FIGURE 6-6 BREAKDOWN OF THE TOTAL SYSTEMS COST .....	118



# CHAPTER 1 INTRODUCTION

## ***1.1. Background of Renewable Fuels***

Fossil fuels, including gasoline and diesel, have long been predominant transportation fuels in the United States. However, the fossil fuels are vulnerable to the fluctuation of oil prices, negative to the environment, and insecure with oil supply dwindling. These challenges have attracted wide attentions from various research disciplines and collectively, they are aggressively working on developing *renewable fuels*, as a viable solution, to substitute the fossil fuels. Renewable fuels are typically derived from renewable biomass energy sources (EPA), and there are many candidate renewable fuel systems, such as biofuel, nature gas, hydrogen, and electricity. Compared to fossil fuels, renewable fuels have similar effectiveness in powering transportation vehicles, and more importantly, they are attractive as they can provide better environmental performance and most of the fuels can be domestically produced within United States.

In order to successfully substitute the fossil fuel systems, each renewable fuel path, such as the biofuel, shall provide better economic and environmental performances and shall be risk-neutral as well. There are two main research directions in reaching this aim: (1) to improve the production technology of the renewable fuel systems, and (2) to provide sustainable and resilient renewable fuel supply chain systems. As a PhD candidate in transportation, my research focuses on the latter one. In particular, I focus on developing the supply chain systems for biofuel. Note that, the major contributions in the methodologies presented in this dissertation can also be applied to other renewable fuel systems with different production technologies.

## **1.2 Research Contributions**

The research focus of this dissertation is on the biofuels that are converted from cellulosic biomass such as biowastes and dedicated energy crops to meet the aggressive goal set by the Renewable Fuels Standard (RFS) with the target of annual production of 36 billion gallons of biofuel by 2022, out of which 16 billion gallons is from the advanced renewable fuels, including cellulosic biofuels (110th U.S. Congress, 2007). A sustainable supply chain system that ensures strong cost competitiveness, environmental benefits and reliability is crucial to facilitate the rapid expansion of biofuel production and delivery in the next few decades.

Such sustainable biofuel supply chain relies on its infrastructure system that supports the movements of feedstocks and biofuels from fields to end users. Typically, there are four major infrastructure layers in support of the supply chain: biomass fields/storage, biorefineries, biofuel blending facilities, and city gates/terminals. Developing a cost effective and operation reliable biofuel supply chain is challenging as it involves interdependent decisions along the supply chain. To model the sustainability of the biofuel supply chain systems, I made four major research contributions:

- Integration of “environmental thinking” into biofuel supply chain system planning and management: This study addresses a strategic multistage expansion (e.g., a decade) of a cellulosic biofuel supply chain system with supplements of corn grain biofuels. A multi-objective, multiyear optimization framework is

proposed and the compromise method is used to seek best-compromise solutions between economic competitiveness and environmental quality of the supply chain while satisfying evolving fuel demand, feedstock resources, and technological constraints. The details of this study are shown in Chapter 3.

- Integrating “Multimodal Transport” into Cellulosic Biofuel Supply Chain Design under Feedstock Seasonality: Due to geographic dispersions between facilities in a cellulosic biofuel supply chain, multimodal transport may be attractive to improve the economic efficiency. A multistage, mixed integer programming model is developed that fully integrates multimodal transport into the cellulosic biofuel supply chain design under feedstock seasonality. Three transport modes are considered: truck, single railcar, and unit train. The goal is to minimize the total cost for infrastructure, feedstock harvesting, biofuel production, feedstock/biofuel storage, and transportation. The details of this study are shown in Chapter 4.
- Mitigation of *conversion technology uncertainty* in the sustainable biofuel system design: The uncertainty inherent in the conversion process arises from the lack of complete knowledge about the production technology. Such deficiency may cause inadequate planning of feedstock supply and refinery configuration, and have adverse effects on the biomass/biofuel logistics performance. This concern motivates me to investigate effective ways to mitigate the impacts of the uncertainty on the biofuel supply chain and develop an advanced stochastic optimization model to tackle this issue. This study combines statistical analysis and stochastic modeling, which allow the integration of the uncertainty into the

decision making of a biofuel supply chain design. The goal is to achieve the best system performance measured by the economic competitiveness and environmental quality. The details of this study are shown in Chapter 5.

- Long-term Energy Supply Chain Sequential Planning under Uncertainties: This work focuses on developing a multistage stochastic programming model to handle the challenges inherent in the decision making for long-term multi-period biofuel supply chain design, which is inevitable under uncertainty from supply, demand or even biofuel conversion technologies. The goal is to minimize the total expected cost over time while satisfying biofuel demand. In this study, I solve the problem using both nested decomposition and decomposition with maximal non-dominated cut. I implement both methods on hypothetical numerical examples to evaluate their performances compared to CPLEX. The multistage stochastic model and the solution method are also applied to a real world case study based on the South Carolina biofuel systems to demonstrate their application on large scale problems. The details of this study are shown in Chapter 6.

These four studies provide my original contribution to the biofuel supply chain design, and more importantly, the general research domain of renewable fuel infrastructure system design and planning. In particular, these studies will help address the following four major questions:

1. How to achieve a cost and environmental friendly biofuel supply chain in the next few decades?
2. Is multimodal transport crucial to the biofuel supply chain design and how to integrate it to mitigate the seasonality issues inherent in the supply chain operations?
3. What kinds of systems strategy should be made to hedge against uncertainty from the conversion technology? and
4. What system expansion strategy should be made to hedge against uncertainties and adapt to the demand market changes over time?

### ***1.3 Structure of this Dissertation***

The remainder of this dissertation is organized as follows. Literature review on biofuel supply chain design will be presented in Chapter 2. The dissertation is composed of four studies, which will be presented in Chapter 3 to Chapter 6 respectively. Chapter 7 will summarize the conclusions of this dissertation and will suggest future research approaches.

## Chapter 2 LITERATURE REVIEW

Prior research efforts on biofuel related supply chain design and planning can be summarized into two categories: *deterministic designs* and *stochastic designs*. The deterministic supply chain design assumes that all parameters are known and fixed, while such assumption has been relaxed in stochastic designs to take into account the uncertainties in the decision making. Depending on the nature of planning process, each of the deterministic and stochastic designs can be divided into two subcategories: *snapshot planning* and *sequential planning*. The snap-shot planning is a simplified view of the problem by assuming that all parameters given would stay unchanged and ignoring the effects of time dynamics. Typically, a snap-shot planning is for annual based system design and may incorporate seasonality to better reflect variations during the course of the year. On the contrary, the sequential planning is mainly from a strategic point of view by recognizing dynamics involved with some supply chain parameters (e.g., demand and technology). The study horizon is normally longer and may extend to multiple years (e.g., 10 years). The planning decisions are made periodically to allow system expansion to meet the changes in the biofuel market. I will organize the literature reviews based on this topology.

### **2.1. Deterministic Biofuel Supply Chain Systems Design**

*Deterministic Snapshot Planning:* There are numerous prior studies falling into this category. For example, Akgul et al. (2010) formulated a mixed integer linear programming model in optimizing biofuel plants locations/sizing, material flows between

sites, required number of transport units, feedstock cultivation and fuel production. The model aimed at minimizing the entire biofuel supply chain system cost. Another study (Bowling et al., 2011) focused on the net profit maximization of the biofuel supply chain, with decisions including operational strategies and configurations of refineries and processing hubs. The model considered nonlinear economic-of-scale behavior of the capital cost function, and reformulated it using disjunctive models. Aksoy et al. (2011) investigated four biofuel conversion technologies, and recommended corresponding supply chain layouts respectively. Kim et al. (2011b) proposed a mixed integer model in selecting fuel conversion technologies, determining biofuel supply chain infrastructure layout, and planning transportation logistics between feedstock sites, conversion facilities and consumer markets.

It is also important to integrate the seasonality, a major characteristic of the biofuel systems, in the biofuel supply chain snapshot planning. . This requires the partition of the one-year study scope into multiple periods (e.g., seasons) to capture the variations in parameters over periods and to provide corresponding detailed operational decisions. For example, Tembo et al. (2003) considered months as the studied periods, and developed a multi-period mixed integer model to identify economical cellulosic feedstock sites, feedstock acquisition, feedstock delivery timing, inventory management, and system configuration. The objective is to maximize the net present value of the ethanol production industry. Another study (An et al., 2011) divided one year design into seasons, and proposed a time-staged profit maximization model for a cellulosic biofuel supply chain from feedstock suppliers to biofuel customers. More recently, in addition to

the cost/profit driven systems development, new research interests arose to integrate sustainability concepts into the biofuel supply chain design, and examples are (Gebreslassie et al., 2013; You et al., 2011; You and Wang, 2011).

*Deterministic Sequential Planning:* There are fewer studies in this category. Huang et al. (2010) developed a multistage mixed integer programming model in planning the biowaste-based cellulosic biofuel system expansion over a multi-year planning horizon. Giarola et al. (2011) addressed the strategic design and planning of the biofuel supply chain by integrating both first-second generation biofuel supply chain systems. A mixed integer multistage multiobjective model was developed to optimize both environmental and financial performances. Another study (Ebadian et al., 2013) focused on the detailed multi-year planning of the storage system for the biomass supply chain system.

Based on existing literatures on deterministic biofuel supply chain design, most of studies (especially for the deterministic sequential planning) only focus on improving the cost efficiency and overlook the environmental impact which is a key aspect in promoting renewable fuel systems. To fill this research void, I will develop sustainable supply chain modeling framework for the deterministic sequential planning of biofuel supply chain in Chapter 3. In addition, all existing literatures in deterministic systems design only consider truck as the transport mode, and ignores the potential benefits of the multimodal transport systems. Therefore, Chapter 4 will initiate a research effort in using multimodal transport systems to further improve the efficiencies in operating the biofuel supply chain.



## **2.2. Stochastic Biofuel Supply Chain Design**

All aforementioned studies on biofuel supply chain systems design are based on deterministic modeling frameworks, which assume that all information is known and fixed. However, uncertainties may exist and can have dramatic impact on the entire supply chain operations (Subrahmanyam et al., 1994). These uncertainty parameters need to be addressed to reduce the impacts of risks on the biofuel supply chain (Awudu and Zhang, 2012). Advanced modeling techniques, two-stage stochastic programming and multi-stage stochastic programming methods are effective methods to deal with uncertainties in the systems design.

*Stochastic Snapshot Planning:* The two-stage stochastic programming method can be effectively applied to the snapshot biofuel supply chain design under uncertainty. Kim et al. (2011a) combined multiple dominant uncertainty parameters into scenarios in the biofuel supply chain design. They used the two-stage stochastic programming method to optimize the overall supply chain profit. Another snapshot design study (Awudu and Zhang, 2013) proposed a stochastic model for planning the biofuel supply chain under demand and price uncertainties, which follow normal distribution and geometric brownian motion respectively. The Monte Carlo simulation technique was applied to discretely sample the continually distributed uncertainty, and the model was then solved with the bender decomposition method. Chen and Fan (2012) incorporated supply and demand uncertainties into the one-year planning of the bioenergy supply chain systems, and used the progressive hedge (PH) method to solve the proposed two-stage stochastic model.

There are also a few biofuel stochastic snapshot studies that considered seasonality. Such one-year, multi-period design usually involves multiple stages for operational decisions. However, due to the complexity of multistage stochastic programming method (Birge and Louveaux, 2011), in my reading scope, all studies simplified the problem to formulate them as two-stage stochastic programming models. For example, Cundiff et al. (1997) modeled impacts of uncertain weather conditions on the biomass production in the biofuel supply chain. The model focused on the upstream supply chain from the fields to the centralized refinery. You (2013) developed a multi-objective stochastic programming model for planning the hydrocarbon bio-refinery supply chains under supply and demand uncertainties. The model was to achieve minimum system cost and downside risk on monthly basis. A multi-cut L-shaped based decomposition method was developed to solve the problem.

Stochastic Sequential Planning: Different from the snapshot design, the sequential planning design usually has planning decisions nested in the successive time stages, which normally requires the use of multistage stochastic modeling framework. Due to the complexity of the modeling and solutions, studies in this category is scarce and the study (Dal-Mas et al., 2011) is probably the only one. The study focused on a multiyear capacity planning of the ethanol supply chain system under feedstock and ethanol price uncertainties. The uncertainty realizations over time were simplified and aggregated to a limited number of scenarios, each of which represents a particular cost or price level over time, assuming that the realized cost or price level will remain unchanged

over time. This simplification makes the two-stage stochastic programming model eligible for this problem.

Most existing studies on stochastic systems design focus on uncertainties from supply, demand and biofuel prices, and no study has been found to consider uncertainty from conversion technology. One contribution of this dissertation is to integrate uncertainties from the conversion technology into the supply chain design, which is presented in Chapter 5.

In addition, it is clear that the system uncertainty is mainly considered in the snapshot systems design, and research efforts in systematically integrating uncertainty mitigation into the long-term sequential decision making are seriously lacking, which however are essentially important to enhance the long-term supply chain resilience in hedging against potential risks. The simplification of the sequential realization of uncertainty by an aggregated set of scenarios in (Dal-Mas et al., 2011) though reduces the modeling complexity, may not fully capture the nature of the uncertainty realization that may be independent over time. To fill this research gap, in Chapter 6, I propose to develop a multistage stochastic modeling framework and corresponding solution methodologies, to design an infrastructure system in support of biofuel supply chain functionality in a long run.

# CHAPTER 3 MULTISTAGE OPTIMIZATION OF SUSTAINABLE SUPPLY CHAIN OF BIOFUELS

## ***3.1 Problem Statement***

Required by the RFS, the biofuel supply chain must not only be economically viable but also be environmentally sustainable. Cellulosic biofuel, produced from crop residues, industrial wastes, and energy dedicated crops, has been deemed as a vital alternative to corn grain based biofuels, for its higher energy production efficiency and better life cycle performances (Jenkins et al., 2007; Zhu and Pan, 2010). This study focuses on characterizing the next-generation economic and environmental sustainable supply chain of cellulosic biofuels, with supplements of corn grain based biofuels.

Achieving a biofuel supply chain with improved life cycle performances requires the integration of the environmental consideration into a supply chain design of biofuels. One of the challenges would be how to maintain low negative impact on the environment while achieving high economic effectiveness. A common approach is to use the multi-objective decision-making approach to seek a set of best alternatives, as the objective of achieving low emissions is usually conflicting with the objective of least cost. Few studies (Gebreslassie et al., 2013; Mele et al., 2009; You, 2013; You et al., 2012; You and Wang, 2011; Zamboni et al., 2009) have investigated the impact of environmental considerations, however, in snapshot biofuel supply chain designs.

To the best knowledge, this study is at first to address a *multiyear* supply chain expansion of biofuels *with an integrated environmental consideration*. As cellulosic

biofuel is still at its early stage of development with no established supply chain (EIA, 2013), the study focuses on developing cellulosic biofuel supply chain with supplement of corn grain based biofuels. A multiobjective (i.e., cost and GHG emission), multistage (multiyear), mixed integer programming model is formulated to create a staged expansion plan for cellulosic biofuel supply chain over long-term (e.g., a decade) and the supplement of corn grain based biofuels. The economic objective is to minimize the total annualized cost of the cellulosic and corn grain based biofuels while the emission objective is to minimize the GHG emissions along the supply chain, including a sequence of feedstock acquisition and transportation, fuel production, and fuel distribution to demand cities as well as the use of corn grain based biofuels. The GHG emissions associated with each process can be quantified by using the GREET (Greenhouse gases Regulated Emissions and Energy use in Transportation) model developed by Argonne National Laboratory (Wang et al., 2005), and their potential environmental impacts were aggregated into an environmental performance indicator (i.e., carbon dioxide equivalent (CO<sub>2</sub>-eq), based on the concept of global warming potential (GWP) (BSI Group, 2011; Forster et al., 2007). In particular, the GHG emissions are limited to three GHG species: CO<sub>2</sub>, CH<sub>4</sub>, and NO<sub>2</sub>. This multistage, multi-objective model is solved by the compromise method (Tamiz et al., 1998) to seek a set of best compromised solutions between the cost and emission objectives.

The remainder of this Chapter is organized as follows. In Section 3.2, we will present the mathematical formulation of a proposed multistage, multi-objective model to integrate economic and environmental considerations under a single modeling framework.

The illustrative case study of California biofuel systems will be presented in Section 3.3, followed by the results in Section 3.4. I will summarize the study in Section 3.5.

### **3.2. Methods**

A deterministic, multi-objective, multistage, mixed-integer program is developed to minimize the total system cost and GHG emissions across the multiple layers of biofuel supply chain (i.e., feedstock fields, refineries, and biofuel terminals at city gates) and throughout the entire expansion horizon (e.g., a decade). This problem requires effective spatial and temporal integration across geographically distributed facilities along with the supply chain. The spatial dimension considers geographic distributions of biomass resources, fuel demands, biorefineries, and roadway network; the temporal dimension relates to the multi-year planning horizon. The temporal dimension is divided into multiple one-year periods  $t \in T$  and decisions are made for each year. The annual fuel demand are satisfied by both cellulosic and corn grain based biofuel.

For *cellulosic biofuel*, as the feedstock yields are aggregated and on annual basis. The feedstock seasonality is neglected and the feedstock storage is thus not included in the supply chain. The infrastructure layers in the supply chain are feedstock fields  $i_l \in N_l^F$  ( $l \in L$ , set of feedstock types), biorefineries  $j \in N^R$ , and biofuel terminals  $m \in N^M$ . Note that the supply chain ends at city gates and further local fuel dispensing to refueling stations is neglected. Both system costs and GHG emissions are dependent on the supply chain layout and operations. For *corn grain based biofuel*, the price and

emissions are exogenously available to the model. The model can be briefly described as follows:

*Inputs:*

- the annual yields of feedstock of each type and annual biofuel demand,
- the geographic distances between infrastructures in the supply chain, processed by geographic information system (GIS),
- cost functions associated with building infrastructures, procuring feedstock, producing fuel, and transporting feedstock and fuel, and
- GHG emission inventories (outputs of the GREET model) associated with feedstock acquisition, fuel production, and transportation.

*Decisions:*

- locations and sizes of new refineries by year,
- capacity expansions of existing refineries by year, and
- feedstock and fuel flows in the supply chain by year.

*Assumptions:*

- a refinery will not shut down once it is operational;
- truck is the only transport mode;
- truck will travel with the shortest path between an origin and a destination; and

- tailpipe emissions are assumed to be offset by the biomass during growth, suggested by studies (Raphael et al., 2009; Wang et al., 2005).

We will first introduce the cost minimization (denoted as  $F_1$ ) and minimization of system GHG emissions objectives (denoted as  $F_2$ ). A compromise model is then used to combine the two objectives in a multi-objective modeling framework, subject to physical, technological, and economic constraints. The notation used in the models is presented in Table 3-1. For consistency, lower-case letters are for parameters and upper-case letters are for decisions variables.

**Table 3-1 Notation**

Sets	
$L$ :	Set of feedstock types, index $l$
$N_l^F$ :	Set of feedstock fields of feedstock type $l \in L$ , index $i_l$
$N^M$ :	Set of cities as demand centers, index $m$
$N^R$ :	Set of potential locations for biorefineries, index $j$
$S$ :	Set of refinery size, index $s$
$T$ :	Set of time phases, index $t$
Parameters	
$a_{i_l,t}$ :	Maximum available feedstock (dry ton) of type $l \in L$ at field $i_l \in N_l^F$ at time $t \in T$
$c^{bp}$ :	Unit biofuel production cost (\$/gallon) at refineries
$c_l^{fa}$ :	Average acquisition cost (\$/dry ton) of harvesting feedstock of type $l \in L$
$c^{dd,b}$ :	Distance-dependent transportation cost (\$/mile/truckload) of biofuel
$c^{dd,f}$ :	Distance-dependent transportation cost (\$/mile/truckload) of feedstock
$c^{lu,b}$ :	Truck loading and unloading cost of (\$/gallon) biofuels
$c^{lu,f}$ :	Truck loading and unloading cost (\$/wet ton) of feedstock
$c^{td,b}$ :	Travel-time dependent transportation cost (\$/hr/truckload) of biofuel
$c^{td,f}$ :	Travel-time dependent transportation cost (\$/hr/truckload) of feedstock



---

$d_{ij}$ :	Distance (miles) between nodes $i$ and $j$
$e_l^{bp}$ :	GHG emission rate (CO <sub>2</sub> -eq. ton/gallon) of biofuel production, $l \in L$
$e_l^{fa}$ :	GHG emission rate (CO <sub>2</sub> -eq. ton/dry ton) of feedstock acquisition, $l \in L$
$e^{Tr}$ :	GHG emission rate (CO <sub>2</sub> -eq. ton/mile/truckload) of transportation
$f_{js}^{Cap}$ :	Annualized capital cost (\$) of refinery at location $j \in N^R$ with size $s \in S$
$k_{m,t}$ :	Biofuel demand (gallons) at city $m \in N^M$ at time $t \in T$
$u_s^R$ :	Refinery annual production capacity (MGY) by size level $s \in S$
$u^{Tr,b}$ :	Truck transportation capacity (gallon/truckload) for biofuel
$u_l^{Tr,f}$ :	Truck transportation capacity (wet ton/truckload) for feedstock, $l \in L$
$v$ :	Average truck travel speed (mile/hr)
$\alpha$ :	Unit cost rate (\$/gallon) of imported corn grain based biofuel
$\beta$ :	GHG emission rate (CO <sub>2</sub> -eq. ton /gallon) of corn grain based biofuel
$\theta_l$ :	Moisture content (%) of feedstock type $l \in L$
$\eta_l$ :	Biofuel conversion rate (gallon/dry ton), $l \in L$

---

Decision Variables

---

$Q_{mt}$ :	amount(gallons) of imported corn grain based biofuel at city $m \in N^M$ at time $t \in T$
$X_{jmt}^b$ :	amount (gallons) of biofuel transported from refinery $j \in N^R$ to city $m \in N^M$ at time $t \in T$
$X_{i_j,t}^f$ :	amount (dry tons) of feedstock of type $l \in L$ transported from field $i_l \in N_l^F$ to refinery $j \in N^R$ at time $t \in T$
$Z_{jst}$ :	=1 if refinery with size $s$ is built at $j \in N^R$ at time $t \in T$ ; =0 otherwise

---

*Objective #1 – Minimization of system cost over planning horizon:*

The biofuel supply chain design consists of decisions, such as feedstock acquisition, biofuel production, and transportation, and they are interdependent. A systems approach is thus utilized to achieve overall lowest system cost over time. The corn grain based biofuel supplements the cellulosic biofuel when it is more economical. The least-cost objective ( $F_1$ ) is formulated in equation (3-1).

$$\text{Minimize } F_1 = \sum_{t \in T} \left\{ \sum_{j \in N^R} \sum_{s \in S} f_{js}^{Cap} Z_{jst} + \sum_{l \in L} \sum_{i_l \in N_l^f} \sum_{j \in N^R} c_l^{fa} X_{ij,t}^f + \sum_{j \in N^R} \sum_{m \in N^M} c^{bp} X_{jm,t}^b + C_t^{FSDel} + C_t^{BFDel} + \sum_{m \in N^M} \alpha Q_{mt} \right\} \quad (3-1)$$

$$\text{where } C_t^{FSDel} = \sum_{l \in L} \sum_{i_l \in N_l^f} \sum_{j \in N^R} \left( \frac{\left( c^{dd,f} + \frac{c^{td,f}}{v} \right) \times d_{ij} \times 2}{u_l^{Tr,f}} + c^{lu,f} \right) \times \frac{X_{ij,t}^f}{(1-\theta_l)} \quad (3-1.a)$$

$$C_t^{BFDel} = \sum_{j \in N^R} \sum_{m \in N^M} \left( \frac{\left( c^{dd,b} + \frac{c^{td,b}}{v} \right) \times d_{jm} \times 2}{u^{Tr,b}} + c^{lu,b} \right) \times X_{jm,t}^b \quad (3-1.b)$$

The cost function (3-1) minimize the total cost of cellulosic biofuel supply chain and the use of corn grain based biofuel ( $\alpha$ ). The cellulosic biofuel supply chain cost includes capital costs associated with the refinery ( $f_{js}^{Cap}$ ), feedstock acquisition cost ( $c_l^{fa}$ ), biofuel production cost ( $c^{bp}$ ), and feedstock and biofuel distribution costs ( $C_t^{FSDel}$  and  $C_t^{BFDel}$ ) respectively formulated in (3-1.a) and (3-1.b). Both distribution costs are composed of distance- and time-dependent costs plus loading/unloading cost and are divided by truck capacity to convert the delivery quantity to number of truckloads. For feedstock transportation, the dry ton measure is converted to wet tons by moisture content (the ratio of water contained in the feedstock, denoted by  $\theta_l$ ), on which the truck capacity of bulk solids is based. Transportation distance is multiplied by two to represent a round trip.

*Objective #2 – Minimization of System GHG Emissions over Planning Horizon:*

The least-GHG emission objective ( $F_2$ ) is formulated in equation (3-2). In particular, the emission rates, measured by the environmental performance indicator CO<sub>2</sub>-eq per mass or liquid unit, are quantified using the GREET model. The three species of GHGs (i.e., CO<sub>2</sub>, CH<sub>4</sub>, and SO<sub>2</sub>) associated with feedstock acquisition, biofuel production, and transportation are considered and their emission rates are respectively denoted by  $e_i^{fa}$ ,  $e^{bp}$  and  $e^{Tr}$  in the model. The emission rate associated with corn grain based biofuel is denoted by  $\beta$ .

Minimize

$$F_2 = \sum_{t \in T} \left\{ \sum_{l \in L} \sum_{i_l \in N_l^f} \sum_{j \in N^R} e_i^{fa} X_{ij,t}^f + \sum_{j \in N^R} \sum_{m \in N^M} e^{bp} X_{jm,t}^b + E_t^{FSDel} + E_t^{BFDel} + \sum_{m \in N^M} \beta Q_{mt} \right\} \quad (3-2)$$

where

$$E_t^{FSDel} = \sum_{l \in L} \sum_{i_l \in N_l^f} \sum_{j \in N^R} \frac{e^{Tr} \times X_{ij,t}^f \times d_{ij} \times 2}{(1 - \theta_l) \times u_l^{Tr,f}} \quad (3-2.a)$$

$$E_t^{BFDel} = \sum_{j \in N^R} \sum_{m \in N^M} \frac{e^{Tr} \times X_{jm,t}^b \times d_{jm} \times 2}{u^{Tr,b}} \quad (3-2.b)$$

Similar to equation (3-1), the emission objective (3-2) minimizes the total GHG emissions along the supply chain of biofuels. The transportation emissions consist of two parts:  $E_t^{FSDel}$  being the emissions from feedstock deliveries and  $E_t^{BFDel}$  being the emissions from biofuel distributions.

*The Objective of Compromise Model:*

The two objectives are integrated into a multi-objective modeling framework by using the compromise method and the objective  $F$  is formulated in equation (3-3). This model aims to find *best-compromise* solutions between economic competitiveness and environmental quality while satisfying the growing biofuel demands, feedstock availability, and technological constraints.

$$\text{Minimize } F = (1 - \lambda)D + \lambda \sum_{i=1}^2 w_i \frac{F_i - F_i^o}{F_i^{ao} - F_i^o} \quad (3-3)$$

$$\text{Subject to } w_i \frac{F_i - F_i^o}{F_i^{ao} - F_i^o} \leq D, \quad i = 1, 2. \quad (3-4)$$

In objective function (3-3),  $F_i^o$  denotes by the optimal result of the  $i^{\text{th}}$  objective (first or second objective in this study) and  $F_i^{ao}$  denotes by the anti-optimal result. In this particular study,  $F_1^o$  denotes the optimal value of objective  $F_1$ ; i.e., the least system cost. The anti-optimal result  $F_1^{ao}$  is obtained in the following way. Decision variables corresponding to  $F_2^o$  (i.e., the lowest emissions) are substituted in objective  $F_1$  and the attained result is called the anti-optimal result,  $F_1^{ao}$ , of objective  $F_1$ . Thus,  $F_1^{ao}$  is greater than or equal to  $F_1^o$ . Note that the denominator  $F_i^{ao} - F_i^o$  is used to normalize the two objectives, which enables the aggregation of objectives with different units (i.e.,

monetary cost for  $F_1$  and emission measurements for  $F_2$ ). The variable,  $D$ , is defined in inequality (3-4).

The preferential weight,  $w_i$ , is valued between 0 and 1, reflecting the relative importance of each objective. A common approach to determine the preferential weights is to use the Analytic Hierarchy Process (AHP) method (Saaty, 1980). In this study, the values will be adopted from existing literatures. The other weighting factor,  $\lambda$ , which is called the aggregation factor, is also valued between 0 and 1. When  $\lambda$  equals 1, the compromise model objective (3-3) becomes:

$$\text{Minimize } F = \sum_{i=1}^2 w_i \frac{F_i - F_i^o}{F_i^{ao} - F_i^o}, \quad (3-5)$$

which is essentially a weighted sum of both objectives and this solution is called *maximum efficiency solution*. On the other hand, when  $\lambda$  equals 0, the objective (3-3) becomes  $f = D$ , subject to constraint (3-4), which is equivalent to

$$\text{Minimize } F = \max \left[ w_1 \frac{F_1 - F_1^o}{F_1^{ao} - F_1^o}, w_2 \frac{F_2 - F_2^o}{F_2^{ao} - F_2^o} \right]. \quad (3-6)$$

This program seeks a perfectly balanced situation between the achievements of both objectives and according to (Tamiz et al., 1998), and it implies that the following equality holds:

$$w_1 \frac{F_1 - F_1^o}{F_1^{ao} - F_1^o} = w_2 \frac{F_2 - F_2^o}{F_2^{ao} - F_2^o}. \quad (3-7)$$

The resulting optimum is called the *maximum equity or equilibrium*. Other values of  $\lambda$  represent intermediate conditions between these two extreme cases. Interested readers are referred to (Linares and Romero, 2000) for details. In this study, both weighting factors  $w$  and  $\lambda$  will be used at the same time.

*Constraint Sets:*

The constraints on feedstock yields, demand, and conversion technological restrictions will be presented as follows.

$$\sum_{l \in L} \sum_{i_j \in N_l^f} \eta_l X_{i_j,t}^f = \sum_{m \in N^M} X_{j,m,t}^b \quad \forall j \in N^R, t \in T \quad (3-8)$$

$$\sum_{s \in S} Z_{jst} \leq 1 \quad \forall j \in N^R, t \in T \quad (3-9)$$

$$\sum_{s \in S} u_s^R Z_{jst} \leq \sum_{s \in S} u_s^R Z_{j,s,t+1} \quad \forall j \in N^R, t \in 1..T-1 \quad (3-10)$$

$$\sum_{m \in N^M} X_{j,m,t}^b \leq \sum_{s \in S} u_s^R Z_{jst} \quad \forall j \in N^R, t \in T \quad (3-11)$$

Equation (3-8) is a flow conservation constraint at refineries, which states that the amount of biofuel produced (right-hand-side of the equation) equals the amount of

converted biomass (left-hand-side of the equation) by relating them to conversion rates. Constraint (3-9) is logic constraint for each time period, stating that a refinery can only have one capacity size if the refinery is operating. Inequality (3-10) allows for refinery capacity expanded discretely and assumes the refinery will never shut down once opened. Constraint (3-11) limits the production amount within the chosen refinery capacity.

$$\sum_{j \in N^R} X_{ij,t}^f \leq a_{i,t} \quad \forall i_l \in N_l^F, l \in L, t \in T \quad (3-12)$$

Feedstock acquisition is limited by its availability in constraint (3-12), and all obtained feedstocks will be delivered to refineries for biofuel production.

$$\sum_{j \in N^R} X_{jm,t}^b + Q_{mt} = k_{mt} \quad \forall m \in N^M, t \in T \quad (3-13)$$

Equation (3-13) allows biofuel city demand to be satisfied by both the cellulosic biofuel and corn-grain based biofuel.

### **3.3 Case Study**

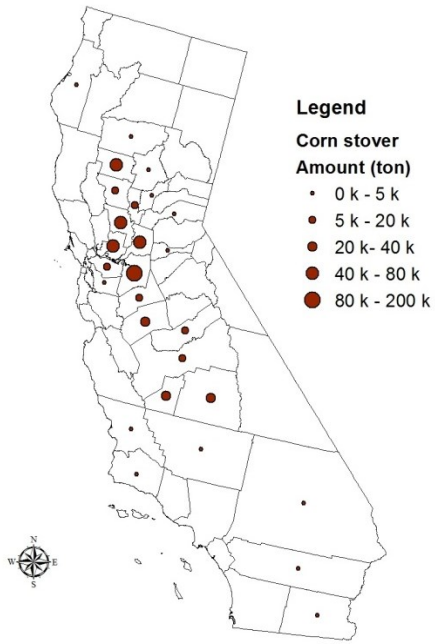
The compromise model has been applied to an illustrative case study of developing cellulosic biofuel supply chain with supplement of corn ethanol in California. California serves as a good case study for two primary reasons. First, the government of California has been aggressively promoting de-carbonating the transportation sector through several

legislations, e.g., AB32 (Global Warming Solution Act), AB1493 and Low Carbon Fuel Standards (California Energy Commission, 2013). In particular, California's Bioenergy Action Plan targets the in-state ethanol production at 40% of the total state's biofuel consumption by 2020 and 75% by 2050, which are equivalent to 350 and 590 Million Gallons per Year (MGY), respectively (Jenkins et al., 2007). Second, with advanced biofuel conversion technologies that use lignocellulosic biomass are anticipated to be ready for commercialization by 2025 (Parker et al., 2007) and given that there are abundant biomass residues from the San Joaquin Valley, i.e., corn stover, and the surrounding Sierra forest, i.e., forest residues, California is in a good position to utilize its resources and promote the cellulosic biofuel industry.

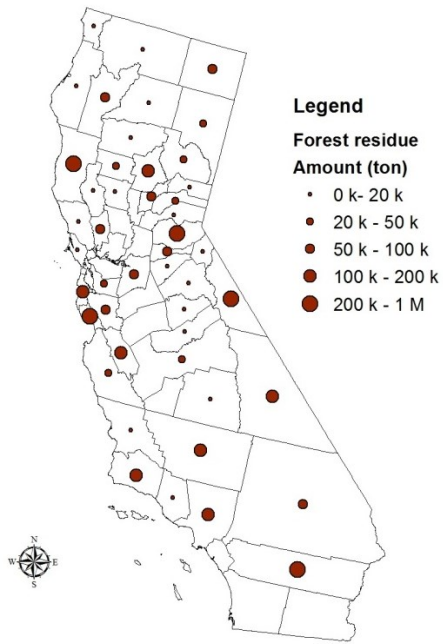
The planning horizon is set between 2015 and 2025, which is consistent with the time frame when the adopted biomass-to-ethanol conversion technology is anticipated to be commercialized. In this case study, biofuel only refers to ethanol and the total demand is projected, based on interpolation and extrapolation, to grow linearly from 272 million gallons per year (MGY) in 2015 to 390 MGY in 2025 (Jenkins et al., 2007). For cellulosic ethanol supply chain, there are 28 candidate refinery locations across the state. A set of 143 cities are considered as demand centers, which are mainly clustered in the populated areas, such as the San Francisco Bay area and the Los Angeles area. The refinery has three capacity levels to choose from at 60, 80 and 100 MGY. The geographic distributions of demand and biomass resources are presented in Figure 3-1. The details on other economic and technological data used for this study are referred to (Xie et al., 2014). For corn ethanol, the average terminal market price of \$2.6/gallon in the Los



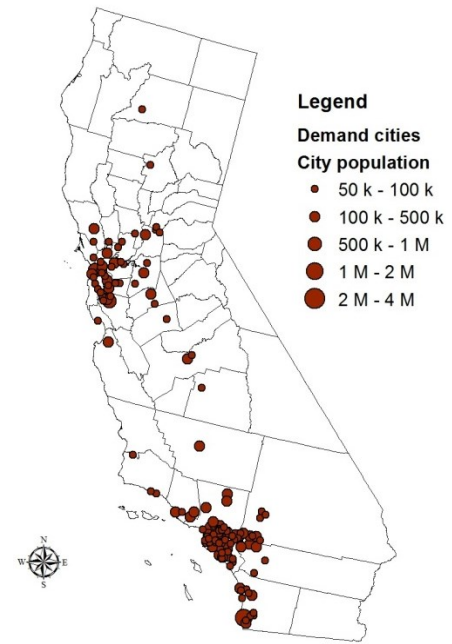
Angeles area and the San Francisco area is used in the baseline case study (California Energy Commission, 2014). According to the historical data, the price can be fluctuating, and thus the impact of a range of corn ethanol prices has been analyzed and results will be reported in subsection 3.2.



(a) Corn stover locations



(b) Forest residues locations



(c) demand centers (city gates)

**Figure 3-1 Maps of Feedstock Supply and Ethanol Demand**

As aforementioned, this study limits the GHG emissions to three species - CO<sub>2</sub>, CH<sub>4</sub>, and NO<sub>2</sub>. The emission rates associated with the cellulosic ethanol production pathway (including the feedstock acquisition and transportation, ethanol production, and transportation within California) are presented in Table 3-2. Each of 2<sup>nd</sup>-to-4<sup>th</sup> columns of the table contains the emission rates of a particular GHG specie, which was quantified using the GREET model and the last column contains the aggregated CO<sub>2</sub>-eq, based on the 100-year GWP (BSI Group, 2011; Forster et al., 2007). The emissions from acquiring forest residues are higher than the corn stover, because more diesel fuels are consumed during stumpage and harvesting (Wu et al., 2006). The emissions from ethanol production is low, since large amount of CO<sub>2</sub> emitted from converting biomass to biofuels offsets the absorbed CO<sub>2</sub> in the biomass growing phase (Raphael et al., 2009; Wang et al., 2005). The emission rate of corn ethanol is equivalent to 0.0085 CO<sub>2</sub>-eq. ton/gallon (converted from 95.66 CO<sub>2</sub>-eq. grams/MJ), which is equivalent to the weighted average emission rate of corn ethanol in California (i.e., 80% is from the Midwest ethanol and 20% is from the California dry mill Wet distillers grains and solubles) (ARB, 2009).

**Table 3-2 GHG Emission Data**

Emission rates		CO <sub>2</sub>	CH <sub>4</sub>	N <sub>2</sub> O	CO <sub>2</sub> -eq
Global warming potentials (GWP)		1	25	298	
Acquisition $e_i^{fa}$ (gram/dry ton)	Corn stover	22,037	25.4	0.27	22,753
	Forest residues	56,184	65.13	0.7	58,020
Production $e_i^{bp}$ <sup>1</sup> (gram/gallon)	Corn stover	7	0.26	0.69	219
	Forest residues	200	0.86	0.63	410
Transportation $e^{Tr}$ (gram/mile/truckload)		2,426	2.8	0.06	2,512

1. Excludes byproduct of electricity

### **3,4 Results and Discussion**

All models were implemented in AMPL (Fourer et al., 2003) and solved using the commercial CPLEX 12.6 solver. All numerical experiments run on a Dell desktop with 8 GB RAM and Intel Core Quad 3.0 GHz processor under Windows 7 environment. This large-scale mixed-integer problem has 924 binary variables, 69,531 continuous variables, and 3,899 linear constraints and the average computational time is 1,200 CPU seconds.

#### **3.4.1 Case Study Results**

In this section, we present results from the case study described above. A pay-off matrix of costs and emissions is obtained by optimizing each objective (i.e.,  $F_1$  and  $F_2$ ) separately over the constraint set. The least-system cost ( $f_1^0 F_1^o$ ) is \$8.3billion, which is the total cost over entire expansion. The corresponding system-wide emission is 7.6 million CO<sub>2</sub>-eq tons. On the other hand, if minimization of GHG emissions is the goal, emission is reduced to 6.8 million CO<sub>2</sub>-eq ton, a 10% reduction, while the system cost is substantially increased by 54% to \$12.8 billion. Analysis of the pay-off matrix indicates that there is a remarkable degree of conflict between the two objectives; and no solution generated by a single objective optimization seems applicable for the problem. These results justify the need of the compromise model.

In the compromise model, the two objectives are aggregated through the mechanisms of preferential weight  $w$  and aggregation factor  $\lambda$ . The preferential weights

are set at  $w_1$  (cost) =0.625 and  $w_2$  (GHG) =0.375 , which are adopted from (Unsihuay-Vila et al., 2011). The choice of aggregation factor  $\lambda$  reflects the preference between system efficiency and equity. *When  $\lambda=1$* , the model objective stated in equation (3-5) aims to achieve the maximum efficiency for both cost and emissions, given the preferential weights  $w$ , the resulting optimal system cost is \$8.5 billion and the GHG emission is 7.0 million CO<sub>2</sub>-eq tons, which respectively presents a 7.9% reduction in GHG emission and a 2.4% increase in cost, relative to the single cost objective model results of 7.6 million CO<sub>2</sub>-eq tons and \$8.3billion. *When  $\lambda=0$* , the model as stated in equations (3-6) and (3-7) aims to perfectly balance the achievements between the two objectives, which further reduces GHG emission to 6.9 million CO<sub>2</sub>-eq tons, or a 9.2% reduction, compromised with a higher system cost at \$8.8 billion, a 6% increment, compared to the single cost objective model results. In the remainder of the section, only the single cost objective solution and the compromise model solution with  $\lambda=1$  and 0 will be reported. A wide range of combinations of preferential and aggregation weights have also been implemented and the results will be reported in subsection of sensitivity analyses.

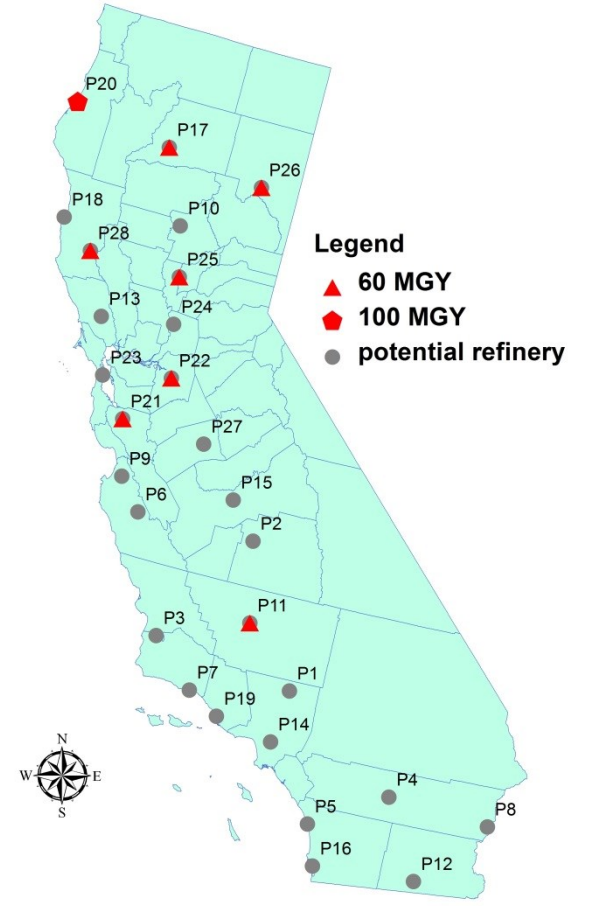
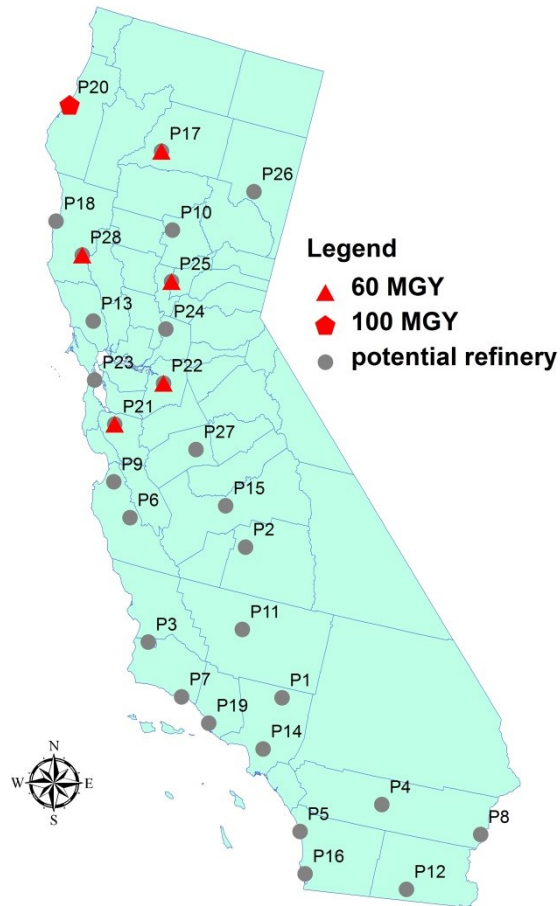
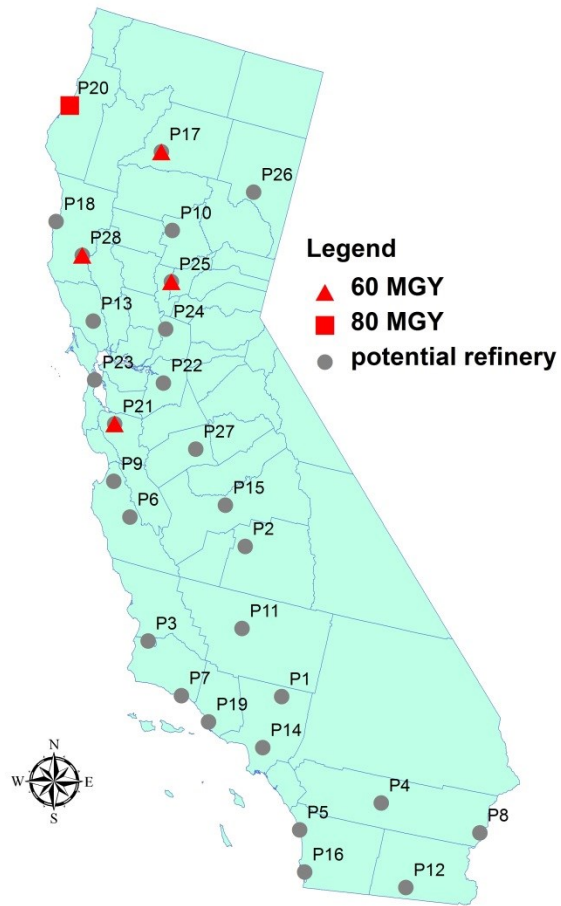
### *System Expansion Strategies*

Table 3-3 shows the refinery system expansion strategies following different modeling objectives, i.e., the single cost objective and the compromise model with  $\lambda=1$  and 0. The results indicate that by the end of planning horizon of 2025 the single-cost objective model yields more *centralized* location pattern (i.e., five refineries) than the results of

compromise model (i.e., eight refineries). This location pattern takes advantage of economics of scales of capital intense refineries, which is consistent with the objective to minimize the total cost while resulting in overall longer delivery distances and higher associated cost. Thus, when emission as another objective is considered in the compromise model ( $\lambda=1$ ), the solution suggests a more dispersed refinery location pattern to help reduce the travel distance and consequently the emissions from transportation, which however requests more refineries than needed, with the total capacity up to 520 MGY by 2025. This redundancy in total refinery capacity is mainly due to the discrete capacity levels (i.e., 60, 80, and 100 MGY) and less capacity redundancy would be expected if capacity variable is continuous. When comparing the two compromise solutions  $\lambda=0$  and  $\lambda=1$ , both solutions share the same location pattern by 2025. However, the scheduling of building new refineries and capacity expansions varies between the two solutions. The  $\lambda=0$  solution tends to have more distributed refinery locations than the  $\lambda=1$  solution at the earlier stages, which helps further reduce emissions, thanks to the higher weight on emission in the objective.

**Table 3-3 Refinery Capacity Expansion (MGY) by Locations over Years (2015~2025)**

Models	locations	2015	2016	2017	2018	2019	2020	2021	2022	2023	2024	2025
Cost objective	#17	60	60	60	60	60	60	80	80	80	80	80
	#20	80	80	80	80	100	100	100	100	100	100	100
	#21	60	60	60	60	60	60	60	60	60	60	60
	#25			60	60	60	60	60	60	80	80	80
	#28	60	60	60	60	60	60	60	60	60	60	60
$\lambda=1$	#11											60
	#17	60	60	60	60	60	60	60	60	60	60	60
	#20	80	100	100	100	100	100	100	100	100	100	100
	#21	60	60	60	60	60	60	60	60	60	60	60
	#22				60	60	60	60	60	60	60	60
	#25	60	60	60	60	60	60	60	60	60	60	60
	#26							60	60	60	60	60
#28	60	60	60	60	60	60	60	60	60	60	60	
$\lambda=0$	#11			60	60	60	60	60	60	60	60	60
	#17	60	60	60	60	60	60	60	60	60	60	60
	#20	80	100	100	100	100	100	100	100	100	100	100
	#21	60	60	60	60	60	60	60	60	60	60	60
	#22	60	60	60	60	60	60	60	60	60	60	60
	#25	60	60	60	60	60	60	60	60	60	60	60
	#26							60	60	60	60	60
	#28	60	60	60	60	60	60	60	60	60	60	60



(a) Year 2015

(b) Year 2020

(c) Year 2025

**Figure 3-2 Example of System Expansion Strategies (Best-Compromised Design with  $\lambda=1$ )**



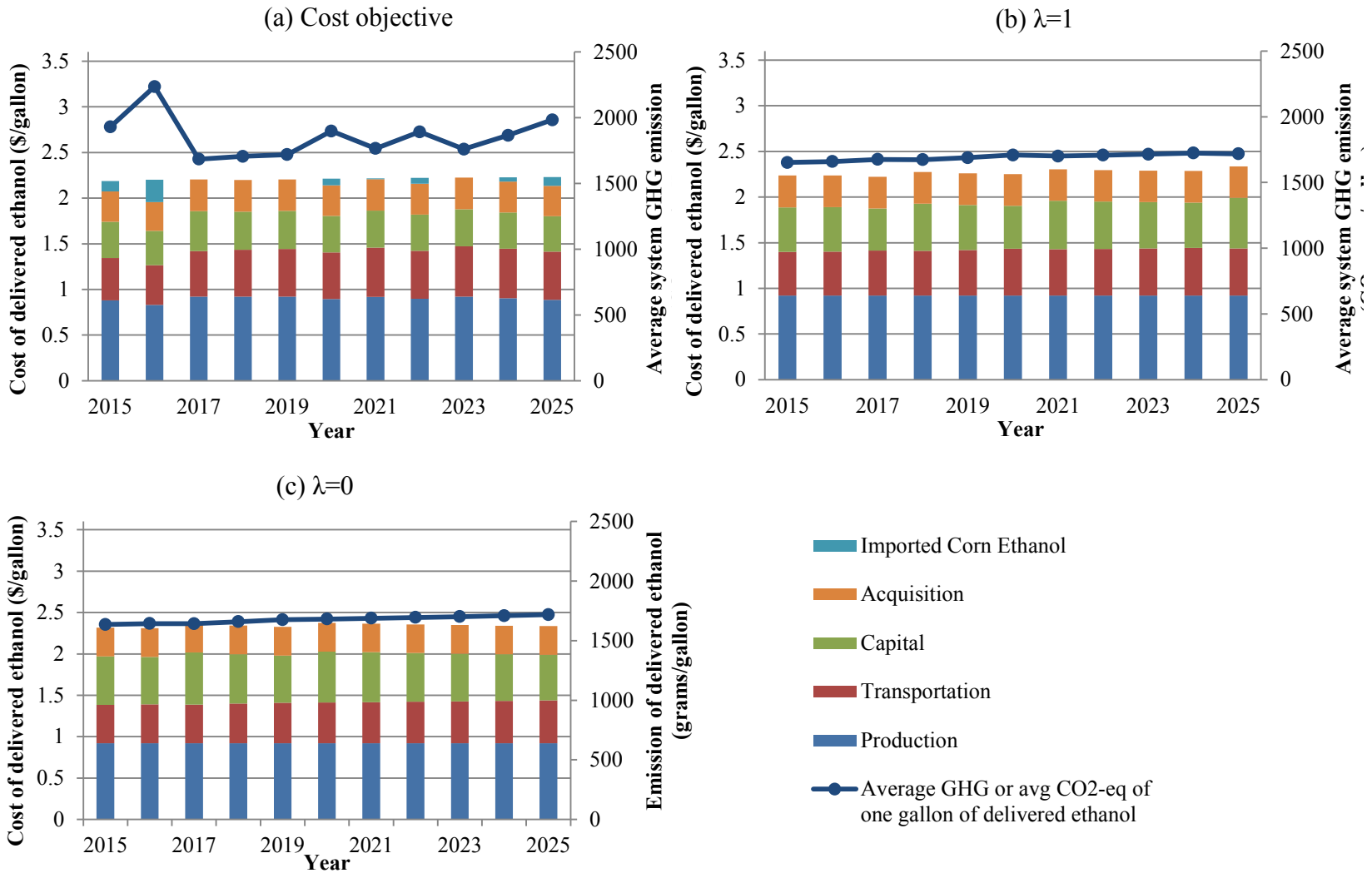


Figure 3-3 Annual Delivered Average Cost and Total GHG Emission in Each Gallon of Ethanol

For illustration purpose, the geographic representation of refinery system expansion is depicted in Figure 3-2(a)-(c) for the compromise solution  $\lambda=1$ . The figures only represent the snapshots of the biofuel supply chain systems in 2015, 2020 and 2025. The system begins with four small-sized (i.e., 60 MGY) refineries at #17, #21, #25 and #28, and one middle-sized (i.e., 80 MGY) refinery at #20 in 2015 and expansions including both opening new refineries and enlarging existing refineries will be undertaken. By 2020, refinery at location #20 will be expanded to 100 MGY from 80 MGY in 2015 and a new small-sized refinery will be built at the location #22 while other refineries remain unchanged. By end of the planning horizon of 2025, another two small-sized refineries will be added to the system at locations #11 and #26. Note that most of the refineries are located in northern part of the state to take the advantage of the proximity to biomass sources and one of the major consumer market in the San Francisco Bay Area.

#### *System Cost and Emission Outcomes*

The total system cost can be broken down to five components: feedstock acquisition cost, refinery capital cost, production cost, and transportation cost of cellulosic ethanol and corn ethanol cost. Transportation cost includes both the delivery costs of feedstock from fields to refineries and fuel from refineries to terminals.

Cost breakdowns and emissions in terms of one gallon of delivered ethanol over time are represented by stacked bars and curves in Figure 3-3(a)-(c) respectively. The average delivered fuel cost is a weighted average delivered cost of both cellulosic and

corn ethanol, which fluctuates in a relatively small range between \$2.2 and 2.4 per gallon. The average emission fluctuates between 1.5 and 2.2 CO<sub>2</sub>-eq kg/gallon, depending on the selected weights between the two objectives. In particular, the single cost objective solution produces higher emissions than the compromise model solutions and the emissions peak when the corn ethanol is used (see Figure 3-3 (a)). This is because corn ethanol has higher GHG emission than the cellulosic ethanol on gallon basis. The compromise models have factored the emission in the objective and thus the emission curve is relatively flat and no corn ethanol is used at all. It is also identified that transportation accounts for substantial portions of both cost (21% ~ 23%) and emission (26% ~ 28%), which justifies the use of the systems approach. From emission perspective, unlike fuel production and feedstock acquisition, for which emission reduction is highly constrained by demand and capital-intensive technology advancement, transportation GHG reduction can be achieved through smart system planning.

#### *Feedstock Portfolio and Use of Corn Ethanol*

Groups of three stacked bars in Figure 3-4 show the annual feedstock acquisition strategies and use of corn ethanol. Since corn stover and forest residues have different biomass-to-ethanol conversion rates, to be consistent, all feedstock acquisition amounts were converted to equivalent ethanol production amounts. For instance, following the solution of the single cost objective solution, within a total demand of 272MGY in 2015, 220MGY are produced from forest residue, 40MGY are produced from corn stover, and

remaining is supplemented from the corn ethanol. As the refinery system is expanded discretely, corn ethanol is used strategically to justify the economic competitiveness between the capacity gaps. In particular, the use of corn ethanol peaks at 9.6% of the total demand in 2016 and the annual average is about 2.2%.

The optimized feedstock portfolio is a result of tradeoffs among multiple factors - conversion rate, acquisition cost rate, emission, moisture content, truck capacity, and feedstock geographic locations to refineries. Rationally, feedstock resources with higher conversion rate but lower acquisition cost are likely to be picked over the others, which is why forest residue dominates the feedstock supply. Corn stover is used mainly due to its proximity to refineries. When the goal of reducing GHG emission is factored in, the use of corn stover increases slightly about 5% for its overall lower life-cycle emissions than forest residues.

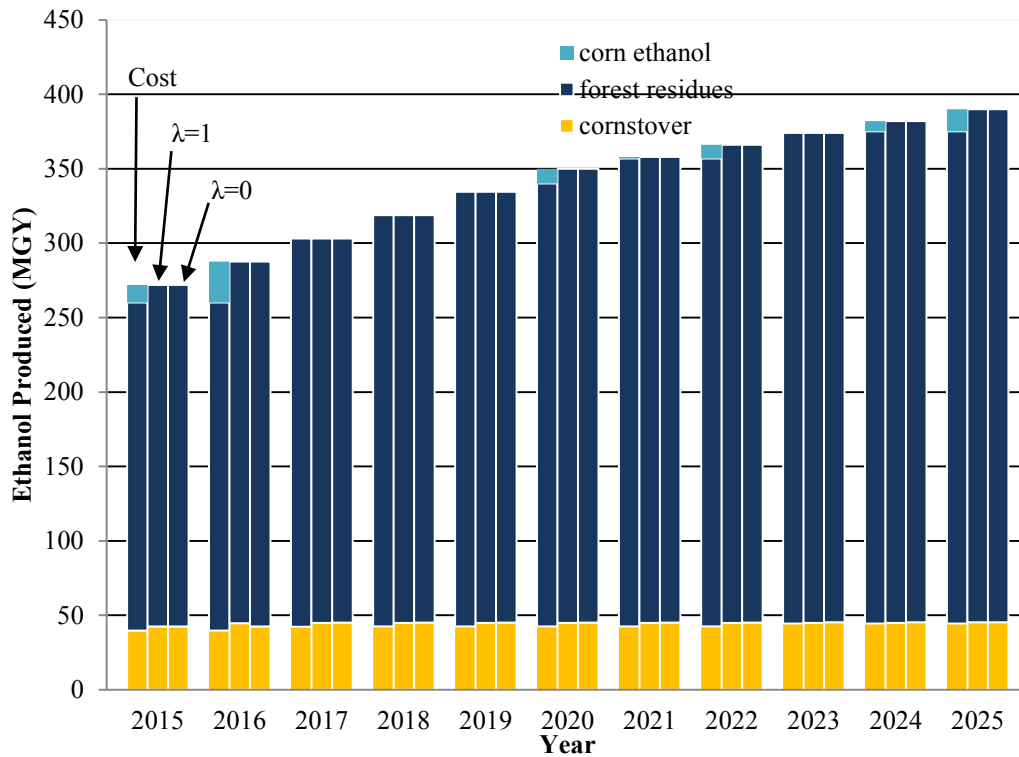


**Figure 3-4 Optimal Feedstock Procurement Portfolio and Use of Corn Ethanol**

### 3.4.2 Sensitivity Analysis

#### *Relationship between Cost and GHG Emission*

A series of numerical experiments were conducted to understand the tradeoffs between cost and GHG emission. We describe a wide range of best-compromise solutions by varying both preferential weight  $w$  ( $w_1 + w_2 = 1$ ) and aggregation factor  $\lambda$  in the compromise model between 0 and 1 with an increment of 0.2. The resulting 36 Pareto-optimal results form a pareto front as shown in Figure 3-5, which indicates a clear trade-off between cost and GHG emissions. By using the compromise method, significant GHG emission reduction is achieved with a small increase of system cost. However, after certain point (e.g., 7.1 million CO<sub>2</sub>-eq tons), pursuing further emission reduction is cost

ineffective. This quantitative trade-off between costs and emissions could be insightful for energy and environment relevant public policies such as carbon-trade, although the analytical results may vary with case studies.

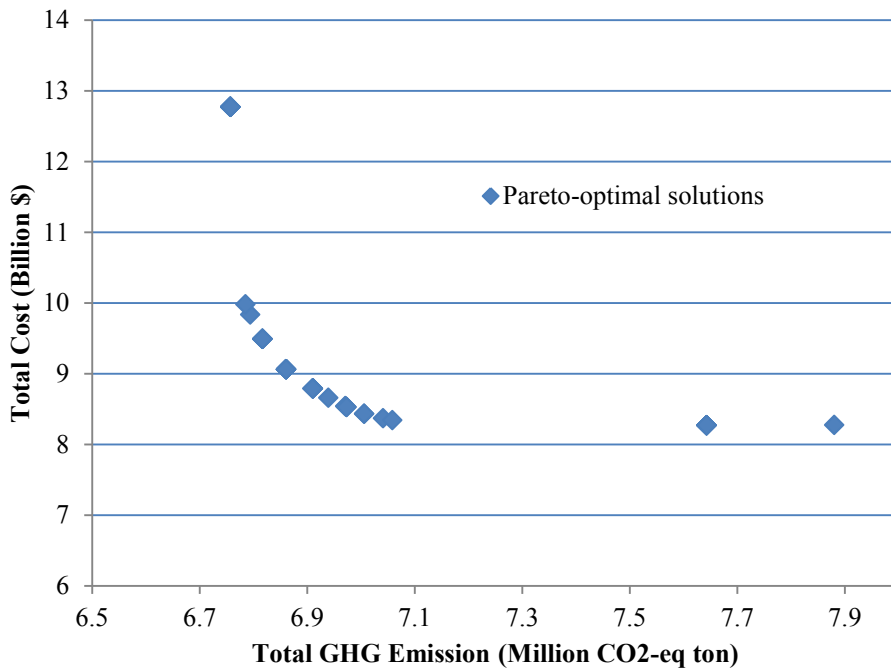


**Figure 3-5 Relationship between Cost and GHG**

*The Impact of Corn Ethanol Price on System*

In the baseline, the average corn ethanol terminal market price of \$2.6/gallon was used. A set of sensitivity analysis of a price between \$1 and \$5 per gallon was conducted and results are plotted in Figure 3-6. When it is down to \$1/gallon, no cellulosic ethanol is produced following the least-system cost solution. However, in the compromise solutions, due to the emission objective factored in, there is still substantial amount of cellulosic ethanol used between 10% and 40% of total demand for the sake of lower emissions,

depending on the objective. With a higher market price of corn ethanol, its usage decreases and no corn ethanol is consumed after the \$3/gallon.

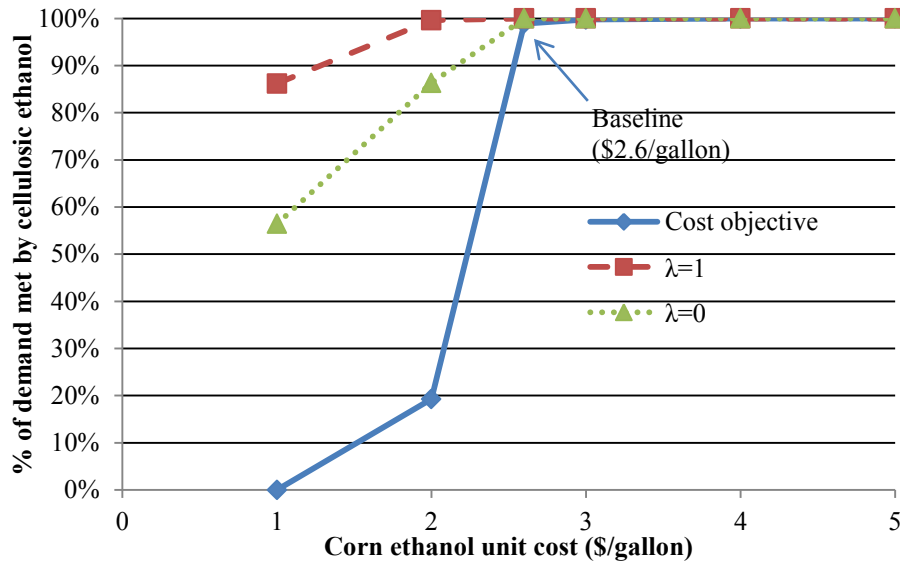


**Figure 3-6 Impact of Corn Ethanol Cost on Cellulosic Ethanol Production**

### 3.5 Summary

In Chapter 3, I developed a new multi-objective, multistage optimization framework for a multiyear planning of supply chain of cellulosic biofuels with supplements of corn grain based biofuels in seeking the best compromise solutions between the economic effectiveness and environmental quality. The model was implemented in an illustrative case study of instate ethanol supply in California. The results show the potentials of cellulosic ethanol as an economically and environmentally sustainable transport fuel alternative to corn ethanol with overall low delivered cost and emission. By using the developed compromise model, significant GHG emissions can be reduced at incremental cost.

# CHAPTER 4 INTEGRATING MULTIMODAL TRANSPORT INTO CELLULOSIC BIOFUEL SUPPLY CHAIN DESIGN UNDER FEEDSTOCK SEASONALITY

## ***4.1 Problem Statement***

In most literature of cellulosic biofuel supply chain design, the importance of transport mode choice has been often overlooked and truck is presumably the only transport mode, despite the fact that geographic dispersion of demand and supply for biofuels makes the use of multimodal transportation very attractive (EERE, 2011). A recent study indicates that the choice of transportation mode, and consequently transportation distances, greatly impact the economic competitiveness of biofuels (Wakeley et al., 2009). Trucks, though flexible, may not always be cost effective, as they may be subject to potential issues such as worsened traffic congestion on highways (USDA, 2007). From modeling perspective, the transport mode choice depends on its availability and is highly correlated to the supply chain configuration. For example, a centralized biorefinery supply chain may benefit more in using a combined rail and truck transport system than a decentralized biorefinery supply chain. Hence, *multimodal transport*, defined as a utilization of at least two transport modes (e.g. truck and rail), will help improve the commercial viability of cellulosic biofuels and should be integrated into the biofuel supply chain design.

In this study, a cost-effective and efficient multimodal transport is proposed for moving *bulk biomass feedstock* and *liquid biofuels* in the cellulosic biofuel supply chain. An integrated multistage, mixed-integer programming model is developed that integrates



the multimodal transport into the design of an entire cellulosic biofuel supply chain in hedging against feedstock seasonality. The goal of the proposed model is to minimize the total annualized system cost including the infrastructure capitals, feedstock harvesting, biofuel production, and transportation across the entire supply chain over a year. Key features that distinguish this study from previous studies and enrich the literature of multimodal transport in biofuel supply chain are at tri-fold from modeling perspective: (1) *feedstock seasonality* is factored into the cellulosic biofuel supply chain through the multistage modeling framework; (2) multimodal transport is integrated throughout a *complete* feedstock-to-end users supply chain design; and (3) explicit transport cost estimate is included and considers fixed cost, travel distance and time dependent costs for three transport modes (i.e., truck, single railcar, and unit train). The optimization model relies on realistic assumptions about the decision variables, the contribution of each decision variable to the objective, the relationship between decision variables, and the constraints. In particular, the multimodal transport system will be used to support the feedstock/biofuel flows in the supply chain to mitigate the effects of feedstock seasonality. These tools are expected to identify transportation system models that overcome additional key market and technical barriers for the cellulosic biofuel distribution system. These barriers, identified in (EERE, 2011), entail no mature distribution infrastructure system for transporting large volumes of biofuel and high delivery cost, due to the incompatibility with the petroleum fuel infrastructure. The proposed model will be evaluated using an illustrative case study of designing a

multimodal cellulosic ethanol supply chain in California and demonstrate the applicability of the model for potential economic improvement.

The remainder of this Chapter is organized as follows. The methods and case study of California will be presented in Section 4.2 and Section 4.3 respectively. The results and discussion will be presented in Section 4.4. I will summarize the study in Section 3.5.

## **4.2 Methods**

### **4.2.1 Description of the Cellulosic Biofuel Supply Chain**

A multimodal based cellulosic biofuel supply chain for multi-period is displayed in Figure 4-1. Three types of transport modes: *truck*, *single railcar*, and *unit train*, are considered and they are differentiated by costs and delivery scheduling. In particular, truck with the most expensive and flexible in delivery scheduling, is usually used for short-haul delivery, while rail (including single railcar and unit train) is normally more efficient for long-haul and high volume transport thanks to the better economies of scale (Mahmudi and Flynn, 2006). A unit train composed of a large number of single railcars (an average of 100) enjoys further improved cost efficiency compared to single rail cars. However, it cannot be scheduled between an origin and a destination until there is substantial volume to ship (e.g., 30 trains per year) and the facilities also have to have compatible equipment to load/unload the unit train (Parker et al., 2008; USDA, 2007).

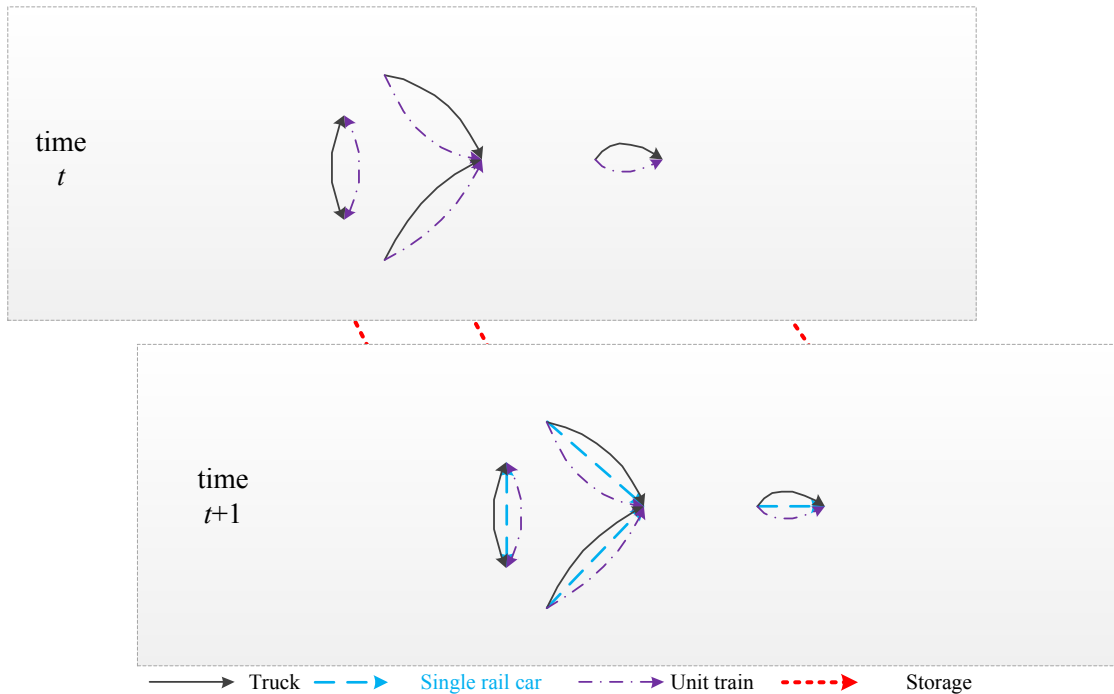


**Figure 4-1 Multistage Multimodal Cellulosic Biofuel Supply Chain Network**

Besides economic incentives, multimodal transport offers greater flexibility in handling feedstock seasonality, coupled with feedstock storage at transshipment hubs in the supply chain. According to (Rentizelas et al., 2009), there are three feedstock storage arrangements - on-field storage, intermediate storage, and storage near refineries. The on-field storage is not considered in this study because of its significant material loss and difficulty in controlling the moisture content over time while the storage near refineries usually only has two-month worth of inventory. The intermediate storage, standing-alone facility neither on nor near feedstock fields and refineries, can accommodate extended storage, thus is considered in the study and placed at transshipment hubs in Figure 4-1 Multistage Multimodal Cellulosic Biofuel Supply Chain Network. They are equipped with necessary facilities for handling multiple types of biomasses and accessible by all

three transport modes. Although a multimodal transport may appear redundant, it helps the supply chain ease the fuel production fluctuations caused by the feedstock seasonality. Different transport modes are employed in a coordinated manner, the greater details will be discussed in the results and discussion section.

A transportation network can be represented by a directed network flow graph  $G(N, A)$ , where  $N$  is the set of nodes on the network and  $A$  is the set of arcs connecting nodes. The biofuel supply chain consists of five infrastructure layers, including feedstock fields  $N_l^F$  ( $l \in L$ , set of feedstock types), transshipment hubs  $N^H$ , refineries  $N^R$ , blending terminals  $N^{BT}$ , and cities  $N^C$ . Thus, the node set  $N$  is a union of all types of facilities in the supply chain, i.e.,  $N = \left( \bigcup_{l \in L} N_l^F \right) \cup N^H \cup N^R \cup N^{BT} \cup N^C$ . Let  $A_m^f$  ( $m \in M$  set of transport modes) be the set of arcs used for transporting feedstocks between feedstock fields, hubs, and refineries, and  $A_m^b$  be the set of arcs used for transporting biofuels. Thus, the supply chain arc set is  $A = \bigcup_{m \in M} \left( A_m^b \cup \left( \bigcup_{l \in L} A_{lm}^f \right) \right)$ .

#### 4.2.2 Transport Cost Models

Due to the complex *transportation cost* structure, an in-depth discussion on the transportation costs will be provided. *For better discernibility, small letters are used to denote parameters and capitalized letters are to denote decision variables throughout the study.* Feedstock and biofuel transportation costs, respectively are formulated in equations (4-1) and (4-2) and each consists of two components: *transportation dependent*

*cost and loading and unloading cost.* The transportation dependent cost is quantity-, travel distance-, and time- (only for trucks) dependent while the loading and unloading cost is only dependent on commodity type and quantity. Please note that the feedstock mass unit in dry ton needs to be converted to wet ton by moisture content factor  $\theta_l$  (%), on which both transportation dependent cost and loading and unloading cost are based.

$$c_{ijlmt}^{FSDel} = u_{ijlm}^f \times I_{ijlmt}^f + \frac{c_m^{lu,f} \times X_{ijlmt}^f}{(1-\theta_l)} \quad \forall (i, j) \in A_{lm}^f, l \in L, m \in M, t \in T \quad (4-1)$$

$$c_{ijlmt}^{BFDel} = u_{ijm}^b \times I_{ijlmt}^b + c_m^{lu,b} \times X_{ijlmt}^b \quad \forall (i, j) \in A_m^b, m \in M, t \in T \quad (4-2)$$

where  $I_{ijlmt}^f$  and  $I_{ijlmt}^b$  are the numbers of units of transport mode  $m \in M$  between node  $i$  and  $j$  in time  $t \in T$  as defined in equations (4-3) and (4-4) for feedstock and biofuel, respectively, and similarly  $u_{ijlm}^f$  and  $u_{ijm}^b$  are the costs per cargo by a transport mode  $m$  as defined in equations (4-7) and (4-8) for feedstock and biofuel. Denote by  $c_m^{lu,f}$  and  $c_m^{lu,b}$  the loading and unloading costs of feedstock (\$/wet ton) and biofuel (\$/gallon) respectively. Let  $X_{ijlmt}^f$  and  $X_{ijlmt}^b$  be the shipping quantities respectively for feedstock and biofuel.

$$\left[ \frac{X_{ijlmt}^f}{w_{lm}^{Tr,f}} \times \frac{1}{(1-\theta_l)} \right] = I_{ijlmt}^f \quad \forall (i, j) \in A_{lm}^f, l \in L, m \in M, t \in T \quad (4-3)$$

$$\left[ \frac{X_{ijmt}^b}{W_m^{Tr,b}} \right] = I_{ijmt}^b \quad \forall (i, j) \in A_m^b, m \in M, t \in T \quad (4-4)$$

where  $w_{lm}^{Tr,f}$  and  $w_m^{Tr,b}$  are respectively the capacities of transportation modes for feedstock and biofuel. For scheduling a *unit train*, inequality (4-5) and (4-6) enforces minimum warranty of shipping volumes ( $\delta$ ) for feedstock and biofuel respectively.

$$I_{ijlm}^f \geq \delta \times Z_{ijlt}^{ut,f} \quad \forall (i, j) \in A_{lm}^f, l \in L, m = \text{"unit train"}, t \in T \quad (4-5)$$

$$I_{ijmt}^b \geq \delta \times Z_{ijt}^{ut,b} \quad \forall (i, j) \in A_m^b, m = \text{"unit train"}, t \in T \quad (4-6)$$

where  $Z_{ijlt}^{ut,f}$  and  $Z_{ijt}^{ut,b}$ , are respectively the binary variables for feedstock and biofuel, which equal one if unit trains are scheduled for an arc  $(i, j) \in A$  in time  $t \in T$ , 0 otherwise.

$$u_{ijm}^f = \begin{cases} (c^{td,f} + c^{u,f}/v) \times d_{ijm} \times 2 & \text{when } m = \text{"truck"} \\ c^{rd,f} \times d_{ijm} + c^{rf,f} & \text{when } m = \text{"single rail car"} \\ (c^{rd,f} \times d_{ijm} + c^{rf,f}) \times \sigma \times \beta & \text{when } m = \text{"unit train"} \end{cases} \quad \forall (i, j) \in A_{lm}^f, l \in L, m \in M \quad (4-7)$$

$$u_{ijm}^b = \begin{cases} (c^{td,b} + c^{u,b}/v) \times d_{ijm} \times 2 & \text{when } m = \text{"truck"} \\ c^{rd,b} \times d_{ijm} + c^{rf,b} & \text{when } m = \text{"single rail car"} \\ (c^{rd,b} \times d_{ijm} + c^{rf,b}) \times \sigma \times \beta & \text{when } m = \text{"unit train"} \end{cases} \quad \forall (i, j) \in A_m^b, m \in M \quad (4-8)$$

in which the trucking cost is multiplied by two to account for round trips. The trucking distance- (i.e.,  $c^{td,f}$  -feedstock and  $c^{td,b}$  -biofuel) and travel time- (i.e.,  $c^{tt,f}$  -feedstock and  $c^{tt,b}$  -biofuel) dependent costs are explicitly included in the definitions. The  $v$  denotes the average truck travel speed. The rail costs are only distance dependent ( $c^{rd,f}$  -feedstock and  $c^{rd,b}$  -biofuel) which have considered labor wages, fuel and other operational costs (Mahmudi and Flynn, 2006) plus the fixed costs ( $c^{rf,f}$  -feedstock and  $c^{rf,b}$  -biofuel). The  $d_{ijm}$  denotes the distance (miles) from node  $i$  to  $j$  for mode type  $m \in M$ . In this study, unit train is comprised of a large number of railcars  $\sigma$  (e.g.,  $\sigma = 100$ ) and its cost is discounted ( $\beta \leq 1$ ) for the improved economies of scale (Parker et al., 2008).

### 4.2.3 Mathematical Formulation for the Multimodal Cellulosic Biofuel Supply Chain

A multistage, mixed-integer model is developed to integrate *multimodal transport* into a biofuel supply chain design under feedstock seasonality. The objective is to minimize the total system cost while satisfying fuel demands. In the model, two sets of decisions: planning decisions and operational decisions are made simultaneously. The *planning decisions* are mainly on the locations and capacities of refineries and terminals, which are made at the beginning of the study period while *operational decisions* on feedstock procurements, feedstock and biofuel deliveries, storage, and fuel production are time dependent, denoted by successive time phases  $t$  and  $t+1$  in Figure 4-1.

The model is briefly described as: given (1) facility capital costs, feedstock procurement unit cost, storage unit cost, transportation unit cost, and biofuel production unit cost, (2) seasonal yields of feedstocks and seasonal ethanol demand, (3) geographic distributions of facilities, and (4) transport modes in different segments of the network, the model makes decisions on (1) locations of transshipment hubs, refineries, and terminals, (2) capacities of refineries and terminals, (3) seasonal feedstock procurement and biofuel production, and (4) seasonal feedstock/biofuel storage and transshipment. The assumptions are transshipment hubs have sufficient capacity and can handle all feedstock types and the unit costs of feedstock procurement and transportation are constant.

Before describing the model, other used notations are firstly presented as follows:

*Supply chain parameters:*

$c_{ip}^R$  Annualized capital cost (\$) of refinery with capacity  $p \in P$  (the set of discrete refinery capacity levels) at location  $i \in N^R$

$c_{iq}^{BT}$  Annualized capital cost (\$) of blending terminal with size  $q \in Q$  (the set of biofuel storage sizes) at location  $i \in N^{BT}$

$c_l^{fp}$  Average feedstock procurement cost (\$/dry ton) for feedstock type  $l \in L$

$c^{bp}$  Biofuel production cost (\$/gallon) at refineries, assuming that it is regardless of the locations of refineries

$c_l^{fs}$  Feedstock storage cost (\$/dry ton) at transshipment hubs for feedstock type



- $l \in L$ , assuming that the storage cost is regardless of locations
- $c^{bs}$  Biofuel storage cost (\$/gallon) at blending terminals
- $w_p^R$  Refinery capacity (gallon) of the size level  $p \in P$
- $w_q^{BT}$  Biofuel storage capacity (gallon) of the size level  $q \in Q$  at blending terminals
- $a_{lit}$  Feedstock availability (dry ton) of type  $l \in L$  at field  $i \in N_i^F$  in time  $t \in T$
- $k_{it}$  Biofuel demand at city  $i \in N^C$  in time  $t \in T$
- $\alpha$  penalty cost of biofuel demand shortage (\$/gallon)
- $\chi_{it}$  Feedstock deterioration rate (%) of type  $l \in L$  during time  $t \in T$  due to storage at transshipment hubs
- $\varphi_i$  Indicator of terminals that can handle unit trains (=1 if blending terminal  $i \in N^{BT}$  can be accessed by unit trains; =0 otherwise)
- $\eta_l$  Biofuel conversion rate (gallon/dry ton), measuring quantity of ethanol produced by one dry ton of feedstock of type  $l \in L$

*Supply chain variables:*

- $Z_{ip}^R$  = 1 if a refinery is opened at  $i \in N^R$  with capacity  $p \in P$ ; 0 otherwise,
- $Z_{iq}^{BT}$  = 1 if a terminal is opened at  $i \in N^{BT}$  with storage size  $q \in Q$ ; 0 otherwise,
- $Y_{lit}$  The quantity (dry ton) of feedstock of type  $l \in L$  procured at field  $i \in N_i^F$  in time  $t \in T$ ,
- $O_{it}$  Biofuel production (gallon) at refinery  $i \in N^R$  in time  $t \in T$ ,

$S_{it}^f$  The quantity (dry ton) of feedstock of type  $l \in L$  stored at hub  $i \in N^H$  at the beginning of time  $t \in T$ ,

$S_{it}^b$  The quantity (gallon) of biofuel stored at terminal  $i \in N^{BT}$  at the beginning of time  $t \in T$ ,

$Q_{it}$  The shortage of ethanol demand (gallon) in city  $i \in N^C$  in time  $t \in T$ .

The complete model is included in (4-9) – (4-21). All variables except binary variables are non-negative continuous.

$$\text{Minimize } F^{\text{CapCost}} + F^{\text{FSProcureCost}} + F^{\text{RpCost}} + F^{\text{StorCost}} + F^{\text{DelCost}} + F^{\text{PenaltyCost}} \quad (4-9)$$

$$F^{\text{CapCost}} = \sum_{i \in N^R} \sum_{p \in P} c_{ip}^R \times Z_{ip}^R + \sum_{i \in N^B} \sum_{q \in Q} c_{iq}^{BT} \times Z_{iq}^{BT} \quad (4-9.a)$$

$$F^{\text{FSProcureCost}} = \sum_{t \in T} \sum_{l \in L} \sum_{i \in N_l^F} c_l^{fp} \times Y_{lit} \quad (4-9.b)$$

$$F^{\text{RpCost}} = \sum_{t \in T} \sum_{i \in N^R} c^{bp} \times O_{it} \quad (4-9.c)$$

$$F^{\text{StorCost}} = \sum_{t \in T} \sum_{l \in L} \sum_{i \in N^H} c_l^{fs} \times S_{it}^f + \sum_{t \in T} \sum_{i \in N^{BT}} c^{bs} \times S_{it}^b \quad (4-9.d)$$

$$F^{\text{DelCost}} = \sum_{t \in T} \sum_{l \in L} \sum_{m \in M} \sum_{(i,j) \in A_m^f} c_{ijlmt}^{FSDel} + \sum_{t \in T} \sum_{m \in M} \sum_{(i,j) \in A_m^b} c_{ijmt}^{BFDel} \quad (4-9.e)$$

$$F^{\text{PenaltyCost}} = \sum_{t \in T} \sum_{i \in N^C} \alpha \times Q_{it} \quad (4-9.f)$$

including (1)-(8)

The objective function (4-9) minimizes the annual total system cost, including refinery and terminal capital cost  $F^{\text{CapCost}}$ , feedstock procurement cost  $F^{\text{FSProcureCost}}$ , biofuel production cost  $F^{\text{RpCost}}$ , feedstock and biofuel storage cost  $F^{\text{StorCost}}$ , feedstock and biofuel delivery cost  $F^{\text{DelCost}}$ , and penalty cost  $F^{\text{PenaltyCost}}$ , respectively formulated in equations (4-9.a) to (4-9.f). In particular, equation (4-9.a) computes the costs associated with system planning decisions, which are invariant of seasons, while equations (4-9.b) to (4-9.f) compute operational cost, which are seasonal dependent.

$$Y_{lit} \leq a_{lit} \quad \forall l \in L, i \in N_l^F, t \in T \quad (4-10)$$

$$Y_{lit} = \sum_{j:(i,j) \in A_{lm}^f} X_{ijlmt}^f \quad \forall l \in L, m = \text{"truck"}, i \in F_l, t \in T \quad (4-11)$$

Constraint (4-10) assures that procurement will not exceed the feedstock seasonal availability and the feedstock flow conservation is observed in constraint (4-11).

$$\sum_{m \in M} \sum_{j:(j,i) \in A_{lm}^f} X_{jilm}^f - \sum_{m \in M} \sum_{k:(i,k) \in A_{lm}^f} X_{iklmt}^f + (1 - \chi_t) \times S_{ilt}^f = S_{il,t+1}^f \quad \forall i \in N^H, l \in L, t \in T \quad (4-12)$$

Equation (4-12) imposes a flow conservation constraint on hubs, which involves both spatial and temporal dimensions. The feedstock storage  $S_{il,t+1}^f$  at the beginning of season  $t+1$ , equals the net feedstock flow  $(\sum_{m \in M} \sum_{j:(j,i) \in A_{lm}^f} X_{jilm}^f - \sum_{m \in M} \sum_{k:(i,k) \in A_{lm}^f} X_{iklmt}^f)$  during

season  $t$  plus the remaining feedstock storage  $S_{it}^f$  from last season which is discounted due to feedstock deterioration  $(1 - \chi_{lt})$  over time.

$$\sum_{p \in P} Z_{ip}^R \leq 1 \quad \forall i \in N^R \quad (4-13)$$

$$\sum_{t \in T} O_{it} \leq \sum_{p \in P} w_p^R \times Z_{ip}^R \quad \forall i \in N^R \quad (4-14)$$

$$\sum_{l \in L} \sum_{m \in M} \sum_{j: (j,i) \in A_m^f} X_{jilm}^f \times \eta_l = O_{it} = \sum_{m \in M} \sum_{j: (i,j) \in A_m^b} X_{ijmt}^b \quad \forall i \in N^R, t \in T \quad (4-15)$$

Constraint (4-13) assures that maximally one capacity can be chosen at each potential refinery location. Constraint (4-14) is a logic constraint, stating that there is no biofuel production unless one is open. Equation (4-15) is a flow conservation constraint for refineries. Note that production variable  $O_{it}$  is redundant, and it remains in the model to simplify the model reading.

$$\sum_{q \in Q} Z_{iq}^{BT} \leq 1 \quad \forall i \in N^{BT} \quad (4-16)$$

$$\sum_{t \in T} \sum_{m \in M} \sum_{j: (j,i) \in A_m^b} X_{jimt}^b \leq \bar{M} \times \sum_{q \in Q} Z_{iq}^{BT} \quad \forall i \in N^{BT} \quad (4-17)$$

$$S_{it}^b \leq \sum_{q \in Q} w_q^{BT} \times Z_{iq}^{BT} \quad \forall i \in N^{BT}, t \in T \quad (4-18)$$

$$\sum_{m \in M} \sum_{j: (j,i) \in A_m^b} X_{jimt}^b - \sum_{m \in M} \sum_{k: (i,k) \in A_m^b} X_{ikmt}^b + S_{it}^b = S_{i,t+1}^b \quad \forall i \in N^{BT}, t \in T \quad (4-19)$$

$$\sum_{t \in T} \sum_{j:(j,i) \in A_m^b} X_{jimt}^b \leq \bar{M} \times \varphi_i \quad \forall i \in N^{BT}, m = \text{"unit train"} \quad (4-20)$$

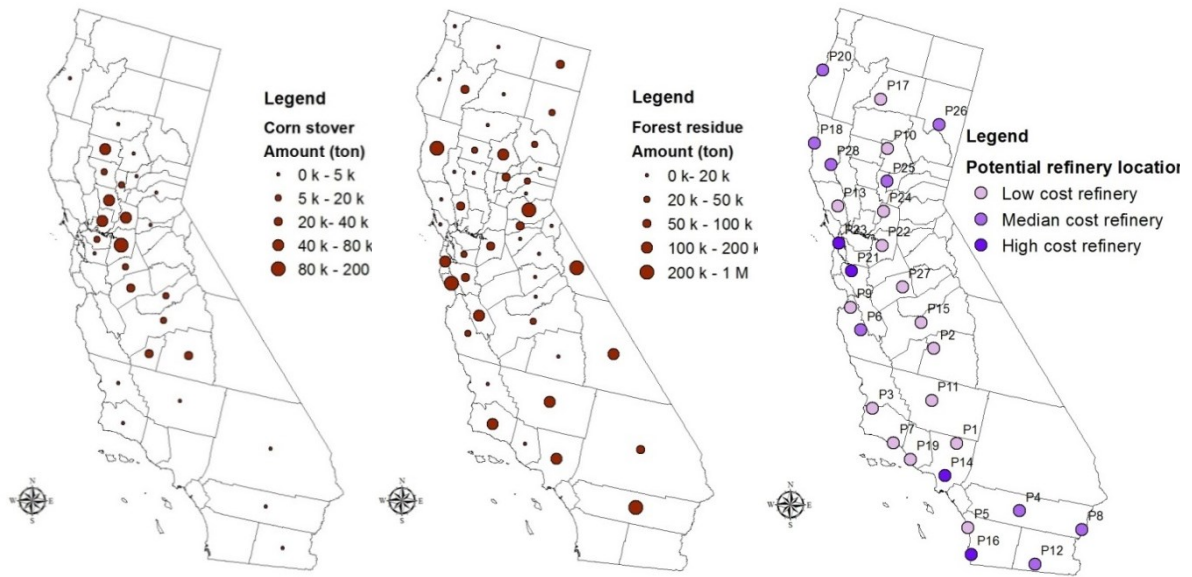
Terminal capacity logic constraint (4-16) can be similarly explained as for constraint (4-13). Constraint (4-17) is a logic constraint, stating that biofuel can only be shipped to the operating terminals. Constraint (4-18) states that the storage cannot exceed the design capacity of terminals. Constraint (4-19) is the flow conservation constraint on terminals, which can be similarly explained as for constraint (4-15) but there is no deterioration over time. Constraint (4-20) specifies the terminals that can handle unit trains.

$$\sum_{j:(j,i) \in A_m^b} X_{jimt}^b + Q_{it} = k_{it} \quad \forall i \in N^C, m = \text{"truck"}, t \in T \quad (4-21)$$

Equation (4-21) ensures that all demands will be satisfied, which can be supplemented by imported fuels ( $Q_{it}$ ) in case of shortage.

### 4.3 Case Study

The model is implemented to a case study of cellulosic ethanol production in California in response to the aggressive public policies in promoting the use of alternative transportation fuels. The whole state of California is considered and facilities in support of the supply chain are geographically distributed (see Figure 4-2), which provides an ideal test bed for the multimodal supply chain design.

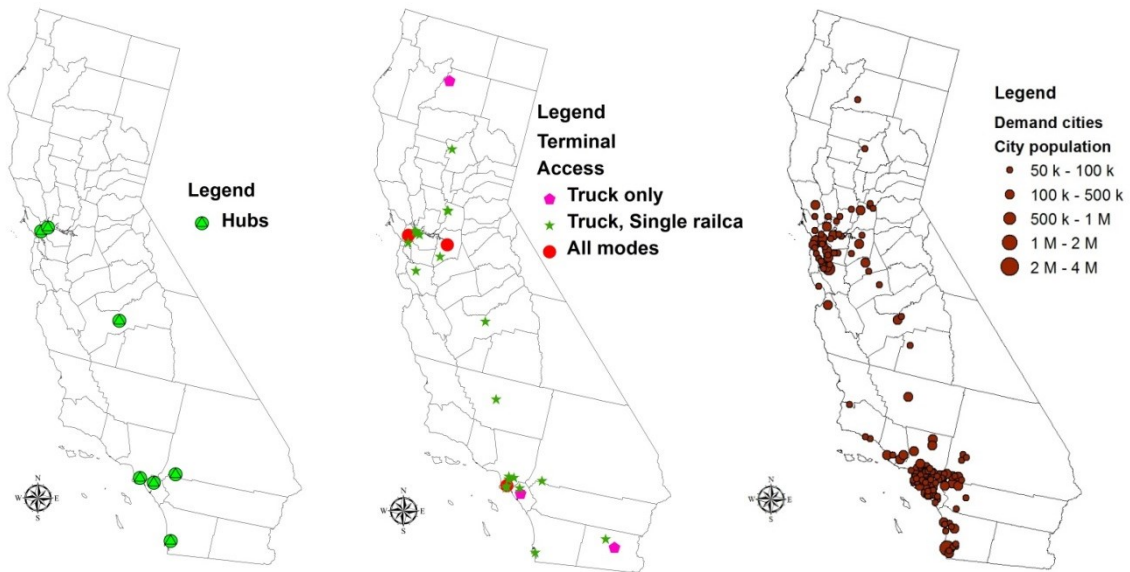


(a) Corn stover locations

(b) Forest residues

(c) Candidate refinery sites

locations



(d) Feedstock hubs

(e) blending terminals

(f) Major ethanol markets

**Figure 4-2 Geographic Distributions of Feedstock Fields, Candidate Refineries, Hubs, Terminals and Major Markets**

Feedstock resources: Two types of feedstock resources, corn stover and forest residues are considered, both of which are abundant in the state of California. The feedstock parameters of these two feedstock types are included in Table 4-1. Feedstock yield varies significantly between different seasons. Corn stover is only available in fall, while forest residue is available in fall, spring and summer. However, compared to feedstock supply, the market demand is relatively stable between various seasons within 2% according to the Energy Information Administration (EIA).

**Table 4-1 Feedstock Parameters<sup>a</sup>**

Feedstock types	Availability (thousand dry ton)	# of sites	Conversion rate ( $\eta_i$ ) <sup>b</sup> (gallon/dry ton)	Moisture content ( $\theta_i$ ) <sup>c</sup> (% mass)	Seasonal deterioration rate ( $\chi_{it}$ ) <sup>d</sup>	Avg. procurement cost $c_i^{fp}$ (\$/dry ton)	Storage cost $c_i^{fs}$ (\$/dry ton)
Corn stover	563	27	80.6	15	10%	35	8
Forest residue	4,268	47	90.2	50	12%	30	2

- a. Feedstock parameters except for seasonal deterioration rate are adapted from (Parker et al., 2008)  
b. The conversion rate measures gallons of ethanol converted from one dry ton of the feedstock.  
c. The moisture content indicates the average quantity of water contented in the feedstock.  
d. Seasonal deterioration rate represents percentage in mass loss of the feedstock over one season.

Refineries: Table 4-2 summarizes the critical refinery parameters. There are 28 candidate refinery sites with three different capital costs due to the varied land price and labor costs along the wide-spread geographic distributions. A variety of other mature biomass refining technology scenarios are also acknowledged for future research (Sims et al., 2010), varying with efficiency, economic, and environmental impacts.

**Table 4-2 Refinery Parameters**

		Low	Median	High
Total # of candidate sites by capital cost level		15	9	4
Capital cost ( $c_{ip}^R$ ) <sup>a</sup> by different capacity ( $w_p^R$ ) (\$million)	60 MGY	25.0	25.6	26.2
	80 MGY	31.3	31.9	32.5
	100 MGY	37.6	38.2	38.8
Production cost ( $c^{bp}$ ) <sup>b</sup> (\$/gallon)		0.92		
Conversion technology considered		LignoCellulosics Ethanol (LCE) via hydrolysis and fermentation conversion technology with Dilute Acid pretreatment process, featuring low cellulose enzyme cost and reasonably high ethanol yields		

a. Refinery capital costs are adopted and converted from (Huang et al., 2010)

b. It is mid-term projection for bioethanol production cost (Office of the Biomass Program, 2009), including pretreatment, production, and distillation and solid recovery costs.

Transshipment hubs: There are 7 hubs that have already been used for freight transshipment in California as potential hub locations for feedstock storage and transshipment. Feedstocks can be stored at hubs over seasons, but will incur seasonal storage costs ( $c_l^{fs}$ ) of \$8/dry ton for corn stover and \$2/dry ton for forest residues (Huang et al., 2013). Feedstock mass lost occurs during the storage, with seasonal deterioration rates ( $\chi_{it}$ ) of 10% for corn stover and 12% for forest residues (Huang et al., 2013).

Terminals: There are 29 candidate sites for terminals with three tank sizes  $w_q^{BT}$ , 4.2, 2.1 and 1.05 million gallons, and their associated costs \$450k, \$765k, and \$1.26m, respectively (Huang et al., 2013). The receiving facilities and blending systems add additional \$310k onto the capital cost  $c_{iq}^{BT}$  of each operating terminal (Huang et al., 2013).

It is assumed that the operational cost is negligible (i.e.,  $c^{bs} = 0$ ).



Demand: Cities with a population more than 50,000 are considered as demand centers, and 143 such cities are chosen in the study. The total annual cellulosic ethanol demand from these demand centers is set to be 272 MGY, according to the California Energy Commission projected cellulosic ethanol demand to 2020 (Jenkins et al., 2007). The annual demand of each city is proportional to the population.

Transportation data: The multimodal transport data is presented in Table 4-3. In this study, two transportation networks are integrated: the highway network and the rail network. It is assumed that deliveries take the shortest paths between any node pairs on the network, prepared in ArcGIS®.

**Table 4-3 Transportation Parameters<sup>a</sup>**

Categories		Truck		Single railcars train		Unit train <sup>c</sup>	
		feedstock	ethanol	feedstock	ethanol	feedstock	ethanol
Cost <sup>b</sup>	Loading/ Unloading ( $c_m^{lu,f}, c_m^{lu,b}$ )	\$5/ wet ton	\$0.02/ gallon	\$5/ wet ton	\$0.015/ gallon	\$5/ wet ton	\$0.015/ gallon
	Time dependent ( $c^{t,f}$ )	\$29/hr/ truckload	\$32/hr/ truckload ( $c^{t,b}$ )	N/A	N/A	N/A	N/A
	Distance dependent ( $c^{td,f}$ )	\$1.2/mile/ truckload	\$1.3/mile/ truckload ( $c^{td,b}$ )	\$2.5/mile/ railcar ( $c^{rd,f}$ )	\$2.5/mile/ / railcar ( $c^{rd,b}$ )	\$200/mile/ unit train ( $c^{rd,f} \times \beta$ )	\$200/mile/ unit train ( $c^{rd,b} \times \beta$ )
	Fixed cost	N/A	N/A	\$2,876/ railcar	\$2,904/ railcar	\$230,000/ unit train	\$232,000/ unit train
Capacity ( $W_{lm}^{Tr,f}, W_m^{Tr,b}$ )		25 wet tons/truck -load	8,000 gallons/ truckload	106.5 wet tons/railca r	33,000 gallons/ railcar	10,650 tons/unit train	3.3 million gallons/unit train
Average travel speed ( $v$ ) (miles/hr)		40		N/A		N/A	

a. adapted from (Parker et al., 2008)

b. it is assumed that unit train has a 20% discount on both of the fixed cost and distance dependent cost (i.e., =20% in the model) for 100 railcars

c. According to (USDA, 2007), the unit train utilization rate is around 30 turns per year and the minimum number of unit trains shipped per season is set to be 8 for each commodity and arc (i.e.,  $\delta = 8$  in the model)

## **4.4 Results and Discussion**

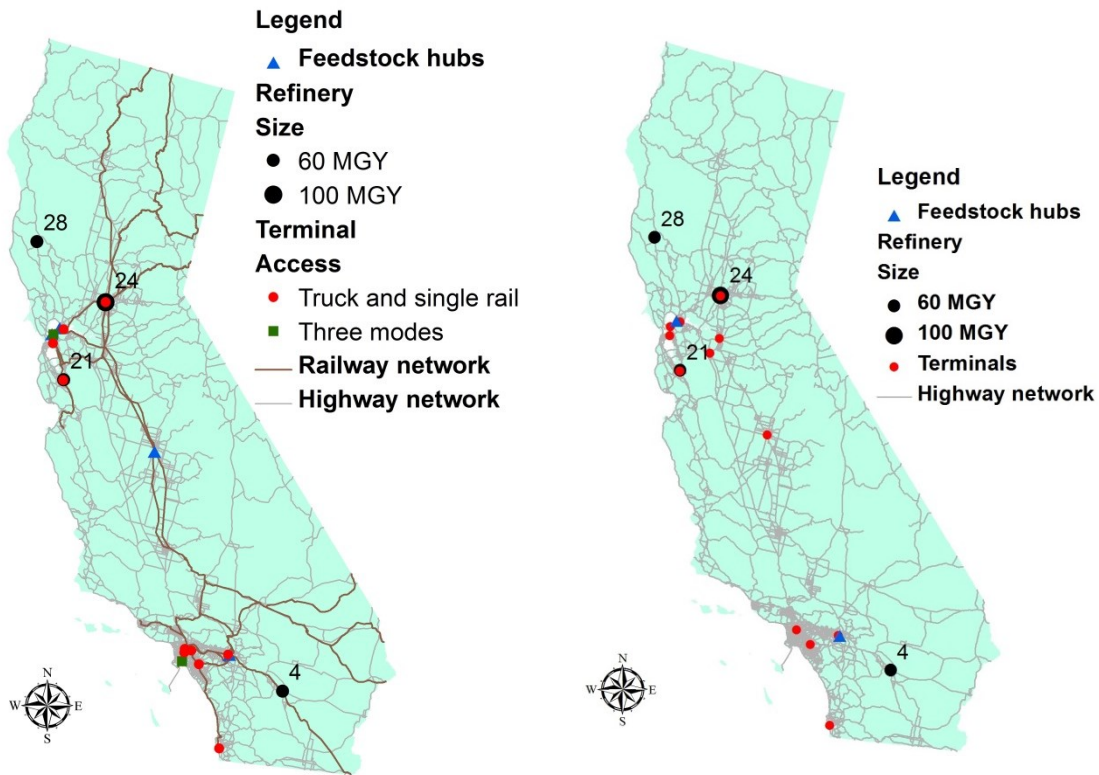
The proposed model is programmed in AMPL (Fourer et al., 2003) and solved using the CPLEX solver 12.4. All the numerical experiments described were run on a Dell desktop with 8 GB RAM and Intel Core Quad 3.0 GHz processor under Windows 7 environment. This large-scale problem has 3,387 binary variables, 38,532 integer variables, 33,377 linear variables, and 40,165 constraints and it was solved in about 3,600 CPU seconds. This section will report the outcomes of baseline case study compared with the single-mode system and sensitivity analysis on the effects of limits on biomass delivery distance.

### **4.4.1 Baseline Case Study Results Compared With Single-Mode Transport**

The penalty cost  $\alpha$  is set as high as \$5/gallon to encourage the instate ethanol production. The resulting ethanol infrastructure system shown in Figure 4-3(a) contains four refineries at locations #4, #21, #24, and #28, 4 transshipment hubs, and 12 terminals. It is a result of the integrated method of facility location design and multimodal transport planning. Note that all four refineries are accessible by road but only three of them at #4, #21, and #24 are accessible by rail. All hubs and terminals are rail accessible, wherein only two terminals (as labeled) can handle all three modes including unit trains. The refinery #24 with largest capacity of 100MGY is located in the central valley area, where major corn stover supply is clustered, for mass ethanol production in the fall season. This production scheduling would help to mitigate the feedstock supply depletion in the

following seasons, and the refineries #21 and #28 are placed for the similar reasons. Only forest residues are available in spring and summer and the refinery #4 extends the consumptions of forest residues. The 4 hubs and 12 large-sized terminals are located proximately to feedstock fields and consumer markets since truck, though the most expensive, is the only eligible transport mode for the segments originating from fields or ending at markets. The geographic dispersions between refineries, hubs, and terminals are compensated by the use of rail wherever applicable.

The multimodal solutions are compared with the single-mode solution by re-running the model as if truck is the only transport mode. The single-mode system layout is shown in Figure 4-3(b), which indicates that fewer (two hubs) are chosen close to major consumer markets as hubs now only provide storage functions and the two solutions have identical refinery configurations.



(a) Multimodal system layout                      (b) Single-mode system layout  
**Figure 4-3 Ethanol Infrastructure Systems**

The details on the feedstock and ethanol flows in the supply chain over seasons are illustrated in Figure 4-4, which shows how storage facilities are used to mitigate seasonal fluctuations and balance fuel production over a year. Multiple transport modes are used based on the travel distance and commodity quantity, which is also subject to facility access restrictions except for trucks. Further investigations reveal that truck is mainly for short-range delivery with an average travel distance of 54 miles while rail is for long-range delivery with a significantly larger distance of 440 miles. As aforementioned, different transport modes can work integrally to achieve better cost efficiency. For instance, to take delivery cost advantage of unit trains with a minimum

shipping quantity of 26.4million dry tons (minimum 8 unit trains/season × 3.3 million dry tons/unit train), ethanol is produced more than it needs in season 3 and the fuel in excess will be used in season 4.

The delivered fuel cost is \$2.16/gallon, in which the production is the major cost contributor accounting for 42.6%. However, the transportation is substantial, totaling 18.2% of the delivered fuel cost. Unlike the challenge in reducing biofuel production cost, which may need to undertake technology breakthrough, transportation cost reduction may be easier to achieve through smart planning, such as using multimodal to replace single-mode transport system in the supply chain. The transport costs by these two solutions are then compared.

Two goals are of particular interest about the two transport systems: efficiency and cost effectiveness. In recognition of the efficiency that is a combined result of quantity shipped and distance traveled, a new pair of measurements were created: dry ton-mile for feedstock and gallon-mile for ethanol. A lower value indicates a more efficient transport mode. The cost effectiveness can be directly measured by the monetary cost. Table 4-4 provides the measures of efficiency and cost effectiveness for two transport systems. The results imply that the single-model (truck) is generally more efficient than the multimodal by 18% ( $= (260.07 - 219.85) / 219.85$ ). This is because if trucking is the only transport mode, trucks do not need to get off the way to send biomass to consolidation points. However, as trucking is more expensive, the multi-modal cuts the total transport cost by \$12.72m= (\$119.86m - \$107.14m) or 10.6%.

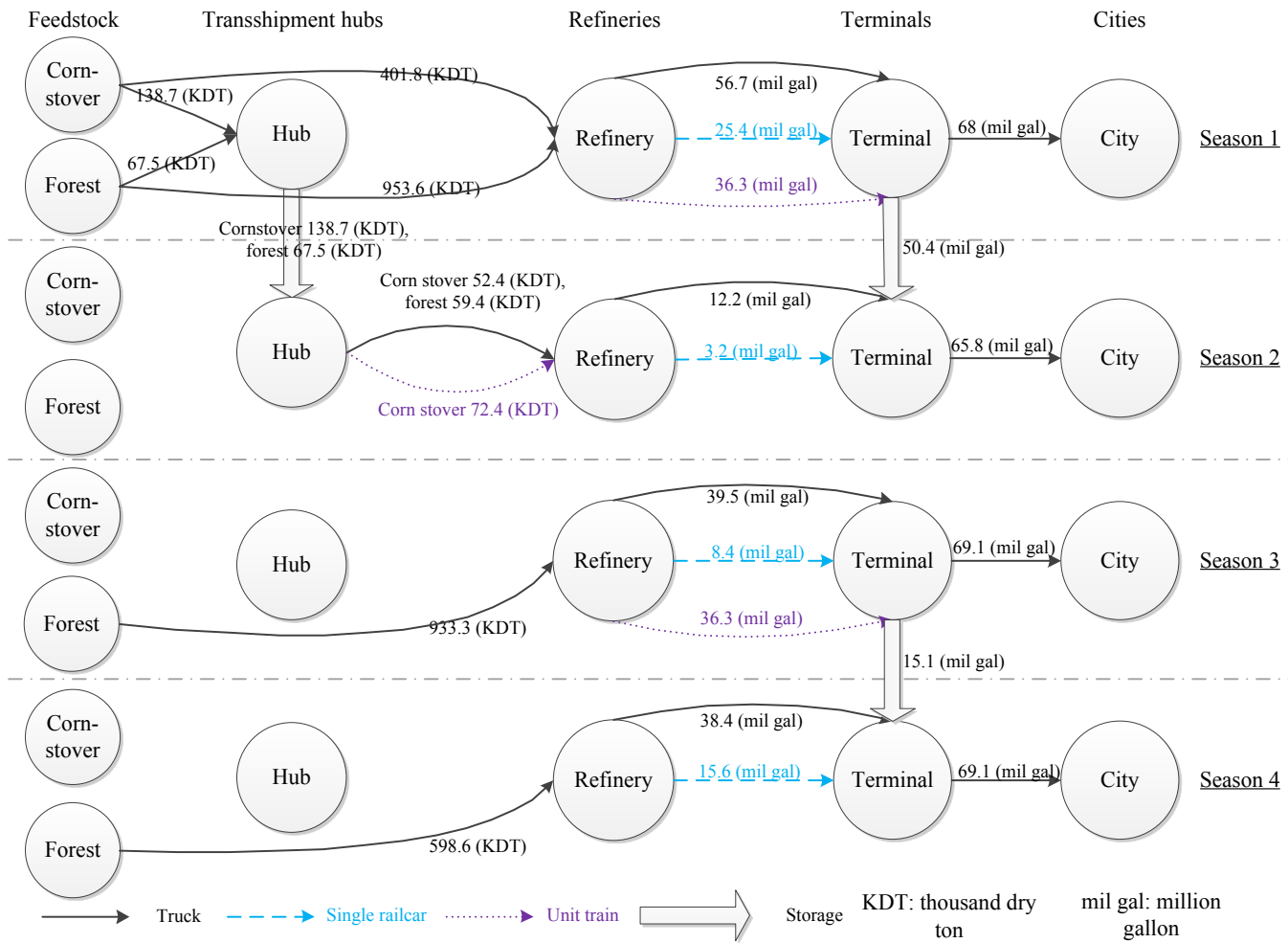


**Figure 4-4 The Diagram of Feedstock and Ethanol Flows over Seasons in The Supply Chain**

**Table 4-4 Measures of Efficiency and Cost for Single-Mode and Multimodal Transports**

Commodity type	Transport modes	Efficiency measurements <sup>a</sup>				Transport cost (\$m)
		Truck	Tingle railcar	Unit train	Total	
Corn stover	multimodal	30.41	0	25.83	56.24	11.82
	single-mode	27.43	NA	NA	27.43	8.18
Forest residues	multimodal	114.21	0	0	114.21	61.30
	single-mode	126.81	NA	NA	126.81	66.26
Ethanol	multimodal	18.92	36.76	33.94	89.62	34.02
	single-mode	65.61	NA	NA	65.61	45.42
Total	multimodal	170.45 for feedstock, 89.62 for ethanol				107.14
	single-mode	154.24 for feedstock, 65.61 for ethanol				119.86

a. million dry ton-mile for feedstock; billion gallon-mile for ethanol.

#### **4.4.2 Effects Of Limits On Biomass Delivery Distance By Truck**

All aforementioned results are free on limits of biomass delivery distance. In the current corn-grain ethanol industry, however, a 50-mile limit on biomass delivery by trucks is normally expected (USDA, 2007). Although the cellulosic ethanol industry may or may not adopt the same limits, the analysis on the effects of the limits on the system operations and cost effectiveness would provide insights for policy makers and industry practitioners.

A 50-mile bound was set on biomass truck delivery coupled with the presence of transshipment hubs in the supply chain. The optimization model was re-ran for both single-mode and multimodal systems and report the resulting refinery configurations, imported ethanol rate, and delivered fuel cost in Table 4-5. For comparison purpose, the baseline results are provided in the last row of the table. Note that all refineries in the table have the same capacity of 60 MGY. The following major observations are made: (1) the distance limit leads to more refineries built in the supply chain. The increased capital

cost makes the delivered fuel cost rise up by 25% (= (\$2.71-\$2.16) /\$2.16); (2) the transshipment hubs make the multimodal supply chain more cost effective, evidenced by the decrease in delivered fuel cost from \$2.91 to 2.71/gallon. This is because the hubs can balance the feedstock availability throughout a year and fewer refineries need to be built; and (3) the single-mode supply chain is more “vulnerable” to the distance limit compared to multimodal. This is because as truck is the only transport mode, whenever the distances between feedstock fields and refineries exceed the limit, ethanol has to be imported to meet demand with penalty cost as indicated by the higher import rates.

**Table 4-5 Outcomes of Including Trucking Distance Limit of 50 Miles**

scenarios		Outcomes		
Transport modes	Hubs <sup>a</sup>	Selected refinery sites	Ethanol import rate <sup>b</sup>	Delivered fuel cost
Multimodal	Yes	#4, #6, #11, #21, #22, #25, #28	10.30%	\$2.71/gallon
Multimodal	No	#4, #6, #7, #11, #14, #21, #22, #25, #28	13.30%	\$2.91/gallon
Single-mode	Yes	#14, #21, #22	68.10%	\$4.20/gallon
Single-mode	No	#14, #21, #22	68.10%	\$4.20/gallon
Baseline (multimodal, no limits)	Yes	#4, #24, #28	0.00%	\$2.16/gallon

a. “yes” indicates that transshipment hubs are available; “no” otherwise

b. Ethanol import rate=Total amount of imported ethanol/Total ethanol demand

As suggested in (Hess et al., 2009), larger distance limits on biomass delivery by truck, e.g., 200 miles, may be considered for future biomass logistics systems to reduce risks from local environmental disturbances, e.g., hurricane, diseases and pest infections. Both single-mode and multimodal systems were tested on a range of distances from 50 to 300 miles. The “unlimited” scenario (i.e., baseline) is also included for comparison



purpose. The resulting delivered fuel costs are plotted in Table 4-5, which can conclude that multimodal system is less cost sensitive to the distance restrictions and a loosened restriction should make system more cost effective.

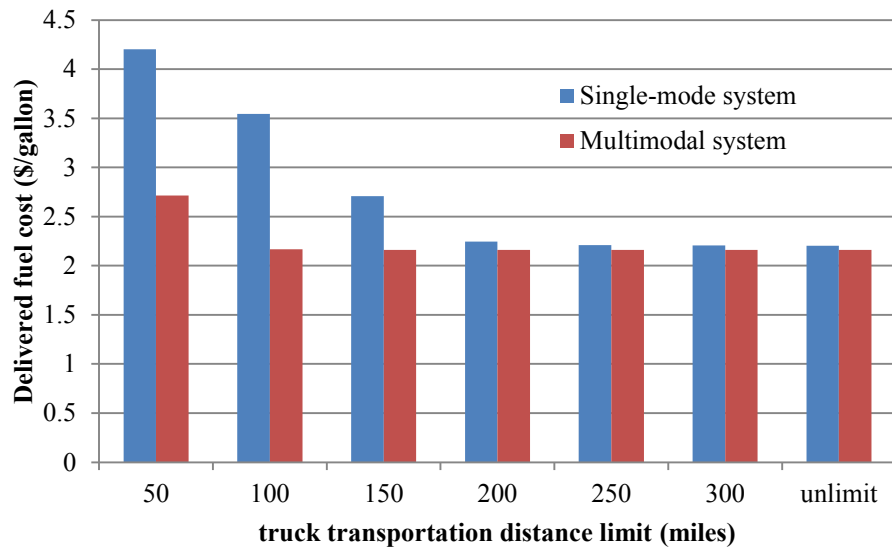


**Figure 4-5 The Effects of Distance Limits on The Delivered Fuel Cost**

## **4.5 Summary**

In Chapter 4, I created a new modeling framework on integrating multimodal transport (truck, single railcar and unit train) into a cellulosic ethanol supply chain design. A multistage, mix-integer programming model was developed to make integral and optimal decisions on the supply chain planning and operations. Through the case study of cellulosic ethanol supply chain design in California, the significance of system components and interactions among them were demonstrated. Compared with single-mode solution, the multimodal solution makes the supply chain more adaptive to

feedstock seasonality, more cost effective, and more capable handling policies on distance limits for biomass truck deliveries.

# **CHAPTER 5 SUSTAINABLE BIOFUEL SUPPLY CHAIN PLANNING AND MANAGEMENT UNDER UNCERTAINTY**

## ***5.1 Problem Statement***

Similar to the study shown in Chapter 3, this study also aims to model sustainability in biofuel supply systems design. In addition to the least-cost objective, this study also includes the environmental objective to reduce carbon footprints in the supply chain. The Argonne GREET model is also used to quantify the life-cycle GHG emissions in the biofuel supply chain.

Another challenge arises from the lack of knowledge in the biofuel supply system planning, such as supply fluctuations, demand variations, and technology efficiency. As shown in Section 2.2, literatures in addressing uncertainty are mainly focused on the uncertainties of feedstock supply or fuel demand. No study has explicitly considered the uncertainty inherent in conversion processes, which can be easily caused by various factors, e.g., chemical composition of the biomass, enzymes, boiler efficiency, etc.

The main contributions of this study are (1) developing a novel multi-objective stochastic programming model that incorporates economic and environmental sustainability in the biofuel supply chain system under uncertainty of conversion process, and (2) using a real-world case study of cellulosic biofuel production in California.

The remainder of the study is organized as follows. Model formulations will be presented in Section 5.2, with a detailed discussion of compromise method. Background information of biomass ethanol production from biowastes in California is described in

Section 5.3. The case study results and discussions will be presented in Section 5.4. Finally, I will summarize the study in Section 3.5.

## **5.2 Methods**

We focus on the planning and management of sustainable biofuel supply chain under uncertainty of conversion technology in an integrative manner. Planning decisions such as, locations and sizes of biorefineries and feedstock procurements are made before the uncertainty is revealed. On the other hand, operational decisions such as, production and transportation can be adjusted based on the actual realization of the uncertain conversion rates. This feature fits well in a stochastic programming framework (Birge and Louveaux, 1997), which recognizes the non-anticipativity of planning decisions while allowing recourse for operational decisions.

In this study, the introduced model includes two competing objectives -least cost and lowest GHG emission. For example, reduction in GHG emission can be achieved by importing more fuels with higher cost.

As a result, a multi-objective optimization modeling framework is proposed to seek non-dominated solutions between the two objectives. In the rest of this section, we first introduce two stochastic model objectives of separate minimization of the expected system cost given in equation (5-1) and minimization of the expected system GHG emissions given in equation (5-2). Then, the two objectives are integrated in a multi-objective model based on the compromise method, also called compromise stochastic model. All notation used in the study is given in Table 5-1.

**Table 5-1 Notations**

Index	
$I_l$	Index $i_l$ , set of feedstock fields of feedstock type $l$
$L$	Index $l$ , set of feedstock types
$J$	Index $j$ , set of potential locations for biorefineries
$M$	Index $m$ , set of demand centers
$\Omega$	Index $\omega$ , set of uncertain scenarios
Parameters	
$c$	Unit ethanol production cost (\$/gallon)
$cap_{b_l}$	Truck bulk solids capacity for feedstock type $l$ (wet ton)
$cap_{lq}$	Truck liquids capacity (gallon)
$capr_j^L$	Minimum required refinery capacity (gallon)
$capr_j^U$	Maximum allowable refinery capacity (gallon)
$d_{ij}$	Distance between node $i$ and $j$ (miles)
$D_m$	Ethanol demand at city $m$ (gallon)
$eh_l$	GHG emission of feedstock harvest of type $l$ (CO <sub>2</sub> eq. ton/dry ton)
$et$	GHG emission of transportation (CO <sub>2</sub> eq. ton/mile/truckload)
$ep_l(\omega)$	GHG emission of ethanol production under scenario $\omega$ by feedstock type $l$ (CO <sub>2</sub> eq. ton/gallon)
$f_j^F$	Annualized fixed capital cost (\$) of refinery at location $j$
$f_j^V$	Annualized variable capital cost (\$/gallon) of refinery at location $j$
$lu_b$	Truck loading and unloading cost of bulk solids (\$/wet ton)
$lu_{lq}$	Truck loading and unloading cost of liquids (\$/wet ton)
$MC_l$	Moisture content of feedstock type $l$ (%)
$p_l$	Average procurement cost of harvesting feedstock of type $l$ (\$/dry ton)
$t_b^d$	Distance dependent transportation cost (\$/mile/truckload) of bulk solids, i.e., the cost of traveling one mile per truckload
$t_b^t$	Travel time dependent transportation cost (\$/hr/truckload) of bulk solids, i.e., the cost of traveling one hour per truckload
$t_{lq}^d$	Distance dependent transportation cost (\$/mile/truckload) of ethanol
$t_{lq}^t$	Travel time dependent transportation cost (\$/hr/truckload) of ethanol
$v$	Average truck travel speed (mile/hr)
$yield_{i_l}$	Maximum available feedstock of type $l$ at field $i_l$ (dry ton)
$\alpha$	Unit penalty cost of ethanol demand shortage (\$/gallon), i.e., cost of

$\eta_l(\omega)$	importing fuels Bioethanol conversion rate (gallon/dry ton) under scenario $\omega$ , measuring quantity of ethanol produced by one dry ton of feedstock of type $l$
<b>Decision Variables</b>	
$cap_j$	Designed refinery capacity (gallon) of refinery $j$
$pr_j(\omega)$	Ethanol production (gallon) at refinery $j$ under scenario $\omega$
$q_m(\omega)$	Shortage of ethanol demand (gallon) in city $m$ under scenario $\omega$
$x_{ij}(\omega)$	Amount (dry ton) of feedstock of type $l$ transported from field $i_l$ to refinery $j$ under scenario $\omega$
$Y_{i_l}$	The quantity (dry ton) of feedstock of type $l$ procured at field $i_l$
$y_{jm}(\omega)$	Amount (gallon) of ethanol transported from refinery $j$ to city $m$ under scenario $\omega$
$z_j$	=1 if refinery at location $j$ is opened; =0 otherwise

### Objective 1: Minimization of System Cost

The system cost consists of costs of planning and operating the biofuel system. The system planning cost is the total of facility capital cost and feedstock procurement cost. The planning decisions are non-distinguishable across all scenarios and their costs are deterministic. The operational decisions are scenario dependent, so are the costs involved in production and delivery. The least expected cost objective  $f_1$  is shown in (5-1).

Minimize

$$f_1 = \sum_{l \in L} \sum_{i_l \in I_l} p_l Y_{i_l} + \sum_{j \in J} (f_j^F z_j + f_j^V cap_j) + E_\omega \left\{ \sum_{j \in J} c \times pr_j(\omega) + TC_1(\omega) + TC_2(\omega) + \sum_{m \in M} \alpha q_m(\omega) \right\} \quad (5-1)$$

where

$$TC_1(\omega) = \sum_{i \in L} \sum_{i_l \in I_l} \sum_{j \in J} \left( \frac{\left( t_b^d + \frac{t_b^t}{v} \right) \times d_{ij} \times 2}{cap_{b_l}} + l_b \right) \times \frac{x_{ij}(\omega)}{(1 - MC_l)} \quad (5-1.a)$$

$$TC_2(\omega) = \sum_{j \in J} \sum_{m \in M} \left( \frac{\left( t_{lq}^d + \frac{t_{lq}^t}{\nu} \right) \times d_{jm} \times 2}{cap_{lq}} + lu_{lq} \right) \times y_{jm}(\omega) \quad (5-1.b)$$

The objective function (5-1) minimizes the expected system cost of the biofuel supply chain. The costs of feedstock logistics  $TC_1$  and fuel distribution  $TC_2$  have similar structures. Both of them convert the transportation quantity into truckloads, and include the time- and distance-dependent costs and loading/unloading costs. Transportation distance is doubled to account for the cost of a round-trip. For feedstock transportation, feedstock dry ton is converted to wet ton by moisture content  $MC_l$ , on which the truck capacity is based. Imports are allowed with a penalty cost of  $\alpha$ , which introduces flexibility in achieving cellulosic biofuel market penetrations and designing greenhouse gas emission regulations.

### **Objective 2: Minimization of System GHG Emissions**

The procurement decision is made before uncertainty is known and thus, the associated emission is deterministic on the first stage, denoted as  $eh_l$ . Emissions of production and transportation decisions are scenario-dependent and included on the second stage, denoted as  $ep_l(\omega)$  and  $et$ , respectively. The objective  $f_2$  is to achieve the lowest expected GHG emissions.

Minimize

$$f_2 = \sum_{l \in L} \sum_{i_l \in I_l} eh_l \times Y_{i_l} + E_\omega \left\{ \sum_{l \in L} \sum_{i_l \in I_l} \sum_{j \in J} ep_l(\omega) \times x_{i_l j}(\omega) \times \eta_l(\omega) + TE_1(\omega) + TE_2(\omega) \right\} \quad (5-2)$$

Where

$$TE_1(\omega) = \sum_{l \in L} \sum_{i_l \in I_l} \sum_{j \in J} \frac{et \times x_{i_l j}(\omega) \times d_{i_l j} \times 2}{(1 - MC_l) \times cap_{b_l}} \quad (5-2.a)$$

$$TE_2(\omega) = \sum_{j \in J} \sum_{m \in M} \frac{et \times y_{jm}(\omega) \times d_{jm} \times 2}{cap_{l_q}} \quad (5-2.b)$$

The objective function (5-2) minimizes the expected GHG emission in the system. Similar to the structure of transportation cost in (5-1), the transportation GHG emissions consist of two parts,  $TE_1$  from feedstock delivery and  $TE_2$  from biofuel distribution.

### Compromise Stochastic Model

The compromise method is used to solve the multi-objective optimization problem. The two stochastic model objectives (5-1) and (5-2) are included in the compromise model given in (5-3) to find the best-compromise solutions of  $f = [f_1, f_2]$ . The problem is transformed to a single-objective, mixed-integer programming model and can be solved using a linear programming solver.

$$\text{Minimize } f = \sum_{i=1}^2 W_i \frac{f_i - f_i^o}{f_i^{ao} - f_i^o} \quad (5-3)$$

In objective function (5-3),  $f_i$  denotes a specific objective function, included in the model.  $f_i^o$  denotes the optimal result of the  $i$ th objective and  $f_i^{ao}$  denotes the anti-optimal



result. For example, the  $f_1^o$  is the optimal value of objective  $f_1$ . The anti-optimal cost  $f_1^{ao}$  is obtained as follows. The decision variables corresponding to  $f_2^o$  are substituted into objective  $f_1$ , and the attained result is the anti-optimal result of objective  $f_1$ . Thus,  $f_1^{ao}$  has a higher system cost than  $f_1^o$ . The denominator  $f_1^{ao} - f_1^o$  normalizes the two objectives considered, which enables the aggregation of the two objectives.

$W_i$  is the preferential weight that reflects the relative importance for each objective and is a reflection of the interests of different societal sectors and public perceptions. The Analytic Hierarchy Process (AHP) (Saaty, 1980) is a popular method used to acquire the weights.

Constraint set

$$\sum_{l \in L} \sum_{i_l \in I_l} x_{i_l j}(\omega) \times \eta_l(\omega) = pr_j(\omega) \quad \forall j \in J, \omega \in \Omega \quad (5-4)$$

$$\sum_{m \in M} y_{jm}(\omega) = pr_j(\omega) \quad \forall j \in J, \omega \in \Omega \quad (5-5)$$

$$capr_j^L z_j \leq cap_j \leq capr_j^U z_j \quad \forall j \in J \quad (5-6)$$

$$pr_j(\omega) \leq cap_j \quad \forall j \in J, \omega \in \Omega \quad (5-7)$$

$$Y_{i_l} \leq yield_{i_l} \quad \forall i_l \in I_l, l \in L \quad (5-8)$$

$$Y_{i_l} \geq \sum_{j \in J} x_{i_l j}(\omega) \quad \forall i_l \in I_l, l \in L, \omega \in \Omega \quad (5-9)$$

$$\sum_{j \in J} y_{jm}(\omega) + q_m(\omega) = D_m \quad \forall m \in M, \omega \in \Omega \quad (5-10)$$

$$z_j = \{0,1\} \quad \forall j \in J \quad (5-11)$$

$$Y_i \geq 0 \quad \forall i \in I, l \in L \quad (5-12)$$

$$x_{ij}(\omega) \geq 0 \quad \forall i \in I, l \in L, j \in J, \omega \in \Omega \quad (5-13)$$

$$y_{jm}(\omega) \geq 0 \quad \forall j \in J, m \in M, \omega \in \Omega \quad (5-14)$$

$$cap_j \geq 0 \quad \forall j \in J \quad (5-15)$$

$$pr_j(\omega) \geq 0 \quad \forall j \in J, \omega \in \Omega \quad (5-16)$$

$$q_m(\omega) \geq 0 \quad \forall m \in M, \omega \in \Omega \quad (5-17)$$

Constraints (5-4) and (5-5) impose flow conservation constraints on refineries. Constraints (5-6) and (5-7) are refinery logic and capacity constraints. Feedstock procurement is limited by its availability in constraint (5-8). Inequality (5-9) requires all procured feedstocks to be delivered to biorefineries. Demand satisfaction is guaranteed by equality (5-10). Constraints (5-11)-(5-17) are integrality and non-negativity constraints.

### **5.3 Case Study**

California is of our particular interest due to the leading role in striving to reduce GHG and promote the use of alternative clean energy. A wide range of policies and programs have been launched to encourage low-carbon fuels. This section will entail the data used for this study.

### 5.3.1 Technical and Economic Data

Two types of biowaste resources – corn stover and forest residues, are considered in this study and both are abundant in California. A total of 28 sites were chosen as the candidate refinery locations based on a set of criteria considering the accessibility to water and transportation infrastructures and zoning requirements. Three different cost levels are assumed for these sites based on their differentiable land prices and labor costs. A set of 143 cities are considered as demand centers and they all have a population of at least 50,000. A road network consisting of local, rural, urban roads and major highways is used. The shortest distances between feedstock fields, refineries, and demand cities were calculated based on this network. The key parameters associated with the feedstock are shown in Table 5-2. All data other than specifically mentioned were adopted from (Parker et al., 2007).

**Table 5-2 Technical and Economic Inputs of Biofuel Supply Chain**

Feedstock inputs			
Feedstock types	Corn stover	Forest residues	
Total annual yields (thousand dry ton)	562	4,268	
Number of nodes at centroid	27	47	
Conversion rate (gallon/dry ton)	80.6	90.2	
Moisture content (% weight)	15	50	
Average procurement cost (\$/dry ton)	35	30	
Refinery inputs			
Categories (by fixed capital cost)	Low	Median	High
Number of candidate sites	15	9	4
Fixed capital cost (\$million)	6.20	6.80	7.40
Variable capital cost (\$/gallon)	0.314		
Production cost (\$/gallon) <sup>1</sup>	0.92		
Technology considered	LignoCellulosics Ethanol (LCE) via hydrolysis and fermentation conversion technology with Dilute Acid		

	pretreatment process		
Refinery capacity range (MGY)	60~100		
Transportation inputs			
Mode	Truck		
Categories (by type)	Corn stover	Forest residues	Ethanol
Cost	loading/unloading	\$5/wet ton	\$0.02/gallon
	Time dependent	\$29/hr/truckload	\$32/h/truckload
	Distance dependent	\$1.2/mile/truckload	\$1.3/mile/truckload
	Diesel Fuel (assumed)	\$2.5/gallon	
Truck capacity	24 wet tons <sup>2</sup>	17 wet tons <sup>2</sup>	8,000 gallons
Average travel speed (miles/hr)	40		

1. This is projected mid-term bioethanol production cost (Office of the Biomass Program, 2009)

2. Adopted from GREET model

Geographic distributions of feedstock and facilities are shown in geographic information system (GIS) maps in Figure 3-1 in Chapter 3. The annual feedstock yields and locations are aggregated at county or city levels to be integrated with transportation network data. The size of each dot is proportional to the feedstock quantity. Corn stover is mainly clustered in the central valley region. Forest residue is widely distributed across the state with higher concentration in the northern part. Potential refinery locations are evenly distributed across the state. High-cost sites are located in metropolitan areas, while the low-cost sites are in remote regions (e.g., the most northern and southern parts of the state). Demand centers are clustered in metropolitan areas. Ethanol demand in 2020 was set as the demand target in this study, which is projected to be 350 million gallons per year (MGY) state wide, given the current blend rate at E5.7. Proportional to the population, the total annual demand from the selected demand centers is 272MGY.

### 5.3.2 GHG Emission Estimates

We adopted classical, process-based LCA techniques in evaluating GHG emissions. To obtain satisfactory estimate, attention has been given to the choice of life stages to be considered. In this study, the CO<sub>2</sub> emissions resulting from the combustion of the biofuel by end users are assumed to be captured by the biomass during growth. Thus, the set of life-cycle stages considered in evaluating emissions in the cellulosic biofuel supply chain include feedstock procurement, feedstock delivery, biofuel production, and biofuel distribution. The life-cycle inventory associated with each process were identified and quantified by using the Argonne GREET model. Emissions of three greenhouse gases (i.e., CO<sub>2</sub>, CH<sub>4</sub>, and NO<sub>2</sub>) shown in Table 5-3 are grouped together in a single indicator in terms of carbon dioxide equivalent emissions (CO<sub>2</sub>-eq), based on the concept of global warming potentials (GWP) (BSI Group, 2011).

**Table 5-3 GHG Emission Estimates**

Emission		CO <sub>2</sub>	CH <sub>4</sub>	N <sub>2</sub> O	CO <sub>2</sub> -eq
Global warming potentials (GWP)		1	25	298	
Procurement (grams/dry ton)	Corn stover	18,143	24.86	0.22	18,830
	Forest residues	21,655	29.67	0.26	22,475
Production <sup>1</sup> (grams/gallon)	Corn stover	7	0.29	0.77	243
	Forest residues	230	2.15	0.89	549
Transportation (grams/mile/truckload)		2,437	3.34	0.06	2,537

1. Excludes byproduct of electricity and it shows average production emissions.

The low emission in biofuel production is because large amount of CO<sub>2</sub> emitted from burnt biomass offsets the absorbed CO<sub>2</sub> in the growing phase (Raphael et al., 2009). The emission from electricity generation as a by-product is out of the scope of the study

and thus omitted. Note that the production emissions in the table are default values (the mean value) in GREET model and they would fluctuate with conversion rates. The transportation emission is dependent on the distance traveled and the number of truckload.

### **5.3.3 Uncertainty in Estimating Conversion Rates**

Most existing studies have assumed that the conversion rate is fixed, which may not be able to hold for general as converting biomass to biofuel involves complicated physical and chemical processes. This study used LignoCellulosics Ethanol (LCE) via hydrolysis and fermentation conversion technology with Dilute Acid pretreatment process, in which chemical composition of the biomass, enzymes, and boiler efficiency may cause uncertainties in estimating conversion rates. Variations in conversion rate affect the decision-making and thus incorporating the uncertainty of conversion technology in managing the biofuel supply chain is important.

Brinkman et al. (2005) have suggested that the conversion rate of feedstock may follow a normal distribution with a deviation of 11 gallon/dry ton from the mean value at 20 and 80 percentiles, where  $\mu=80.6$  and  $90.2$  gallon/dry ton for corn stover and forest residue and  $\sigma=13.1$  gallon/dry ton. We then created a set of 10 discrete scenarios with equal probability to approximate the normal distribution as shown in Figure 5-1. Each scenario takes the same area size and the expected value is used as the conversion rate under that particular scenario. The scenario-dependent conversion rates are shown in Table 5-4. According to the GREET model (Wang et al., 2005), production emission varies with the conversion rate and thus the associated production emissions are scenario-

dependent in Table 5-4. Both the conversion rate and production GHG emission are the input data, which represent the conversion technology uncertainty.

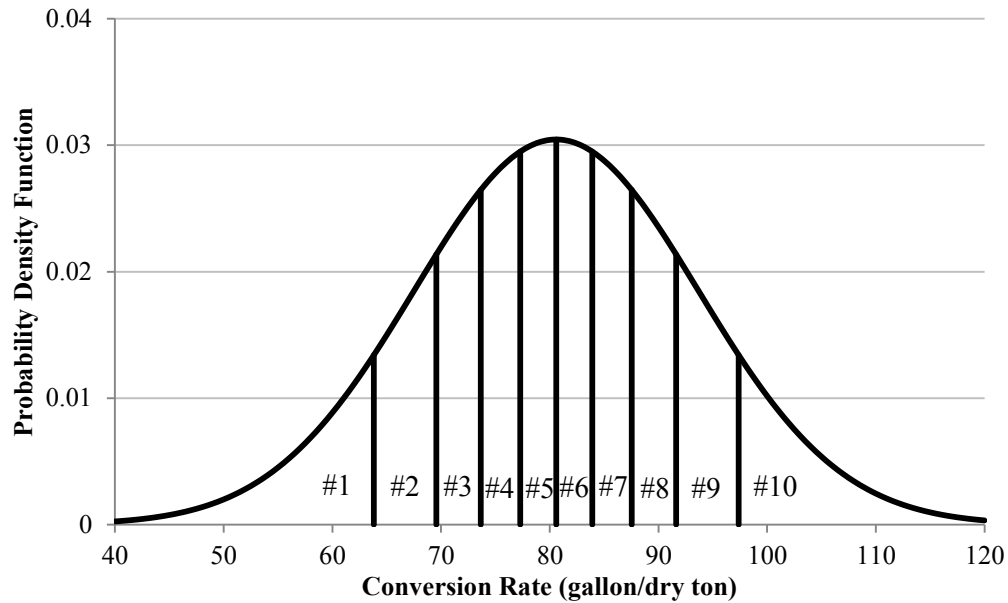


**Figure 5-1 Scenario Generations For Uncertain Conversion Rates Of Corn Stover**

**Table 5-4 Scenario-Dependent Conversion Rates and Emissions**

Scenario	Conversion rate		Production GHG emission	
	Corn stover	Forest residues	Corn stover	Forest residues
	gallon/dry ton		CO <sub>2</sub> -eq gram/gallon	
#1	58	67	333	638
#2	67	77	290	596
#3	72	81	271	578
#4	76	85	259	565
#5	79	89	248	554
#6	82	92	239	545
#7	86	95	230	536
#8	89	99	221	526
#9	94	104	211	515
#10	104	113	194	497

## 5.4 Results and Discussion

The compromise stochastic model was programmed in AMPL (Fourer et al., 2003) and solved using a commercial solver CPLEX. This study tends to focus on the analysis of effects of uncertainty on the multi-objective modeling.

### *Planning strategies by stochastic program vs. deterministic program*

In handling multiple possibilities of randomness, a common engineering approach is to examine each scenario separately. A solution generated with perfect information of the scenario is called wait-and-see (WS) solution and they are deterministic. In this study, there are ten WS solutions and they perform the best in their particular scenarios. However, WS solutions may vary drastically across scenarios and may not be able to find a representative solution. One remedy would be aggregating all scenarios into a representative scenario by using the expected value and then solve the corresponding deterministic problem. The solution is called the expected solution. These two deterministic approaches are conceptually simple and easy to implement, but may not be reliable given uncertain decision making environment.

**Table 5-5 System Planning Strategies and Outcomes**

		SP soln	Wait-and-See Solutions										Exp. soln	
			#1	#2	#3	#4	#5	#6	#7	#8	#9	#10		
Refinery Size (MGY)	#17	60	60	65	60	60	60	60	60	60	60	60	60	60
	#20	87	66	75	80	83	87	90	93	94	92	88	88	
	#22	65	60	72	72	69	65	62	60	60	60	60	63	
	#25	NA	60	NA	NA	NA	NA	NA	NA	NA	NA	NA	NA	NA



	#28	60	60	60	60	60	60	60	60	60	60	64	61
	Total capacity	272	306	272	272	272	272	272	273	274	272	272	272
Feed-stock proc. (million dry tons)	Corn stover	0.5	0.5	0.5	0.5	0.5	0.5	0.5	0.5	0.5	0.5	0.5	0.5
	Forest Residue	2.9	3.6	3.1	2.9	2.7	2.6	2.5	2.4	2.3	2.2	2	2.6
Total system cost (billion \$)		0.63	0.69	0.64	0.62	0.61	0.60	0.59	0.58	0.58	0.57	0.55	0.59
Total GHG emission (million tons of CO <sub>2</sub> -eq)		0.37	0.47	0.43	0.41	0.39	0.38	0.36	0.35	0.34	0.33	0.31	0.37

In this study, we compare our stochastic solution to the deterministic solutions by using the ten scenarios described in Table 5-4. The penalty cost is set at \$5/gallon to mandate the required level of in-state ethanol production. The weighting factors are assumed to be 0.8 and 0.2 for cost and GHG objectives (i.e.,  $W_1=0.8$  and  $W_2=0.2$ ), reflecting a higher preference on the cost reduction. Table 5-5 exhibits the resulted system planning strategies - system layout and feedstock procurement and outcomes of system costs and emissions. For example, the SP solution requires four biorefineries to be placed at locations #17, 20, 22, and 28, and their designed sizes are 60, 87, 65, 60MGY, respectively. The four biorefineries consume half million dry tons of corn stover and 2.9 million dry tons of forest residues.

As the WS based planning strategies vary with scenarios, a method that produces single strategy is in need. Both the stochastic and expected solutions place refineries at the same locations and have the same total capacity with different allocations. This is because the demand is fixed and the varied conversion rates only affect the amount of feedstocks procured for biofuel production, particularly from forest residues. Corn stover

is clustered in central valley area and the remotely located is abandoned for economics and environmental purposes.

### *Solution performance evaluations*

The planning strategies of SP and expected solutions are evaluated against the same ten scenarios to understand the differences in handling uncertainty. We set the second objective to prefixed emission inventory levels between 0.1 and 0.45 million tons of CO<sub>2</sub> eq, which are the lowest and highest levels across all possible scenarios. The multi-objective model becomes a single-objective model of minimizing cost with emission caps in the constraint set. The system cost of both solutions under each of the ten scenarios is attained and plotted in Figure 5-2.

The horizontal axis in Figure 5-2 represents the prefixed emission levels and the vertical axis represents relative system cost saved by using the SP solution over the expected solution. The positive values indicate that the SP solution outperforms the expected solution, vice versa. The top and bottom bars of the box plot indicate the maximum and minimum cost savings. The upper and lower edges of boxes represent the cost savings at 75 and 25 percentiles, respectively. For instance, when emission cap is 0.45 million tons of CO<sub>2</sub> eq. (the most left box in the figure), the SP solution can save up to 10.6% and there is a 25% of chance save at least 6.6%.

The cost savings vary with the prefix emission levels. Although SP solution is more costly than the expected solution shown mainly due to the difference in feedstock procurement strategy as indicated in Table 5-5, in general it outperforms the expected

solution when higher emission is allowed. This is because the SP solution features higher in-state production, which is cheaper than importing fuels but resulting higher GHG. When the prefixed GHG emission level decreases, the increasing stringent emission requirement forces the system to raise fuel imports, regardless of the in-state production capacity, and thus the SP solution becomes less preferable.

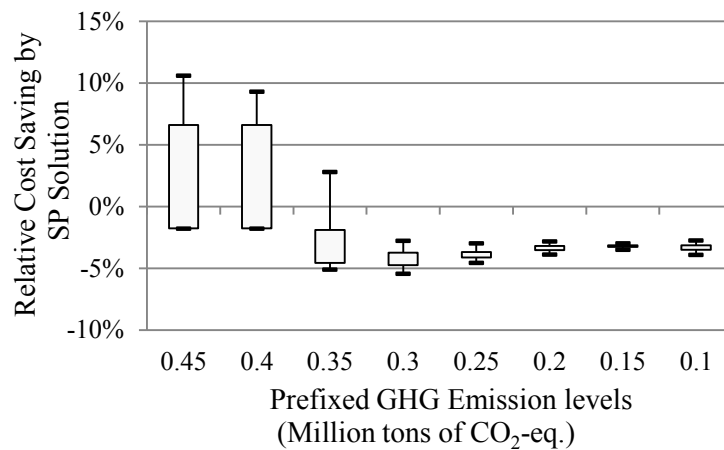


**Figure 5-2 Box Plots Of Relative Cost Savings By The Sp Solution**

## 5.5 Summary

In Chapter 5, I developed an advanced model to integrate sustainability concept and uncertainty into biofuel supply chain management. A mixed-integer, compromise stochastic programming model that combines strategic and tactical system decision making has been developed, with a goal of achieving the best-compromise solution in achieving economic and environmental sustainability under the uncertainty of conversion technology. Through the analysis, I found that (1) uncertainty with conversion technology has impact on system planning and management, especially on feedstock

procurement strategy; (2) stochastic method over the deterministic methods provides more cost-effective solutions, but the effects may vary with the GHG emission restrictions.

# CHAPTER 6 MULTISTAGE SEQUENTIAL PLANNING OF LONG-TERM BIOFUEL SUPPLY CHAIN PLANNING UNDER UNCERTAINTIES

## **6.1 Background**

This study is focused on a long-term sequential establishment of an efficient biofuel supply chain system against uncertainty by integrating the planning and operations of an entire supply chain.

A long-term planning of a supply chain needs to take into account the spatial distributions of involving infrastructures coupled with the effects of time dynamics. In addition, strategic supply chain planning and management needs to adapt to the uncertainties that could be caused by weather variations, natural or man-made disasters, technology improvement, or even the changes in public policy and mandates on biofuels. Proactive strategic decisions for hedging against uncertainty thus are crucial in mitigating the adverse impacts of uncertainty and achieving economic effectiveness. In the context of a multi-period or multistage planning, uncertainty is revealed in a sequential manner that is distinct from a single-stage or snapshot planning in which uncertainty is assumed to be revealed only once. *The challenge is how to make sequential decisions under uncertainty that is not known a priori over time.*

Among these literatures on biofuel supply chain design shown in Chapter 2, the study (Dal-Mas et al., 2011), perhaps, is most relevant to our study, which is concerned about a strategic design of biofuel supply chain for multiple years. However, the two-

stage stochastic programming framework that is adopted in their study comes with two major approximations. First, the planning decisions are made only once at the beginning of the entire planning horizon. This assumption is more defensible for a one-shot or single-period system design. In a transition state where infrastructure is built sequentially over time, such as biofuel supply chain, a dynamic model that captures the growth of the system should be adopted. Secondly, in terms of modeling evolving information, it is assumed that the complete information of the uncertain supply chain parameters is immediately revealed once the planning decisions are made at the beginning of the planning horizon. This simplification helps reduce the modeling complexity, but may cause deviation from the reality. Realistically, we should model information of the uncertain parameters in a sequential manner, meaning that the random parameters become known gradually over time. A multistage stochastic programming framework thus would suit better.

Multistage stochastic supply chain design problems aim at finding the best supply chain planning strategies adaptive to time dynamics, including location decisions, procurement, production, and distribution to support efficient operations of the whole supply chain (Nickel et al., 2012). Readers are referred to (Melo et al., 2009) for general supply chain design and management problems and to (Nickel et al., 2012) in particular for recent progress in multistage stochastic supply chain design problems. The multistage stochastic programming method is not particularly new and has been used in a range of applications, including electricity power system (Hochreiter and Wozabal, 2010; Pereira and Pinto, 1991; Shiina and Birge, 2003), financial portfolio management (Consigli and

Dempster, 1998; Golub et al., 1995; Gulpinar et al., 2002; Kouwenberg, 2001), and water resource management (Archibald et al., 1999; Li et al., 2006; Li et al., 2008; Watkins et al., 2000; Zhou et al., 2013).

The key feature that distinguishes this study from most existing efforts on biofuel supply chain is the integration of physical design and operational management as a whole in seeking long-term reliable strategies against uncertainty. Facility spatiality, time dynamics, and uncertainty are integrated into a multistage stochastic programming framework. Optimal strategies on refinery, feedstock procurement, biofuel production, and feedstock and fuel deliveries are sought simultaneously to achieve the least expected total cost. The problem is formulated as a mixed integer multistage stochastic programming problem with integer recourse based on the paths in a scenario tree. Two solution algorithms based on nested decomposition (ND) (Birge and Louveaux, 1997) and maximal non-dominated cuts (Sherali and Lunday, 2013) are developed to overcome the computational challenges of the problem. We justify the proposed model and evaluate the solution algorithms using hypothetical numerical experiments. A case study of South Carolina is used to demonstrate the applicability of the model in evaluating the economic potential and system effectiveness of converting forest residues to bioethanol and phased supply chain infrastructure system expansions over 15 years.

The remainder of the study is organized as follows. The multistage stochastic model and the corresponding solution methods are presented and discussed in Section 6.2. Section 6.3 presents two case studies. The case study results are presented in Section 6.4. Finally, I will summarize the study in Section 3.5.

## **6.2 Methods**

In this section, I first describe the main characteristics of the studied problem, including the structure and dimensions of the biofuel supply chain, as well as the main features of the planning and operational decision variables. I will then discuss the evolution of uncertainty and modeling assumptions, followed by the complete model formulation. Finally I will develop corresponding solution methods.

### **6.2.1 Modeling Background**

The multi-period biofuel supply chain designs spans over both spatial and temporal dimensions. The spatial dimension comes from the geographical distribution of the feedstock supply, facility locations, and demand sites, including the following infrastructure layers:

- Feedstock fields, where biomass is collected;
- Refineries, where biomass is converted into biofuel; and
- City gates, where blended fuels are distributed to consumer markets.

Note that the supply chain ends at city gates and that further fuel dispensing to individual refueling stations is omitted in this study. The temporal dimension is brought by the multi-year planning. The planning horizon is typically divided into stages, denoted by  $t=0, \dots, T$ , where zero is the beginning of the planning horizon and  $T$  is the final stage. Note that the length of a time stage varies, e.g., one year or multiple years. The effects of



feedstock seasonality and storage facilities for feedstock and biofuels are neglected as decisions are aggregate on an annual basis in this study.

Strategic planning of this supply chain includes designing the physical configuration of the supply chain system such as locations and the sizes of the production facilities, while operational decisions include procurement strategy of the feedstock, production amount, and transportation flows between different layers of the supply chain. Designing such a complex system is not trivial due to several tradeoffs in the system. For example, a centralized facility takes advantage of economies of scale, but may result in higher transport cost. A choice of larger refinery capacity may be costly at the beginning, but may mitigate the risk of future fuel supply shortage. By integrating the physical design of supply infrastructure and the operations, this study captures the system interdependence and balances the tradeoffs in both temporal and spatial dimensions.

### **6.2.2 Planning and Operational Decisions under Uncertainty**

In addition to system interdependence and time dynamics, biofuel supply chains are vulnerable to uncertainties. Handling uncertainty imposes another modeling challenge, especially for a long-term system planning. Planning decisions are usually made before the uncertain supply chain parameters (e.g., feedstock supply or fuel demand) become known. For a multistage planning problem, planning decisions are made sequentially and once implemented, they are not easily modified. On the other hand, operational decisions can be adjusted based on the actual realizations of uncertain parameters. This feature fits well in a multistage stochastic programming framework, which recognizes the non-

anticipativity of planning decisions for each stage while allowing recourse for operational decisions in the subsequent stages (Birge and Louveaux, 1997). In particular, the planning decisions are assumed to be made at the beginning of each stage  $t=1,\dots,T$  or the end of stage  $t-1$  and once made the decisions are not able to change during the stage  $t$ . The operational decisions for each stage  $t=1,\dots,T$  are made during the current stage  $t$ , in response to the planning decisions.

The *planning decisions* include:

- locations of new refineries (integer variables), and
- capacity expansion of existing refineries (integer or continuous variables).

The *operational decisions* (all continuous variables) include:

- fuel production,
- feedstock procurement,
- feedstock and fuel transportation, and
- fuel imports at penalty if demand is not satisfied.

### 6.2.3 Evolvement of Uncertainty

Uncertainty is described by a set of discrete scenarios. For the entire planning horizon, a tree of scenarios is built, such as the scenario tree shown in Figure 6-1 for three time stages. Without loss of generality, biofuel demand is assumed uncertain and the exact demand is realized at the beginning of each stage. For illustration purpose, an *uncertainty realization*, denoted by  $\xi_t \in \Xi_t$ ,  $t=1,\dots,T$ , is either high or low, which is represented by a

*branch arc* of the tree. A  $t$ -stage scenario, denoted by  $k_t$ , consists of sequence of uncertainty realizations  $(\xi_1, \dots, \xi_t)$ , and  $k_t \in \Xi_1 \times \Xi_2 \times \dots \times \Xi_t, t=1, \dots, T$ . Thus, a scenario is described by a path on the tree from root (i.e., the beginning of the planning horizon) to stage  $t$ . For example, there are four scenarios in stage 2 represented by the four nodes. Node (2, 1) describes a scenario of having high demands in both the first and second stages. At stage 0, no uncertainty has been revealed, and the 0-stage scenario  $k_0$ , is a dummy scenario for the purpose of modeling formality. We denote by  $K_t$  the set of  $t$ -stage scenarios,  $K_t \equiv \Xi_1 \times \Xi_2 \times \dots \times \Xi_t$  and  $K_t = K_{t-1} \times \Xi_t, t=1, \dots, T$ , assuming that uncertainty realizations are independent over time. Each  $t$ -stage scenario  $k_t, t=1, \dots, T$  has a unique parent (also known as ancestor)  $(t-1)$ -stage scenario, denoted as  $a_{k_t}$ . For example, the scenario described by node (2, 2) has only one parent scenario described by node (1, 1). However, each  $t$ -stage scenario  $k_t, t=0, \dots, T-1$  has a set of child (also known as descendent) scenarios in stage  $t+1$ , denoted by set  $D_{k_t}$ . For example, the scenarios described by nodes (3, 3) and (3, 4) are both the child scenarios of the scenario described by node (2, 2).

The multistage stochastic program is developed based on the paths in the scenario tree. In particular, the planning decisions for a time stage  $t=1, \dots, T$  are made at the beginning of time stage  $t$  or equivalently the end of time stage  $t-1$  when the scenario  $k_{t-1}$  is fully realized. For example, the planning decision for time stage 3 will be made after 2-stage scenario  $k_2$  is fully revealed. Note that the planning decisions for the last stage are

made under the scenario  $k_{T-1}$ . On the other hand, the operational decisions for each time stage  $t$  are assumed to be made under scenario  $k_t$ . For example, the operational decisions for stage 3 are made under 3-stage scenario  $k_3$ .

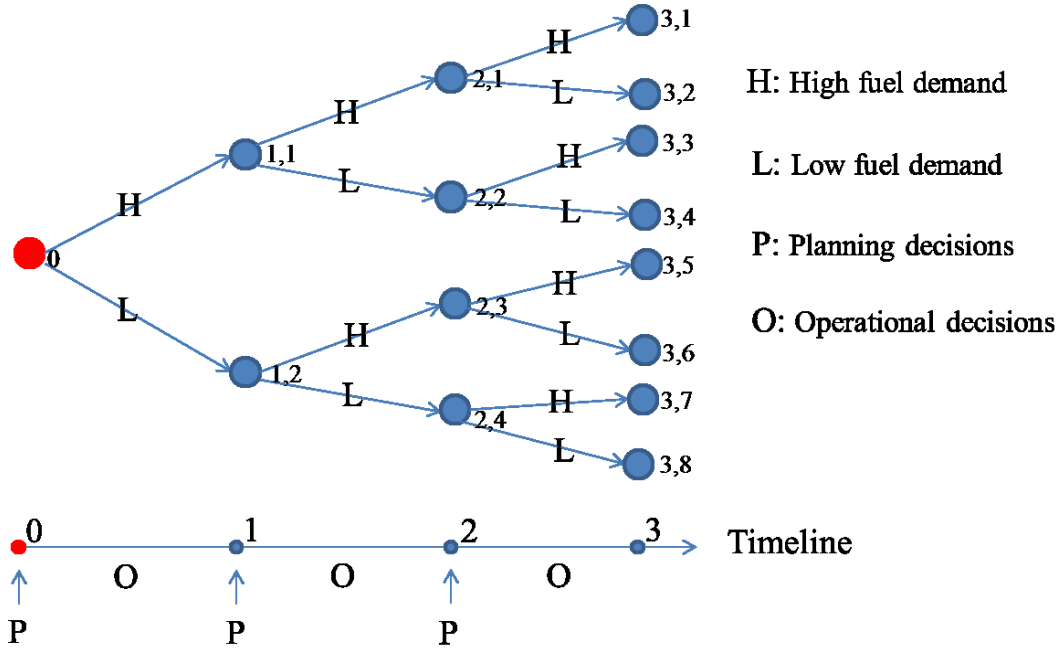


**Figure 6-1 A Scenario Tree with Three Periods and Two Realizations for Each Period**

We denote by  $p_{k_t}$  the probability of the  $t$ -stage scenario  $k_t$ ,  $t=0,\dots,T$  and  $\bar{p}_{\xi_t}$  the probability of uncertainty realization  $\xi_t$ ,  $t=1,\dots,T$ . Given that uncertainty realizations are independent between time stages, the probability of a  $t$ -stage scenario  $p_{k_t}$  (except for stage 0) can be represented by  $p_{k_t} = \prod_{t'=1,\dots,t} \bar{p}_{\xi_{t'}}$  and  $\sum_{k_t \in K_t} p_{k_t} = 1$ ,  $t=0,\dots,T$ . For example, if both demand realizations as shown in Figure 1 have equal probabilities, the probability

of each 1-stage scenario  $k_t$  (a total of two scenarios) is 0.5, i.e.,  $p_{k_t}=0.5$ . The probabilities of each 2- and 3-stage scenarios (totaling four and eight scenarios, respectively) are 0.25 ( $= 0.5^2$ ) and 0.125 ( $= 0.5^3$ ), respectively.

#### 6.2.4 Mathematical Formulation

A multistage mixed-integer stochastic programming model is formulated. Here we present it in a general form. An exact formulation is problem specific and dependent on a number of factors, including network topology, uncertainty sources, and planning horizon. The general formulation presented in this section demonstrates the critical properties of the multistage stochastic program of the biofuel supply chain, which helps develop appropriate solution methods as discussed in Section 6.3. All parameters and decision variables used in the model are defined first, followed by the model presented in (6-1)-(6-4).

Parameters:

$\xi_t$	Uncertainty realization (defined in Section 6.2.3) at stage $t$ , $\xi_t \in \Xi_t$ , $t=1, \dots, T$
$k_t$	$t$ -stage scenario (defined in Section 6.2.3), $k_t \in K_t$ , $t=0, \dots, T$
$p_{k_t}$	Probability of the $t$ -stage scenario $k_t \in K_t$ , $t=0, \dots, T$
$a_{k_t}$	Parent scenario of scenario $k_t \in K_t$ , $t=1, \dots, T$
$c_{k_t}^P$	Planning decision cost vector, given $k_t \in K_t$ , $t=0, \dots, T-1$

- $c_{k_t}^O$  Operational decision cost vector, given  $k_t \in K_t$ ,  $t=1, \dots, T$
- $A_t$  Recourse matrix for  $t$ -stage planning decisions,  $t=0, \dots, T-1$
- $B_t$  Recourse matrix for  $t$ -stage operational decisions,  $t=1, \dots, T$
- $R_{k_t}$  Technology matrix for constraints on planning decisions,  $k_t \in K_t$ ,  $t=1, \dots, T-1$
- $S_{k_t}$  Technology matrix for constraints on operational decisions,  $k_t \in K_t$ ,  $t=1, \dots, T$
- $b_{k_t}$  Right-hand-side matrix for constraints on planning decisions,  $k_t \in K_t$ ,  
 $t=0, \dots, T-1$
- $d_{k_t}$  Right-hand-side matrix for constraints on operational decisions,  $k_t \in K_t$ ,  
 $t=1, \dots, T$

Decisions:

- $z_{k_t}$  Planning decision vector made at the beginning of stage  $t+1$ ,  $t=0, \dots, T-1$ ,  
 $k_t \in K_t$ .
- $x_{k_t}$  Operational decision vector made during stage  $t$ ,  $t=1, \dots, T$ ,  $k_t \in K_t$ .

### Multistage Stochastic Biofuel Supply Chain Problem

Minimize:

$$c_{k_0}^P z_{k_0} + E_{\xi_1} \left\{ c_{k_1}^P z_{k_1} + c_{k_1}^O x_{k_1} + \dots + E_{\xi_t} \left\{ c_{k_t}^P z_{k_t} + c_{k_t}^O x_{k_t} + \dots + E_{\xi_T} \left\{ c_{k_T}^O x_{k_T} \right\} \right\} \dots \right\} \quad (6-1)$$

Subject to:

$$A_0 z_{k_0} = b_{k_0} \quad (6-2)$$

$$-R_{k_t} z_{k_{t-1}} + A_t z_{k_t} = b_{k_t} \quad \forall k_t \in K_t, k_{t-1} = a_{k_t}, t=1, \dots, T-1 \quad (6-3)$$

$$-S_{k_t} z_{k_{t-1}} + B_t x_{k_t} = d_{k_t} \quad \forall k_t \in K_t, k_{t-1} = a_{k_t}, t=1, \dots, T \quad (6-4)$$

$$z_{k_t} \in \mathbb{R} \quad \mathbb{Z} \quad \forall k_t \in K_t, t=0, \dots, T-1$$

$$x_{k_t} \geq 0 \quad \forall k_t \in K_t, t=1, \dots, T$$

The objective (6-1) minimizes the total cost of planning and operations of biofuel supply chain over the entire planning horizon. As uncertainty is revealed over time, both planning and operational decisions of current stage are dependent on the planning decisions made *a priori* and thus nested in the objective function (6-1). In addition, importing biofuels is allowed to supplement unsatisfied fuel demand with a penalty cost.

Constraint (6-2) describes physical (e.g., candidate locations) and economic (e.g., budget) constraints in establishing refineries at the beginning of planning horizon. Constraint set (6-3) depicts relationships on planning decisions  $z_{k_{t-1}}$  and  $z_{k_t}$  in two consecutive time stages on new refineries or capacity expansions. Constraint set (6-4) describes relationships between planning decisions ( $z_{k_{t-1}}$ ) and operational decisions ( $x_{k_t}$ ) in each time stage, e.g., the logic relationship between the existence of refineries and biofuel production within designed capacity. This constraint set also describes relationships among operational decisions themselves, mainly on feedstock and biofuel flow conservations at fields, refineries, and demand centers. Note that the recourse matrices  $A_t$  and  $B_t$  in the model are assumed to be fixed and independent of uncertainty scenarios while all other parameters are scenario dependent.

For a discrete set of uncertainty scenarios, this multistage stochastic program can be solved by deriving the deterministic equivalent program (Louveaux, 1986). The complexity can be greatly reduced if a multistage stochastic program possess the property of block-separable recourse (Louveaux, 1986).

**Proposition 1:** *The multistage stochastic program presented in (6-1) - (6-4) has the block-separable recourse property.*

**Proof:** According to the definition 2.1 of the property of block-separable recourse (Shiina and Birge, 2003), a multistage stochastic program has block-separable recourse if the following two conditions are satisfied. *First*, for all stages, decision vectors can be decomposed to aggregate and detailed level decisions, which are  $z_{k_t}$ ,  $k_t \in K_t$ ,  $t=0, \dots, T-1$ , and  $x_{k_t}$ ,  $k_t \in K_t$ ,  $t=1, \dots, T$ , respectively in our model. *Second*, the structures of objective function and constraint matrices at each stage satisfy the following two partitions:

(1) For each  $t$ -stage scenario  $k_t \in K_t$ ,  $t=0, \dots, T$ , the objective function can be written in the form of  $f_{k_t} = c_{k_t}^P z_{k_t} + c_{k_t}^O x_{k_t}$ ; and

(2) The constraint matrices conform with the  $(z_{k_t}, x_{k_t})$  separation as:

$$\begin{bmatrix} -R_{k_t} & 0 \\ -S_{k_t} & 0 \end{bmatrix} \times \begin{bmatrix} z_{k_{t-1}} \\ x_{k_{t-1}} \end{bmatrix} + \begin{bmatrix} A_t & 0 \\ 0 & B_t \end{bmatrix} \times \begin{bmatrix} z_{k_t} \\ x_{k_t} \end{bmatrix} = \begin{bmatrix} b_{k_t} \\ d_{k_t} \end{bmatrix}. \quad \square$$

**Proposition 2** (Louveaux, 1986): *A multistage stochastic program with block separable recourse is equivalent to a two-stage stochastic program, where the first-stage is the*



extensive form of the aggregate level problems, and the value function of the second stage is the sum (weighted by the appropriate probabilities) of the detailed level recourse functions for all  $t$ -stage scenarios.

From the proposition 2, the multistage stochastic program with the property of *block-separable recourse* can be transformed into a two-stage stochastic program with recourse. The problem turns out to be the one that has first stage mixed integer variables and continuous second stage variables. The deterministic equivalent for the multistage stochastic program with block-separable recourse can be written as (6-5)-(6-7).

### Deterministic Equivalent for the Multistage Stochastic Biofuel Supply Chain

**Problem:**

$$\text{Minimize: } \sum_{t=0}^{T-1} \sum_{k_t \in K_t} p_{k_t} c_{k_t}^P z_{k_t} + \sum_{t=0}^{T-1} \sum_{k_t \in K_t} G_{k_t} \quad (6-5)$$

Subject to:

Including constraints (6-2)-(6-3)

$$G_{k_t} = \min_{k_{t+1} \in D_{k_t}} \sum p_{k_{t+1}} g_{k_{t+1}} \quad \forall k_t \in K_t, t=0, \dots, T-1 \quad (6-6)$$

$$g_{k_{t+1}} = \min \left\{ c_{k_{t+1}}^O x_{k_{t+1}} \mid B_{t+1} x_{k_{t+1}} = d_{k_{t+1}} + S_{k_{t+1}} z_{k_t}, x_{k_{t+1}} \geq 0 \right\} \quad \forall k_t \in K_t, k_{t+1} \in D_{k_t}, t=0, \dots, T-1 \quad (6-7)$$

$$z_{k_t} \in \mathbb{R} \quad \mathbb{Z} \quad \forall k_t \in K_t, t=0, \dots, T-1$$

In the objective function (6-5), the first term is the total expected planning cost over time weighted by the corresponding probabilities and the second term is the total expected operational cost, which is a sum of recourse functions over all stages. The recourse function is written in (6-6) for each stage. The operational cost  $g_{k_{t+1}}, k_{t+1} \in D_{k_t}$  is defined in (6-7) for each scenario.

## **6.2.5 Solution Methods**

Nested decomposition (ND) can be readily applied to solve block-separable multistage stochastic linear programs (Louveaux, 1986). We compose the deterministic equivalent program into a mixed integer master problem and linear subproblems. The ND is presented in Section 6.2.5.1. It is integrated with strategically generated maximal non-dominated cuts (Sherali and Lunday, 2013) for improved decomposition convergence in Section 6.2.5.2.

### **6.2.5.1 Nested Decomposition (ND)**

Nested decomposition (Birge, 1985) uses an outer linearization approximation based on the L-shaped method for two-stage stochastic programs (Slyke and Wets, 1969). ND is to approximate recourse functions based on the duality theory of linear programs, which has been primarily used to solve quadratic multistage program (Louveaux, 1980) and linear multistage program (Birge, 1985) and has been improved by developing a parallel implementation method by Birge et al. (1996) to solve large-scale problems. The properties of this method are explicitly elucidated in (Birge and Louveaux, 1997).

Another series of algorithmic studies focuses on reducing scenario size. For example, Pereira and Pinto (1991) uses stochastic dual dynamic programming method to hedge against an exponential increase in the number of states by approximating recourse functions of a stochastic dynamic program with piecewise linear functions, which is recently enhanced by the abridged nested decomposition method (Donohue and Birge, 2006).

All those solutions are limited to the problems with continuous recourse and may not be applicable to solve a stochastic program with integer recourse, as the cuts in those decomposition methods are generated based on the duality theory of linear programs. However, if a multistage stochastic program holds the special block-separability property, ND can be readily applied to solve the derived two-stage stochastic program that has first stage mixed integer variables and continuous second stage variables such that the integer recourses are lifted (Louveaux, 1986). Note that the first stage still keeps a multistage nested structure, but it becomes more tractable due to the reduced problem size. The second stage consists of independent linear subproblems, which can be effectively handled by any off-the-shelf solvers (e.g., CPLEX). Successful applications of ND in solving multistage stochastic programs include a power system expansion problem (Shiina and Birge, 2003) and a financial portfolio management problem (Edirisinghe and Patterson, 2007).

In this study, our deterministic equivalent problem (6-5)–(6-7) is decomposed into (i) a *reduced master problem* (RMP) that contains the first-stage mixed integer decision variables and new continuous variable vector  $\theta_k$  that approximates recourse functions

$G_{k_t} = \min \sum_{k_{t+1} \in D_{k_t}} p_{k_{t+1}} g_{k_{t+1}}$ ,  $k_t \in K_t$ ,  $t=0, \dots, T-1$  in (6-6), and (ii) a series of subproblems, each of which contains only second-stage continuous decisions. As unsatisfied biofuel demand is to be fulfilled by using imported biofuels with a penalty cost, this problem has a *relatively complete recourse* and feasibility cut constraint can thus be omitted.

**Reduced Master Problem (RMP):**

$$\text{Minimize: } \sum_{t=0}^{T-1} \sum_{k_t \in K_t} p_{k_t} c_{k_t}^P z_{k_t} + \sum_{t=0}^{T-1} \sum_{k_t \in K_t} \theta_{k_t} \quad (6-8)$$

Subject to:

$$A_0 z_{k_0} = b_{k_0} \quad (6-2)$$

$$-R_{k_t} z_{k_{t-1}} + A_t z_{k_t} = b_{k_t} \quad \forall k_t \in K_t, k_{t-1} = a_{k_t}, t=1, \dots, T-1 \quad (6-3)$$

$$\theta_{k_t} \geq \sum_{k_{t+1} \in D_{k_t}} p_{k_{t+1}} \bar{\pi}_{k_{t+1}, n} (d_{k_{t+1}} + S_{k_{t+1}} z_{k_t}) \quad \forall k_t \in K_t, t=0, \dots, T-1, n=1, \dots, N \quad (6-9)$$

$$z_{k_t} \in \mathbb{R} \quad \mathbb{Z} \quad \forall k_t \in K_t, t=0, \dots, T-1$$

In this formulation, the recourse functions are not known explicitly in advance. Thus, the optimality cuts (6-9) are added to approximate it, where  $n$  is the index of the number of optimality cuts  $N$ . The optimal solution to the master problem is obtained by solving the mixed integer program. Let  $\bar{z}_{k_t}$  and  $\bar{\theta}_{k_t}$ ,  $\forall k_t \in K_t$ ,  $t=0, \dots, T-1$ , be the optimal solutions to the master problem. Then each subproblem for  $(t+1)$ -stage scenario  $k_{t+1} \in D_{k_t}$

is solved at the optimal solution of the master problem. The dual subproblem is presented in (6-10) – (6-11), in which  $\pi_{k_{t+1}}$  is dual vector associated with the constraint in (6-7).

**Dual subproblem (SP) for (t+1)-stage scenario,  $k_{t+1} \in D_{k_t}, k_t \in K_t, t=0, \dots, T-1,$**

$$g_{k_{t+1}}^D = \max \pi_{k_{t+1}}^T (d_{k_{t+1}} + S_{k_{t+1}} \bar{z}_{k_t}) \quad (6-10)$$

Subject to

$$B_{t+1}^T \pi_{k_{t+1}} \leq c_{k_{t+1}}^O, \pi_{k_{t+1}} \in \mathbb{R} \quad (6-11)$$

Since the primal problem is feasible due to the relatively complete recourse property, the feasible region (6-11) is bounded and nonempty according to the duality theory so that there is no extreme ray in the feasible region. Let  $\bar{\pi}_{k_{t+1}}$  be the optimal solution to the SP and  $\bar{g}_{k_{t+1}}^D$  be the attained optimal objective value  $k_{t+1} \in D_{k_t}$ . If  $\bar{\theta}_{k_t} < \sum_{k_{t+1} \in D_{k_t}} p_{k_{t+1}} \bar{g}_{k_{t+1}}^D$ , the optimality cut (6-9) is added to the RMP and updates  $N = N + 1$ .

The ND for the multistage stochastic model is summarized as following:

**Step 0. Initialize bounds:**

Set Lower bound (LB) =  $-\infty$ , Upper bound (UB) =  $+\infty$ , and tolerance error =  $\varepsilon$ .

**Step 1. Solve the master problem:**

Solve the RMP problem, and update optimal solution values  $\bar{z}_{k_t}$  and  $\bar{\theta}_{k_t}$ ,  $\forall k_t \in K_t$

$$, t=0, \dots, T-1; \text{ Set LB} = \sum_{t=0}^{T-1} \sum_{k_t \in K_t} p_{k_t} c_{k_t}^P \bar{z}_{k_t} + \sum_{t=0}^{T-1} \sum_{k_t \in K_t} \bar{\theta}_{k_t} .$$

**Step 2. Solve the subproblems:**

Solve the SP for  $(t+1)$ -stage scenario,  $k_{t+1} \in D_{k_t}, k_t \in K_t, t=0, \dots, T-1$ , and update

corresponding optimal solution value  $\bar{\pi}_{k_{t+1}}$  and objective value  $\bar{g}_{k_{t+1}}^D$ ; Set UB =

$$\sum_{t=0}^{T-1} \sum_{k_t \in K_t} p_{k_t} c_{k_t}^P \bar{z}_{k_t} + \sum_{t=0}^{T-1} \sum_{k_t \in K_t} \sum_{k_{t+1} \in D_{k_t}} p_{k_{t+1}} \bar{g}_{k_{t+1}}^D .$$

**Step 3. Add optimality cuts:**

If  $\bar{\theta}_{k_t} < \sum_{k_{t+1} \in D_{k_t}} p_{k_{t+1}} \bar{g}_{k_{t+1}}^D$  for any  $t$ -stage scenario  $k_t \in K_t$ ,  $t=0, \dots, T-1$ , the optimality

cut (6-9) is added to the RMP.

**Step 4. Convergence check:**

If  $(\text{UB} - \text{LB})/\text{UB} < \varepsilon$ , then stop; otherwise go to Step 1.

### 6.2.5.2 Nested Decomposition with Maximal Non-dominated Cuts (ND-

### Max)

To accelerate the convergence of decomposition method, Magnanti and Wong (1981); (1990) set forth a seminal work on generating *non-dominated* or *Pareto optimal* cuts to tighten the Benders cuts. Their work however possesses potential difficulties, as highlighted in later studies (Mercier et al., 2005; Papadakos, 2008; Santoso et al., 2005), which are involved in searching “core points” and solving a two-fold increase in the

number of linear programs for the generation of cuts. Sherali and Lunday (2013) proposed a new algorithmic strategy that utilizes a preemptively small perturbations to generate *maximal* non-dominated Benders cuts to improve the effectiveness of decomposition methods. Although the maximal non-dominated cuts is not as strict as the non-dominated cuts, it is expected to be more direct and computationally effective (Sherali and Lunday, 2013). Here we adopt the maximal non-dominated cuts to accelerate the convergence of the ND in section 6.2.5.1.

Let us revisit the SP in (6-10)-(6-11). When the SP is degenerate, there may exist multiple optimal solutions to the SP given the first-stage decision  $\bar{z}_{k_t}$  from the RMP. We denote by  $\bar{\Pi}_{k_{t+1}}, k_{t+1} \in D_{k_t}, k_t \in K_t, t=0, \dots, T-1$ , the set of optimal solution as:

$$\bar{\Pi}_{k_{t+1}} \equiv \left\{ \pi_{k_{t+1}} \in \Pi_{k_{t+1}} \mid g_{k_{t+1}} = \bar{g}_{k_{t+1}} \right\}, \text{ where } \Pi_{k_{t+1}} \equiv \left\{ \pi_{k_{t+1}} \in \mathbb{R} \leq c_{k_{t+1}}^o \right\} \quad (6-12)$$

Given  $\pi_{k_{t+1}} \in \bar{\Pi}_{k_{t+1}}$ , the optimality cut (6-9) can be re-written as:

$$\theta_{k_t} \geq \sum_{k_{t+1} \in D_{k_t}} p_{k_{t+1}} \left( \pi_{k_{t+1}} d_{k_{t+1}} + \sum_{j=1}^m \pi_{k_{t+1}} s_{k_{t+1},j} z_{k_t} \right) \quad (6-13)$$

where  $s_{k_{t+1},j}$  denotes the  $j^{\text{th}}$   $j=1, \dots, m$ , column of matrix  $S_{k_{t+1}}$ .

**Definition of a Maximal Non-dominated Cut** (Sherali and Lunday, 2013): for (6-13) to be “non-dominated, or more distinctly, to be maximal, there must not exist any  $\pi'_{k_{t+1}} \in \bar{\Pi}_{k_{t+1}}$  so that  $\pi'^T_{k_{t+1}} d_{k_{t+1}} \geq \pi^T_{k_{t+1}} d_{k_{t+1}}$  and  $\pi'^T_{k_{t+1}} s_{k_{t+1},j} \geq \pi^T_{k_{t+1}} s_{k_{t+1},j}$ ,  $j=1, \dots, m$ , with at least one of these  $(m+1)$  inequalities being strict”.

The generation of the maximal non-dominated cuts is considered as obtaining a Pareto optimal solution to a multi-objective linear program in (6-14).

$$\text{Maximize } \left\{ \pi_{k_{t+1}}^T d_{k_{t+1}}, \pi_{k_{t+1}}^T s_{k_{t+1},1}, \pi_{k_{t+1}}^T s_{k_{t+1},2}, \dots, \pi_{k_{t+1}}^T s_{k_{t+1},m} : \pi_{k_{t+1}} \in \bar{\Pi}_{k_{t+1}} \right\} \quad (6-14)$$

The multi-objective program can be solved by using the weighted-sum method,

$$\text{Maximize } \left\{ \pi_{k_{t+1}}^T d_{k_{t+1}} + \sum_{j=1}^m \pi_{k_{t+1}}^T s_{k_{t+1},j} \lambda_j : \pi_{k_{t+1}} \in \bar{\Pi}_{k_{t+1}}, \forall \lambda_j \in \mathbb{R}, m \right\} \quad (6-15)$$

where  $\lambda_j$  is any positive weighting vector.

However, obtaining a complete optimal solution set  $\bar{\Pi}_{k_{t+1}}$  to (6-15) is difficult as finding all optimal solution needs to identify all extreme points in the feasible region of the set  $\bar{\Pi}_{k_{t+1}}$ . Instead of solving the SP first to formulate  $\bar{\Pi}_{k_{t+1}}$  as in (6-12) and subsequently solving (6-13), we can combine these two steps in a preemptive priority multiple objective program, where we wish to first maximize  $\pi_{k_{t+1}}^T d_{k_{t+1}} + \pi_{k_{t+1}}^T s_{k_{t+1}} \bar{z}_{k_t}$  (i.e., to solve the dual SP), and among alternative optimal solutions to this problem, we wish to maximize  $\pi_{k_{t+1}}^T d_{k_{t+1}} + \sum_{j=1}^m \pi_{k_{t+1}}^T s_{k_{t+1},j} \lambda_j$ . We denote this preemptive priority multi-objective program as follows:

$$\text{Maximize } \left\{ \pi_{k_{t+1}}^T (d_{k_{t+1}} + s_{k_{t+1}} \bar{z}_{k_t}) \ll \pi_{k_{t+1}}^T \left( d_{k_{t+1}} + \sum_{j=1}^m s_{k_{t+1},j} \lambda_j \right) : \pi_{k_{t+1}} \in \bar{\Pi}_{k_{t+1}} \right\} \quad (6-16)$$

As shown by Sherali and Lunday (2013), there exists a  $\mu > 0$  small enough such that the following combined weighted-sum problem equivalently solves (6-16):



**Revised Dual Subproblem (SP2) for scenario**  $k_{t+1} \in D_{k_t}, k_t \in K_t, t=0, \dots, T-1$ :

$$\text{Maximize } \left\{ \pi_{k_{t+1}}^T (d_{k_{t+1}} + s_{k_{t+1}} \bar{z}_{k_t}) + \mu \left( \pi_{k_{t+1}}^T (d_{k_{t+1}} + \sum_{j=1}^m s_{k_{t+1},j} \lambda_j) \right) : \pi_{k_{t+1}} \in \Pi_{k_{t+1}} \right\} \quad (6-17)$$

An optimality cut that is formed by using the optimal solution  $\bar{\pi}_{k_{t+1}}$  to (6-17) is the maximal non-dominated cut, which replaces (6-9) in the ND solution procedure. We call the revised decomposition method the ND-Max.

### 6.3 Case Study

In this section, we consider two types of case studies. The first one is composed of a set of hypothetical numerical experiments to test computational performance of developed decomposition method. The second one is the case study of South Carolina to justify the implementation of the methodologies in real world large scale problems.

#### 6.3.1 Case I: Numerical Experiments

Let  $(N, A)$  be a network where  $N$  and  $A$  are the sets of nodes and links in the network respectively. Here,  $N$  consists of a set of feedstock sites  $N^F$ , a set of candidate refinery locations  $N^R$ , and a set of demand centers (e.g., major cities)  $N^C$ ; that is,  $N = N^F \cup N^R \cup N^C$ . The arc set  $A$  represents highway network that connects nodes. A finite planning horizon is considered with each time stage being one year.

Three discrete refinery capacity levels of 60, 80 and 100 million gallons per year (MGY) are considered for numerical experiments. A new refinery capacity can be at any

level and expanded over time unless it is already at its maximum capacity of 100 MGY. We consider demand to be uncertain. In particular, it is assumed that a demand  $d_i^t$  at location  $i$  in  $t$  is increased by  $\alpha_{\xi_i} d_i^0$  from  $t-1$ , where  $\alpha_{\xi_i}$  is percentage increase for uncertainty realization  $\xi_i \in \Xi_i$  and  $d_i^0$  is the baseline (year 0) demand at location  $i$ . The equation  $d_i^t = d_i^{t-1} + \alpha_{\xi_i} d_i^0$  is used to estimate the demand over time under uncertainty. For an illustration purpose, we assume that there are only three possible realizations - low, medium, and high demands, with equal probability for all time stages and that  $\alpha_{\xi_i}$  is 0%, 10%, and 20% respectively for low, medium, and high demand realizations, which holds fixed over time. A high penalty cost of \$5/gallon is imposed in this model. All other technical and economic parameters are adopted from (Xie et al., 2014), including refinery capital costs, feedstock moisture content, transportation costs, and biomass-to-biofuel conversion rates.

*Numerical experiment setups:*

Three different numerical experiments are designed as follows:

1. Varied network sizes (three different sizes), with a three-year planning horizon.
2. Varied planning horizons (i.e., 3, 4, and 5 years), with a fixed network size.
3. Varied number of uncertainty realizations in each year (i.e., 3, 5, and 9 realizations), with a fixed planning horizon and a network size.

The baseline case is the one with the smallest network size, three-year planning horizon, and three demand realizations each year. We randomly generated 10 instances

for each numerical experiment, totaling 70 instances - 10 instances for the baseline case and 20 instances each for the numerical experiments with different network sizes, planning horizons, and demand realizations. In each instance, *distances* between nodes on the network, *feedstock yields*, and *demands* are all randomly generated. In particular, the *distances* are generated as:  $\text{distance} = \text{rand}(20,100) / \text{rand}(0.1,1)$ , where  $\text{rand}(a, b)$  is a uniform random number between  $a$  and  $b$ . The generated distances are most likely in a range between 20 and 100 miles. The annual *feedstock yields* and *demands* are uniformly distributed between 0.1 and 1 million dry tons and between 5 and 50 MGY respectively. Note that the randomly generated demand is the  $d_i^0$  in the equation  $d_i^t = d_i^{t-1} + \alpha_{\xi_i} d_i^0$  and demand in the subsequent time stages is  $d_i^t$ . A time limit of 3 CPU hours is set for all numerical experiments. If the problem cannot be solved to optimum by the time limit, the best solution found is reported.

### **6.3.2 Case II: Waste-Based Bioethanol Production in South Carolina**

Reports and studies (Harris et al., 2004; SCRA, 2012) have shown that South Carolina, especially the 17 counties along I-95 highway corridor, has the great potential of producing cellulosic ethanol from biowaste resources and that the high-profit cellulosic biofuels will help boost the economic development in that region which is a traditional agricultural zone and less developed. We explicitly develop a multistage stochastic biofuel supply chain model to explore the economic potential of establishing a supply chain of biofuel between 2015 and 2030. This illustrative case study aims to help better

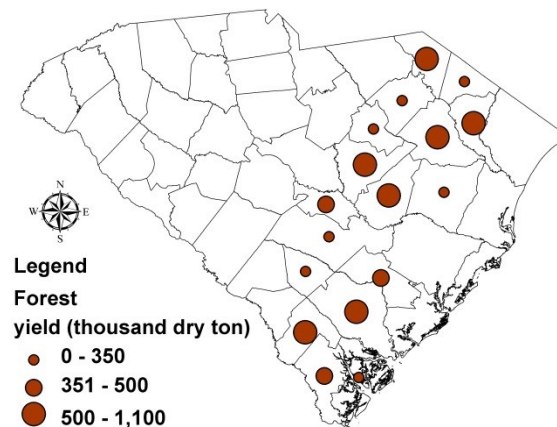
understand how the multistage stochastic method can help adapt planning decisions to evolving uncertainty. Data inputs of the case study are shown as the following.

Feedstock resource: forest residue is abundant in the 17 counties for future for cellulosic biofuel production (SCRA, 2012). In this study, the annual feedstock yields and locations are aggregated at county levels by using Geographic Information System (GIS) software packages (e.g., ArcGIS). To integrate feedstock resource data with transportation network data, it is assumed that feedstock produced in a county is available at the centroid node of that zone. The geographic distribution of forest residue is plotted in Figure 6-2 (a), in which the size of each dot is proportional to the feedstock quantity. The total annual yield is 8.26 million dry tons. The biomass-to-biofuel conversion rate of 80.6 gallons/dry ton, the moisture content of 15% weight, and the average procurement cost of \$35/dry ton are all adopted from our previous study (Xie et al., 2014).

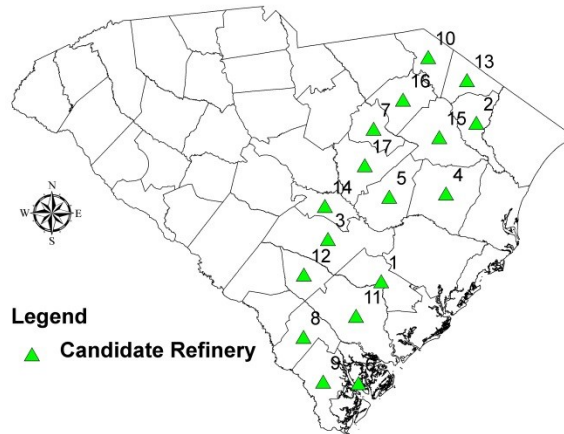
Potential biorefineries: Candidate refinery sites are subject to a number of critical factors, such as the accessibility to water, transportation infrastructures, and zoning requirements if there is any. However, without explicit information, we assume that all 17 counties are legitimate for biorefineries and that the candidate refinery sites are located at the centroid nodes of counties to be integrated with transportation network data (see Figure 6-2 (b)). For illustration purpose, we assume that the refinery capacity is in a range between 60 and 100 MGY (Parker et al., 2007). The total capital cost is the sum of the fixed and variable capital costs. The annualized fixed capital cost is \$6.157m, based on a 20 year return with a 10% rate of return, while the variable capital cost depends on the capacity of the biorefinery and is \$0.314 per gallon (Parker et al., 2007). A mid-term

(2025-2030) projection of biofuel production cost of \$0.92/gallon (Office of the Biomass Program, 2009) is considered, which includes pretreatment, production, distillation, and solid recovery costs.

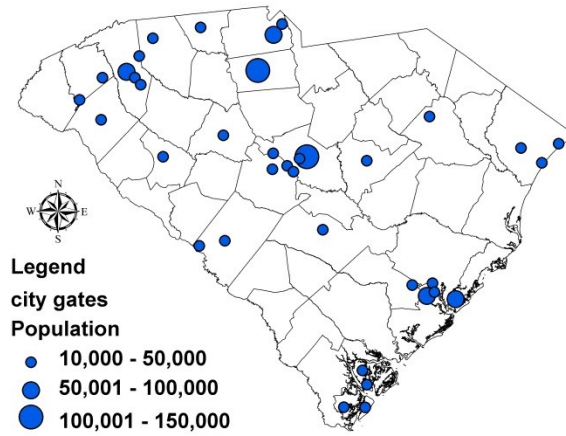
*Demand centers*: Cities with population greater than 10,000 in South Carolina (see Figure 6-2 (c)) plus Atlanta, Georgia are considered as demand centers, totaling 38 cities. The Columbia, Charleston, and Atlanta metropolitan areas are three largest consumer markets. With a 10% ethanol blend wall (i.e., E10), there is a total of 95 MGY consumed annually (EIA, 2014). The ethanol consumption of each city is assumed proportional to its population, which is the baseline (year 0) demand in our model.



(a) Locations of forest residues



(b) Candidate locations of refineries



(c) Demand centers

**Figure 6-2 Maps of Feedstock Fields, Refineries and Demand Centers**

*Transportation:* All feedstock and fuel transportation will be completed by using trucks. In order to estimate the transportation costs within the supply chain, a GIS-based transportation network is used, which contains existing major highways. The shortest distances between feedstock fields, refineries, and city gates are calculated based on the network. Table 6-1 summarizes transportation technical properties (trucking capacity and travel speed) and transportation costs (loading/unloading cost, time/distance dependent cost) required by the model. In particular, in Table 6-1, the time dependent cost consists

of labor and capital cost of trucks, and distance dependent cost includes fuel, insurance, maintenance, and permitting cost.

**Table 6-1 Transportation Inputs**

	Liquids	Bulk solids
Truck Capacity	8,000 gallons	25 wet tons
Travel Speed	40 mph	40 mph
Loading/unloading	\$0.02/gallon	\$5/wet ton
Time dependent	\$32/hr/truckload	\$29/hr/truckload
Distance dependent	\$1.30/mile/truckload	\$1.20/mile/truckload

Source: (Parker et al., 2007)

*Planning horizon and demand uncertainties:* The entire planning horizon of 15 years is partitioned into three stages, each of which spans five years. Planning decisions are made at the beginning of years 1, 6, and 11 while operational decisions are made for every year. The ethanol demand is assumed to be uncertain with three equally distributed realizations  $\alpha_{\xi_i}$ ,  $\forall \xi_i \in \Xi_i$  and set to be 5%, 10%, and 15% respectively for low, medium, and high demand realizations. During the five-year period, the annual demand increases linearly with an increment of  $\alpha_{\xi_i} d_i^0$ , where  $d_i^0$  is the baseline demand at location  $i$ .

## **6.4 Results and Discussion**

All problems were programmed in AMPL (Fourer et al., 2003) and all numerical implementations were conducted on a Dell desktop with 8GB RAM and Intel Core Quad 3.0 GHz processor under Windows 7 environment.

### 6.4.1 Case I Results

Table 6-2 ~ Table 6-4 report the average solution time, number of instances that exceeds the time limit, and the maximum optimality gap for the three numerical experiments. For CPLEX, the optimality gap is between the best bound of relaxed problem and the best integer. For the ND and the ND-Max, it is the convergence gap:  $(UB - LB)/LB$  with a predefined  $\varepsilon = 0.01\%$ . The rows in the table correspond to the different numerical experiments, where the baseline case is duplicated in the first row in each table for comparison purposes. For the numerical instances that are solved to optimum (i.e., zero optimality gap), the objective values attained by the ND and ND-Max are the same as CPLEX. Table 6-2 ~ Table 6-4 indicate that the solution time rises on average for all solutions methods when the problem size increases with network size, planning horizon, or number of demand realizations. Among the three solution approaches, the ND-Max outperforms the others for its lower solution times and smaller optimality gaps on average.

**Table 6-2 Performances of Solution Methods for Different Network Sizes**

Size of Network *	CPLEX			ND			ND-Max		
	Avg. solution time (CPU sec)	# of instances exceeding time limit	Max opt. gap (%)	Avg. solution time (CPU sec)	# of instances exceeding time limit	Max opt. gap (%)	Avg. solution time (CPU sec)	# of instances exceeding time limit	Max opt. gap (%)
16/7/16	406	0	0	148	0	0	106	0	0
24/11/24	4,233	3	0.08	3,035	0	0	1,775	0	0
32/15/32	8,992	8	0.21	5,797	3	0.31	4,607	2	0.07

Note \*: A/B/C: A is number of feedstock fields; B is number of candidate refineries; and C is number of cities.



**Table 6-3 Performances of Solution Methods for Different Planning Horizons\***

Planning length (years)	CPLEX			ND			ND-Max		
	Avg. solution time (CPU sec)	# of instances exceeding time limit	Max opt. gap (%)	Avg. solution time (CPU sec)	# of instances exceeding time limit	Max opt. gap (%)	Avg. solution time (CPU sec)	# of instances exceeding time limit	Max opt. gap (%)
Three	406	0	0	148	0	0	106	0	0
Four	5,609	5	0.18	1,073	0	0	834	0	0
Five	8,401	7	0.13	2,572	0	0	1,682	0	0

Note \*: The numerical experiments were conducted with a fixed network size of 16/7/16.

**Table 6-4 Performances of Solution Methods for Different Number of Realizations Each Year\***

Number of realizations each year	CPLEX			ND			ND-Max		
	Avg. solution time (CPU sec)	# of instances exceeding time limit	Max opt. gap (%)	Avg. solution time (CPU sec)	# of instances exceeding time limit	Max opt. gap (%)	Avg. solution time (CPU sec)	# of instances exceeding time limit	Max opt. gap (%)
Three	406	0	0	148	0	0	106	0	0
Five	2,179	1	0.08	504	0	0	381	0	0
Nine	6,321	5	0.36	2,373	0	0	1,490	0	0

Note \*: The numerical experiments were conducted with fixed the network size of 16/7/16 and a three-year planning horizon.

All comparisons above are based on the average performances of different solution methods, which may neglect possible variations in performances between instances. Here we report the solution performance for each of the 70 instances in terms of the ratios of computing times. It is computed by dividing solving times of the ND and ND-Max by the CPLEX's for every instance. A ratio that is less than one indicates that the decomposition method outperforms CPLEX, and vice versa. Note that we exclude three instances that cannot be solved to optimality by either the ND or the ND-Max within the preset time limit. We plot the ratios of the remaining 67 instances in Figure 6-3.

The horizontal axis denotes seven different ranges of ratios and the vertical axis is the corresponding cumulative probability. From the figure, there are about 82% and 74% probabilities respectively that the ND-Max and the ND perform better than CPLEX. However, when problems are relatively easy (e.g., baseline case), CPLEX can outperform the decompositions, resulting in the ratios that are greater than one. The results of these numerical experiments render us confidence of applying the ND-Max to solve the real-world case study of South Carolina.

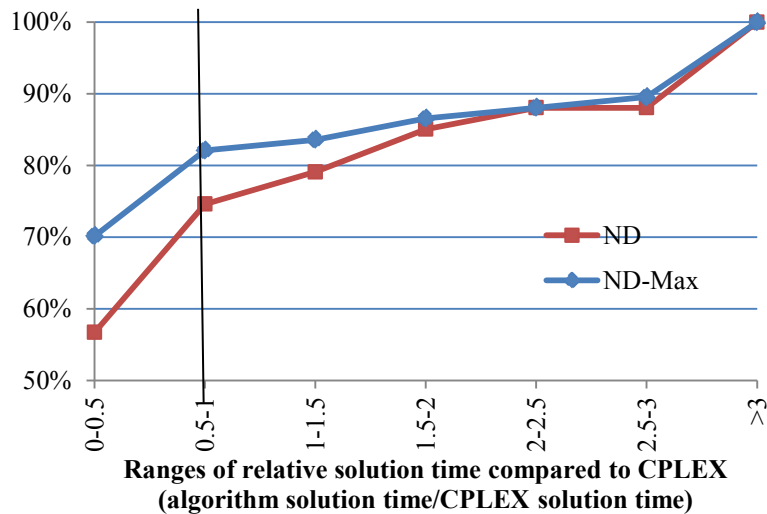


**Figure 6-3 Cumulative Distributions of the Ratios of Solving Times of ND and ND-Max to the Solving Times of CPLEX**

### 6.4.2 Case II Results

The problem has 221 binary variables, 196,651 continuous variables, and 18,066 constraints and is solved by using the ND-Max to an optimality gap of 1% for 2.7 CPU hours.

*Planning decisions:* the optimal planning decisions over the 15-year planning horizon are demonstrated in the diagram shown in Figure 6-4, in which the first number in the parentheses denotes the number of refinery built so far and the second number describes the total capacity. For example, at the beginning of the planning horizon, two refineries are built with a total capacity of 153 MGY to satisfy the demand the in first five years. The planning decisions for stage 2 (i.e., years between 6 and 10) are made upon the full realizations of the uncertainty in stage 1. If it is a low demand ( $\alpha_{\xi_t} = 5\%$ ), the planning decision made at the beginning of year 6 for the next five years is to build no new refinery but upgrade the total capacity to 177 MGY. Similarly, if a medium demand (i.e.,  $\alpha_{\xi_t} = 10\%$ ) is realized, the total capacity of the existing two refinery is expanded to their maximum capacities of 200 MGY. However, if a high demand (i.e.,  $\alpha_{\xi_t} = 15\%$ ) occurs, a new refinery has to be added in order to assure that the total biofuel production capacity can reach 225 MGY. Similarly, the planning decision for stage 3 occurs at the beginning of year 11 and anticipates the uncertain demand for the years from 11 to 15.

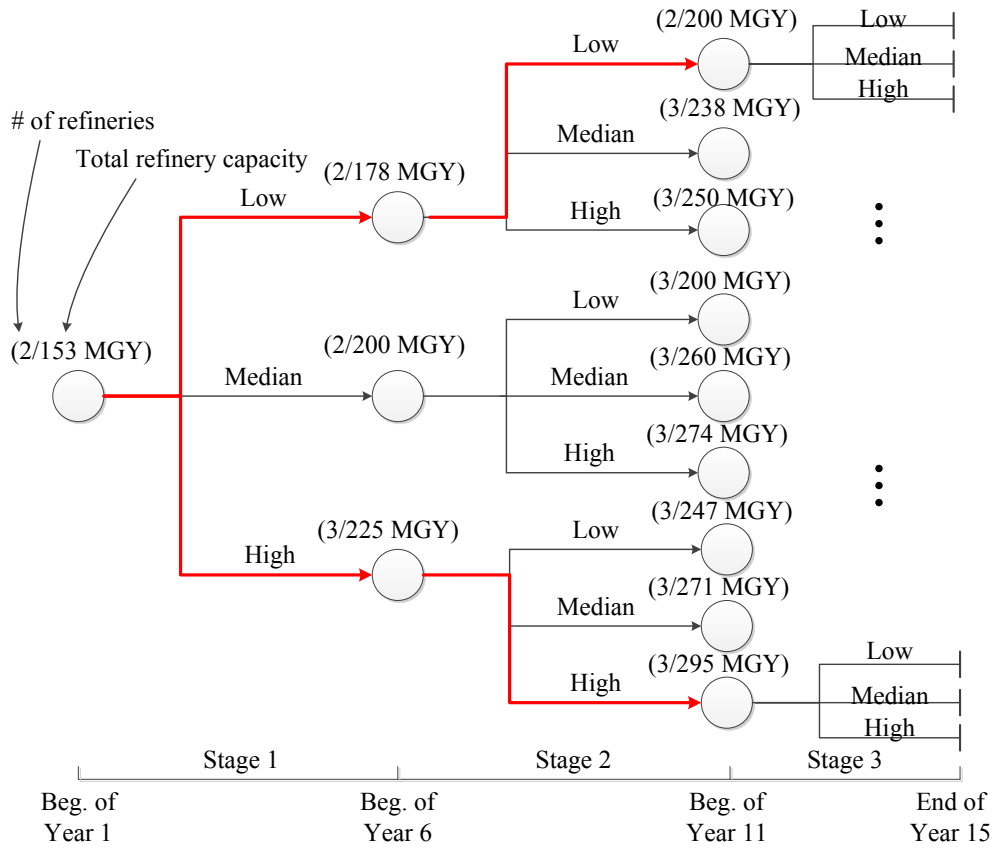


**Figure 6-4 A Diagram of Planning Decisions over Time**

The geographic locations of the refineries are demonstrated in Figure 6-5 for two specific scenarios, which are in correspondent with the low and high demands throughout the planning horizon as highlighted in Figure 6-4, and the capacities of the refineries are presented in Table 6-5. For both scenarios, locations #5 and #17 are selected to build refineries to take advantage of their proximities to feedstock fields and –Columbia area, which is one of major demand centers. For the scenario of high demand, one more refinery at location #11 is selected to supplement the demand from Charleston which is another major demand center in this case study.

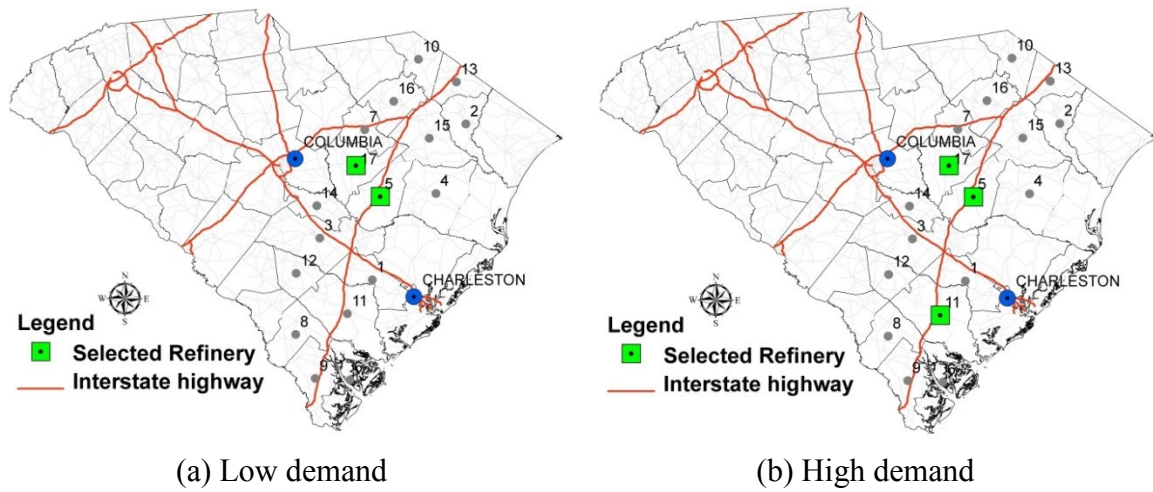


**Figure 6-5 Refinery Layouts under Two Demand Scenarios**

**Table 6-5 Refinery Capacities by Scenarios**

Scenarios	Refinery locations	Year 1	Year 6	Year 11
Low demand	#5	64 MGY	89 MGY	100 MGY
	#17	89 MGY	89 MGY	100 MGY
High demand	#5	64 MGY	76 MGY	100 MGY
	#11	Not open	60 MGY	95 MGY
	#17	89 MGY	89 MGY	100 MGY

*Breakdown of the total cost:* The total expected system cost is about \$5 billion over 15 years and the resulting average delivered fuel cost is about \$1.95 per gallon of ethanol. The breakdown of the total expected cost in Figure 6-6 indicates that the production cost accounts for almost half and that transportation cost is also substantial accounting for 10% the total cost, which justifies that an effective supply chain is crucial. The penalty cost (2% of the total cost) mainly incurs to meet the high demand scenario of Atlanta, which offsets the instate production and transportation costs.

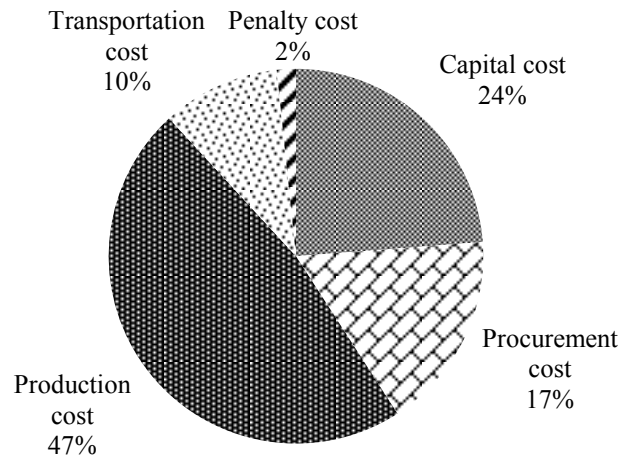


**Figure 6-6 Breakdown of the Total Systems Cost**

*The Value of Multistage Stochastic Model*

Prior research on long-term biofuel supply chain planning presumes that sequential decisions are made with certainty (Ebadian et al., 2013; Giarola et al., 2011; Huang et al., 2010). We are particularly interested in understanding how much economic value a stochastic modeling method can contribute to a decision making under uncertainty, relative to its deterministic counterpart, considering the extra modeling and computational efforts involved in the stochastic model.

We base our evaluation on the Value of the Stochastic Solution (VSS) (Birge and Louveaux, 1997), which is defined as the difference between the *expected result* of using the *expected value* problem solution (EEV) and the result of *here-and-now* (or *recourse problem*) solution (RP); that is,  $VSS=EEV-RP$ . The EEV is the expected outcome of the deterministic solution that is obtained by taking the expectation of uncertainty scenarios as inputs while the RP is the expected outcome of using the stochastic solution under

uncertainty, which is the optimal objective value of the stochastic model. The VSS for a multistage stochastic program is calculated for each stage. The results of VSS presented in Table 6-6 indicate that the stochastic solutions help reduce the cost for each stage and such benefit increases with higher demand over time, with a total cost saving up to \$71m or 1.42% (= \$71m/\$5b).

**Table 6-6 The VSSs by Stages**

Stages	Time Periods	EEV (\$m)	RP (\$m)	VSS (\$m)
1	1 <sup>st</sup> ~5 <sup>th</sup> years	1,231	1,225	6
2	6 <sup>th</sup> ~10 <sup>th</sup> years	1,687	1,657	30
3	11 <sup>th</sup> ~ 15 <sup>th</sup> years	2,141	2,106	35
Total	1 <sup>st</sup> ~15 <sup>th</sup> years	5,059	4,988	71

In this case study, the benefit of stochastic solution may seem low. It may be due to the relatively low variations in demand realizations and the assumption of linearly demand growth over time. It may also be attributed by the absence of storage facilities in the supply chain, resulting in the lack of buffers in mitigating discrepancy caused by uncertainties. From modeling perspective, the choice of a specific formulation is problem specific and one would not know if a multistage stochastic model is worthwhile until all the modeling and computational efforts are made. However, how to identify the bound at early stage that better informs an appropriate formulation without having to completely solve the entire problem may be a worthy research question for the future.

## **6.5 Summary**

In Chapter 6, I presented a new research endeavor in biofuel supply chain design, which addresses the coupled effects of time dynamics and uncertainty, by integrating planning and operational decisions into a multistage stochastic programming framework. In this study, planning decisions are determined sequentially along with evolving uncertainty realizations while achieving a least-cost supply chain of biofuel for the entire planning horizon. I formulate a multistage stochastic mixed integer program with integer recourse. By utilizing the property of block separable recourse, we develop two decomposition methods based on nested decomposition (ND) and integrated maximal non-dominated cuts (ND-Max) to solve the multistage stochastic program. I justified the model and evaluated the performances of the decompositions using hypothetical numerical experiments with different network sizes, planning horizon, and number of uncertainty realizations. The ND-Max is identified as the most effective solution method by the 70 randomly generated instances and is used to solve the illustrative case study of South Carolina. It is found that the forest residue based bioethanol system in South Carolina can be economically feasible with an average delivered ethanol cost of \$1.95 per gallon via rigorous long-term system planning. Through the case study, we also demonstrate how planning decisions are adapted to evolving uncertainty on geographic resolution. The multistage stochastic solution is shown to be more cost effective than the deterministic counterpart through the analysis of the value of stochastic solutions.



## **CHAPTER 7 CONCLUSIONS**

### ***7.1 Summary of Dissertation***

In the transportation energy field, this dissertation presents a couple of new research endeavors in planning and designing sustainable supply chains for the future renewable fuel systems. Taking the biofuel systems as an example, the dissertation demonstrated the importance of integrating “environmental thinking” into the supply chain planning, adopting multimodal transportation to improve the supply chain operations, providing strategies in mitigating uncertainty from conversion technology, and developing advanced modeling framework of the sequential planning of the supply chain against uncertainties in a long run. The integration of these novel supply chain design features is proved to successfully sustain the biofuel supply chain systems and is expected to provide guidance in designing other renewable fuel supply chain systems.

### ***7.2 Research Impacts of Dissertation***

This dissertation has innovative research impacts on both transportation systems domain and operations research domain.

In the broad transportation systems domain, instead of relying on traditional engineering methodologies, this dissertation demonstrated the importance of using systems approaches in answering challenging transportation related problems. For example, through smart systems design, I showed that it is promising in identifying novel solutions such as multimodal transportation in improving the efficiency of biofuel supply chain operations. In particular for the transportation energy society, this dissertation

showed the value of supply chain systems design in promoting renewable energy systems. By adopting the advanced model frameworks developed in this dissertation, decision makers can reduce the systems cost and improve environmental quality for the renewable energies.

In the operations research domain, this dissertation developed several advanced models and solution methods. Especially in Chapter 6, an advanced multistage stochastic programming model was developed with efficient algorithms. Such effort is not only brand new in the transportation field, but also innovative in the operations research domain. The methodologies can be generalized and applied to other operations research emphasized multistage stochastic problems.

### ***7.3 Limitations of Dissertations***

One major limitation of this dissertation is that the four studies did not provide methodologies in validating the proposed models. Although the mathematical correctness of the models has been proved during the implementation process, it is still questionable if or not the models can effectively represent the real world application. However, such effort is time consuming and hardly achieved especially for the biofuel systems, for there is no existing commercialized cellulosic ethanol supply chain that could validate the model. Given the research limitation during the PhD study, validating the models is not the focus of this dissertation and can be part of the future works.

Another major limitation arises from the lack of analysis in evaluating the interaction between different innovative solutions proposed in four studies. Although the

dissertation showed that each of the proposed models can improve the biofuel supply chain independently, these models shall be integrated into one complete model to design the supply chain systems. However, because of the computational challenges, this dissertation did not make this integration.

## **7.4 Future Works**

For future work, one immediate research approach is how to integrate the novel concepts presented in the four studies into one complete model. For example, the environmental objective (presented in Chapter 3 and Chapter 5) and the multimodal transport systems (presented in Chapter 4) can be integrated into the sequential stochastic modeling framework (presented in Chapter 6). Such effort is not trivial from the modeling prospective, and more importantly, it contributes to additional computational challenges. Thus, advanced solution methods, such as local branching and approximation methods, may be adopted to further improve the computational performance.

Another important future work is based on the multistage stochastic model developed in Chapter 6. Most existing literatures in biofuel supply chain design is either under deterministic environment or under stochastic environment but ignoring the time dynamics. The study enacts a new research approach to consider both time dynamics and uncertainties in the renewable fuel supply chain systems design. For future implementations, a natural step is to incorporate the storage facilities in the supply chain to handle the feedstock seasonality and allows for biofuel storage. However, the resulting formulation may not possess the property of block-seperability and algorithmic

development will be another concerted efforts. Fortunately, recent endeavor on solving multistage stochastic integer programs have already set path toward, such as a linear programming based approximation scheme to exploit the decomposable structure and seek a feasible solution (Ahmed et al., 2003) and a parallelizable Branch-and-Fix Coordination algorithm for solving multistage mixed 0-1 stochastic problems (Escudero et al., 2012). Another direction is to explore the effects of different optimization formulations on the solution quality and the relations with the types of uncertainty and their realizations. This research can also be enriched by incorporating more realistic considerations, such as considering multiple types of feedstocks, multimodal transport systems, and realistic trucking distances.

Finally, a complete decision making framework shall be developed which also includes model validation and calibration. This effort is important for the proposed models to be validate and applicable at different temporal and geographical dimensions.

## BIBLIOGRAPHY

110th U.S. Congress, 2007. Energy Independence and Security Act of 2007, *H.R.6*.

Ahmed, S., King, A., Parija, G., 2003. A Multi-Stage Stochastic Integer Programming Approach for Capacity Expansion under Uncertainty. *Journal of Global Optimization* 26(1), 3-24.

Akgul, O., Zamboni, A., Bezzo, F., Shah, N., Papageorgiou, L.G., 2010. Optimization-Based Approaches for Bioethanol Supply Chains. *Industrial & Engineering Chemistry Research* 50(9), 4927-4938.

Aksoy, B., Cullinan, H., Webster, D., Gue, K., Sukumaran, S., Eden, M., Sammons, N., 2011. Woody biomass and mill waste utilization opportunities in Alabama: Transportation cost minimization, optimum facility location, economic feasibility, and impact. *Environmental Progress & Sustainable Energy* 30(4), 720-732.

An, H., Wilhelm, W.E., Searcy, S.W., 2011. A Mathematical Model to Design A Lignocellulosic Biofuel Supply Chain System with A Case Study Based on A Region in Central Texas. *Bioresource Technology* 102(17), 7860-7870.

ARB, 2009. Detailed California-Modified GREET Pathway for Corn Ethanol. Air Resources Board.

Archibald, T.W., Buchanan, C.S., McKinnon, K.I.M., Thomas, L.C., 1999. Nested Benders Decomposition and Dynamic Programming for Reservoir Optimisation. *The Journal of the Operational Research Society* 50(5), 468-479.

- Awudu, I., Zhang, J., 2012. Uncertainties and Sustainability Concepts in Biofuel Supply Chain Management: A Review. *Renewable and Sustainable Energy Reviews* 16(2), 1359-1368.
- Awudu, I., Zhang, J., 2013. Stochastic Production Planning for A Biofuel Supply Chain under Demand and Price Uncertainties. *Applied Energy* 103(0), 189-196.
- Birge, J., Donohue, C., Holmes, D., Svintsitski, O., 1996. A parallel implementation of the nested decomposition algorithm for multistage stochastic linear programs. *Mathematical Programming* 75(2), 327-352.
- Birge, J., Louveaux, F., 1997. *Introduction to Stochastic Programming*. Springer.
- Birge, J.R., 1985. Decomposition and Partitioning Methods for Multistage Stochastic Linear Programs. *Operations Research* 33(5), 989-1007.
- Birge, J.R., Louveaux, F., 2011. *Introduction to Stochastic Programming*, 2nd ed. Springer, New York.
- Bowling, I.M., Ponce-Ortega, J.M.a., El-Halwagi, M.M., 2011. Facility Location and Supply Chain Optimization for a Biorefinery. *Industrial & Engineering Chemistry Research* 50(10), 6276-6286.
- Brinkman, N., Wang, M., Weber, T., Darlington, T., 2005. Well-to-Wheels Analysis of Advanced Fuel/Vehicle Systems — A North American Study of Energy Use, Greenhouse Gas Emissions, and Criteria Pollutant Emissions.
- BSI Group, 2011. PAS 2050:2011: Specification for the Assessment of the Life Cycle Greenhouse Gas Emissions of Goods and Services. BSI British Standards Institution.
- California Energy Commission, 2013. <http://www.energy.ca.gov/>.

California Energy Commission, 2014. Fuel Ethanol Terminal Market Price - 18 Month History, [http://www.energyalmanac.ca.gov/transportation/ethanol\\_graphs/ethanol\\_18-month.html](http://www.energyalmanac.ca.gov/transportation/ethanol_graphs/ethanol_18-month.html). Access Date: 02/19/2014.

Chen, C.-W., Fan, Y., 2012. Bioethanol Supply Chain System Planning under Supply and Demand Uncertainties. *Transportation Research Part E: Logistics and Transportation Review* 48(1), 150-164.

Consigli, G., Dempster, M.A.H., 1998. Dynamic stochastic programming for asset-liability management. *Annals of Operations Research* 81(0), 131-162.

Cundiff, J.S., Dias, N., Sherali, H.D., 1997. A linear Programming Approach for Designing A Herbaceous Biomass Delivery System. *Bioresource Technology* 59(1), 47-55.

Dal-Mas, M., Giarola, S., Zamboni, A., Bezzo, F., 2011. Strategic design and investment capacity planning of the ethanol supply chain under price uncertainty. *Biomass and Bioenergy* 35(5), 2059-2071.

Donohue, C.J., Birge, J.R., 2006. The Abridged Nested Decomposition Method for Multistage Stochastic Linear Programs with Relatively Complete Recourse. *Algorithmic Operations Research* 1(1).

Ebadian, M., Sowlati, T., Sokhansanj, S., Townley-Smith, L., Stumborg, M., 2013. Modeling and analysing storage systems in agricultural biomass supply chain for cellulosic ethanol production. *Applied Energy* 102(0), 840-849.

Edirisinghe, N.C.P., Patterson, E.I., 2007. Multi-period stochastic portfolio optimization: Block-separable decomposition. *Annals of Operations Research* 152(1), 367-394.

EERE, 2011. Ethanol Distribution. U.S. Department of Energy.

EIA, 2013. Cellulosic biofuels begin to flow but in lower volumes than foreseen by statutory targets.

EIA, 2014. Prices, Sales Volumes & Stocks by State

([http://www.eia.gov/dnav/pet/pet\\_sum\\_mkt\\_dcu\\_SSC\\_a.htm](http://www.eia.gov/dnav/pet/pet_sum_mkt_dcu_SSC_a.htm)).

EPA, Renewable and Alternative Fuels (<http://www.epa.gov/otaq/fuels/alternative-renewablefuels/index.htm>).

Escudero, L.F., Araceli Garín, M., Merino, M., Pérez, G., 2012. An algorithmic framework for solving large-scale multistage stochastic mixed 0–1 problems with nonsymmetric scenario trees. *Computers & Operations Research* 39(5), 1133-1144.

Forster, P., Ramaswamy, V., Artaxo, P., Berntsen, T., Betts, R., Fahey, D., Haywood, J., Lean, J., Lowe, D., Myhre, G., Nganga, J., Prinn, R., Raga, G., Schultz, M., Van Dorland, R., 2007. Changes in atmospheric constituents and in radiative forcing, Cambridge, United Kingdom, pp. 129-234.

Fourer, R., Gay, D., Kernighan, B., 2003. *AMPL: A Modeling Language for Mathematical Programming*, 2nd ed. Duxbury Press, Boston.

Gebreslassie, B.H., Slivinsky, M., Wang, B., You, F., 2013. Life Cycle Optimization for Sustainable Design and Operations of Hydrocarbon Biorefinery via Fast Pyrolysis, Hydrotreating and Hydrocracking. *Computers & Chemical Engineering* 50, 71-91.

Giarola, S., Zamboni, A., Bezzo, F., 2011. Spatially explicit multi-objective optimisation for design and planning of hybrid first and second generation biorefineries. *Computers & Chemical Engineering* 35(9), 1782-1797.



- Golub, B., Holmer, M., McKendall, R., Pohlman, L., Zenios, S.A., 1995. A stochastic programming model for money management. *European Journal of Operational Research* 85(2), 282-296.
- Gulpinar, N., Rustem, B., Settergren, R., 2002. Multistage Stochastic Programming in Computational Finance, In: Kontoghiorghes, E., Rustem, B., Siokos, S. (Eds.), *Computational Methods in Decision-Making, Economics and Finance*. Springer US, pp. 35-47.
- Harris, R.A., Adams, T., Hiott, V., Lear, D.V., Wang, G., Tanner, T., Frederick, J., 2004. Potential for Biomass Energy Development in South Carolina
- Hess, J.R., Kenney, K.L., Ovard, L.P., Searcy, E.M., Wright, C.T., 2009. Commodity-Scale Production of an Infrastructure-Compatible Bulk Solid from Herbaceous Lignocellulosic Biomass. Idaho National Laboratory, Idaho Falls, ID.
- Hochreiter, R., Wozabal, D., 2010. A Multi-stage Stochastic Programming Model for Managing Risk-optimal Electricity Portfolios, In: Rebennack, S., Pardalos, P.M., Pereira, M.V.F., Iliadis, N.A. (Eds.), *Handbook of Power Systems II*. Springer Berlin Heidelberg, pp. 383-404.
- Huang, Y., Chen, C.-W., Fan, Y., 2010. Multistage Optimization of The Supply Chains of Biofuels. *Transportation Research Part E: Logistics and Transportation Review* 46(6), 820-830.
- Huang, Y., Fan, Y., Chen, C.-W., 2013. An Integrated Biofuel Supply Chain against Feedstock Seasonality and Uncertainty. *Transportation Science (In press)*.

- Jenkins, B., Dempster, P., Gildart, M., Kaffka, S., 2007. California Biomass and Biofuels Production Potential (Draft). California Energy Commission.
- Kim, J., Realff, M.J., Lee, J.H., 2011a. Optimal design and global sensitivity analysis of biomass supply chain networks for biofuels under uncertainty. *Computers & Chemical Engineering* 35(9), 1738-1751.
- Kim, J., Realff, M.J., Lee, J.H., Whittaker, C., Furtner, L., 2011b. Design of biomass processing network for biofuel production using an MILP model. *Biomass and Bioenergy* 35(2), 853-871.
- Kouwenberg, R., 2001. Scenario generation and stochastic programming models for asset liability management. *European Journal of Operational Research* 134(2), 279-292.
- Li, Y.P., Huang, G.H., Nie, S.L., 2006. An interval-parameter multi-stage stochastic programming model for water resources management under uncertainty. *Advances in Water Resources* 29(5), 776-789.
- Li, Y.P., Huang, G.H., Nie, S.L., Liu, L., 2008. Inexact multistage stochastic integer programming for water resources management under uncertainty. *Journal of Environmental Management* 88(1), 93-107.
- Linares, P., Romero, C., 2000. A Multiple Criteria Decision Making Approach for Electricity Planning in Spain: Economic versus Environmental Objectives. *The Journal of Operational Research Society* 51(6), 736-743.
- Louveaux, F., 1986. Multistage stochastic programs with block-separable recourse, In: Prékopa, A., Wets, R.B. (Eds.), *Stochastic Programming 84 Part II*. Springer Berlin Heidelberg, pp. 48-62.

- Louveaux, F.V., 1980. A Solution Method for Multistage Stochastic Programs with Recourse with Application to an Energy Investment Problem. *Operations Research* 28(4), 889-902.
- Magnanti, T.L., Wong, R.T., 1981. Accelerating Benders Decomposition: Algorithmic Enhancement and Model Selection Criteria. *Operations Research* 29(3), 464-484.
- Magnanti, T.L., Wong, R.T., 1990. Decomposition methods for facility location problems, P. B. Mirchandani & R. L. Francis (Eds.), *Discrete location theory*. Hoboken: Wiley, pp. 209–262.
- Mahmudi, H., Flynn, P., 2006. Rail vs truck transport of biomass. *Applied Biochemistry and Biotechnology* 129(1), 88-103.
- Mele, F.D., Guillén-Gosálbez, G., Jiménez, L., 2009. Optimal Planning of Supply Chains for Bioethanol and Sugar Production with Economic and Environmental Concerns. *Computer Aided Chemical Engineering* 26, 997-1002.
- Melo, M.T., Nickel, S., Saldanha-da-Gama, F., 2009. Facility location and supply chain management – A review. *European Journal of Operational Research* 196(2), 401-412.
- Mercier, A., Cordeau, J.-F., Soumis, F., 2005. A computational study of Benders decomposition for the integrated aircraft routing and crew scheduling problem. *Computers & Operations Research* 32(6), 1451-1476.
- Nickel, S., Saldanha-da-Gama, F., Ziegler, H.-P., 2012. A multi-stage stochastic supply network design problem with financial decisions and risk management. *Omega* 40(5), 511-524.

- Office of the Biomass Program, 2009. Biomass Multi-Year Program Plan, Energy Efficiency and Renewable Energy, U.S. Department of Energy.
- Papadakos, N., 2008. Practical enhancements to the Magnanti–Wong method. *Operations Research Letters* 36(4), 444-449.
- Parker, N., Tittmann, P., Hart, Q., Lay, M., Cunningham, J., Jenkins, B., 2007. Strategic Development of Bioenergy in the Western States Development of Supply Scenarios Linked to Policy Recommendations, Task 3: Spatial Analysis and Supply Curve Development. Western Governors' Association.
- Parker, N., Tittmann, P., Hart, Q., Lay, M., Cunningham, J., Jenkins, B., 2008. Strategic assessment of bioenergy development in the west: Spatial analysis and supply curve development. Western Governors' Association.
- Pereira, M.V.F., Pinto, L.M.V.G., 1991. Multi-stage stochastic optimization applied to energy planning. *Mathematical Programming* 52(1-3), 359-375.
- Raphael, S., Ausilio, B., Nilay, S., 2009. The Greenhouse Gas Emissions Performance of Cellulosic Ethanol Supply Chains in Europe. *Biotechnology for Biofuels* 2(1).
- Rentizelas, A.A., Tolis, A.J., Tatsiopoulos, I.P., 2009. Logistics issues of biomass: The storage problem and the multi-biomass supply chain. *Renewable and Sustainable Energy Reviews* 13(4), 887-894.
- Saaty, T.L., 1980. *The Analytic Hierarchy Process: Planning, Priority Setting, Resource Allocation*. McGraw Hill International.

- Santoso, T., Ahmed, S., Goetschalckx, M., Shapiro, A., 2005. A stochastic programming approach for supply chain network design under uncertainty. *European Journal of Operational Research* 167(1), 96-115.
- SCRA, 2012. I-95 Corridor, South Carolina: Resources to Support Revitalization through Clean Energy and Biotechnology.
- Sherali, H., Lunday, B., 2013. On generating maximal nondominated Benders cuts. *Annals of Operations Research* 210(1), 57-72.
- Shiina, T., Birge, J., 2003. Multistage stochastic programming model for electric power capacity expansion problem. *Japan J. Indust. Appl. Math.* 20(3), 379-397.
- Sims, R.E.H., Mabee, W., Saddler, J.N., Taylor, M., 2010. An overview of second generation biofuel technologies. *Bioresource Technology* 101(6), 1570-1580.
- Slyke, R.M.V., Wets, R., 1969. L-Shaped Linear Programs with Applications to Optimal Control and Stochastic Programming. *SIAM Journal on Applied Mathematics* 17(4), 638-663.
- Subrahmanyam, S., Pekny, J.F., Reklaitis, G.V., 1994. Design of Batch Chemical Plants Under Market Uncertainty. *Industrial & Engineering Chemistry Research* 33(11), 2688-2701.
- Tamiz, M., Jones, D., Romero, C., 1998. Goal Programming for Decision Making: An Overview of the Current State-of-the-Art. *European Journal of Operational Research* 111(3), 569-581.

- Tembo, G., Epplin, F.M., Huhnke, R.L., 2003. Integrative Investment Appraisal of a Lignocellulosic Biomass-to-Ethanol Industry. *Journal of Agricultural and Resource Economics* 28(03).
- Unsihuay-Vila, C., Marangon-Lima, J.W., Zambroni de Souza, A.C., Perez-Arriaga, I.J., 2011. Multistage Expansion Planning of Generation and Interconnections with Sustainable Energy Development Criteria: A Multiobjective Model. *International Journal of Electrical Power & Energy Systems* 33(2), 258-270.
- USDA, 2007. Ethanol Transportation Backgrounder.
- Wakeley, H.L., Hendrickson, C.T., Griffin, W.M., Matthews, H.S., 2009. Economic and Environmental Transportation Effects of Large-Scale Ethanol Production and Distribution in the United States. *Environmental Science & Technology* 43(7), 2228-2233.
- Wang, M., Wu, Y., Elgowainy, A., 2005. Operating Manual for GREET: Version 1.7. Argonne National Laboratory.
- Watkins, D.W., McKinney, D.C., Lasdon, L.S., Nielsen, S.S., Martin, Q.W., 2000. A scenario-based stochastic programming model for water supplies from the highland lakes. *International Transactions in Operational Research* 7(3), 211-230.
- Wu, M., Wang, M., Huo, H., 2006. Fuel-Cycle Assessment of Selected Bioethanol Production Pathways in the United States.
- Xie, F., Huang, Y., Eksioglu, S., 2014. Integrating multimodal transport into cellulosic biofuel supply chain design under feedstock seasonality with a case study based on California. *Bioresource Technology* 152(0), 15-23.

- You, F., 2013. Design of Biofuel Supply Chains under Uncertainty with Multiobjective Stochastic Programming Models and Decomposition Algorithm, In: Andrzej, K., Ilkka, T. (Eds.), *Computer Aided Chemical Engineering*. Elsevier, pp. 493-498.
- You, F., Tao, L., Graziano, D.J., Snyder, S.W., 2011. Optimal design of sustainable cellulosic biofuel supply chains: Multiobjective optimization coupled with life cycle assessment and input–output analysis. *AIChE Journal*, n/a-n/a.
- You, F., Tao, L., Graziano, D.J., Snyder, S.W., 2012. Optimal Design of Sustainable Cellulosic Biofuel Supply Chains: Multiobjective Optimization Coupled with Life Cycle Assessment and Input–Output Analysis. *AIChE Journal* 58(4), 1157-1180.
- You, F., Wang, B., 2011. Life Cycle Optimization of Biomass-to-Liquid Supply Chains with Distributed–Centralized Processing Networks. *Industrial & Engineering Chemistry Research* 50(17), 10102-10127.
- Zamboni, A., Bezzo, F., Shah, N., 2009. Spatially Explicit Static Model for the Strategic Design of Future Bioethanol Production Systems. 2. Multi-Objective Environmental Optimization. *Energy & Fuels* 23(10), 5134-5143.
- Zhou, Y., Huang, G.H., Yang, B., 2013. Water resources management under multi-parameter interactions: A factorial multi-stage stochastic programming approach. *Omega* 41(3), 559-573.
- Zhu, J.Y., Pan, X.J., 2010. Woody biomass pretreatment for cellulosic ethanol production: Technology and energy consumption evaluation. *Bioresource Technology* 101(13), 4992-5002.